

DTIC

OPY

N00014-37-K-0152

12  
4

Final Report: 2-D and 3-D Magnetic Inversion Studies in the South Atlantic

Ken C. Macdonald,  
Department of Geological Sciences and Marine Science Institute  
University of California, Santa Barbara 93106

Other collaborating scientists: S.M. Carbotte, S. Welch, S.P. Miller, U.C.S.B.; P.J. Fox, U.R.I.;  
P. Vogt, N.R.L.; S. Cande, L.D.G.O.

SDIC  
ELECTE  
APR 26 1989  
D & D

AD-A207 068

Our long range goals have been to achieve an understanding of crustal accretion along the Southern Mid-Atlantic Ridge. We address this problem with a combined analysis of bathymetry and sea surface magnetic data from two extensive SeaBeam surveys of the ridge between 25°-28° S and 30°-38° S. We are particularly interested in how crustal accretion may differ from accretion processes in other areas spreading at faster and slower rates as spreading rates in the South Atlantic area fall within a transitional range in which the axial rift valley begins to disappear.

The great clarity of magnetic recording in the oceanic crust of the South Atlantic has enabled us to carry out a very thorough analysis of the magnetic data which, in turn, has provided us with powerful constraints on models of volcanic and tectonic crustal generation processes at slow spreading rates. Analysis of the magnetic data has included both 2-D and 3-D inversions which remove skewness and the effects of bathymetry. From 2-D analysis we have identified isochron boundaries and constructed spreading rate history models, thus defining the evolution of the ridge-axis discontinuities in the region. We have examined transition widths for evidence of any variation in the crustal accretion process with time or location. From 3-D analysis we have created maps of crustal magnetization that reveal zones of enhanced magnetization possibly related to fractionation processes in the axial magma chamber.

Major Conclusions

Interval spreading rates, which reflect the stability through time of the spreading process, indicate that spreading within each ridge segment has been asymmetric with the sense of asymmetry often changing from one interval (~0.8 my duration) to the next. Averaged over longer time periods (>1.0 my) however, the sense of asymmetry has generally remained the same.

Full interval spreading rates for adjacent ridge segments differ by 10% on average. These differences, which exceed our measurement errors and are substantially more than the expected change with changing proximity to the pole of rotation for the South American and African plates, reflect non-rigid behavior. Total opening rates from 25°-27°30' S have decreased by 20-30% from anomaly 4' to 2'.

Full rates since the Jaramillo have increased in the 25°-27°30' S area. We see this same pattern for only one ridge segment within 31°-34° 30' S, although our data coverage here is less extensive. The changes in spreading rates we see may be of global significance or may point to significant errors in the anomaly time scale.

Magnetization highs of comparable magnitude are located at both the large offset Cox fracture zone and short offset 33°30' S discordant zone-ridge intersections. These magnetization highs persist off axis and can be traced in places beyond anomaly 2'.

Within the past 10.0 my, the Moore transform fault has evolved from a classic ridge-perpendicular feature with an offset of over 25 km to an oblique-trending second order ridge-axis discontinuity 9.5 km in length. The change occurred between 2.5 and 1.8 my and involved a rift

Approved for public release  
Distribution Unlimited

289 4 25 192

propagation 'event' which transferred crust of anomaly 2-2' time from the east to west flank of the ridge. Since that time, the Moore discontinuity has migrated north approximately 12 km.

There is additional evidence for rift propagation "events" during the same time interval in the vicinity of the 33°30' S discontinuity and since anomaly 2 time at the 31°15' S discontinuity.

Discordant zones within both survey areas have systematically lengthened or shortened by ~10 km during the time interval from 1 my to 4 my while larger-offset fracture zones have remained comparatively constant in length. Changing offset along these short-offset discontinuities may be a mechanism by which the plate boundary responds to changes in plate motion. However, the sense in which the length of each offset has evolved (i.e., lengthening or shortening) is not simply related to the sense of offset (i.e., right or left lateral) across each discontinuity, and could not reflect one simple adjustment of the entire plate boundary in this region to a change in the direction of plate opening.

Individual ridge segments within our study area have independent spreading histories in that the amount and sense of asymmetric spreading and total opening rates for adjacent ridge segments differ. Independent spreading histories may reflect significant decoupling in the mantle source region for these ridge segments and we conclude that ridge segments may respond independently to changes in plate motion giving rise to discordant zone length variability.

#### Publications

\*Carbotte, S.M., S. Welch, K.C. Macdonald, and S.P. Miller. Spreading rates, rift propagation, and fracture zone offset histories for the past 5 myrs on the Mid-Atlantic Ridge; 25°-28° S and 31°-34° S, submitted to Mar. Geophys. Res.

\*Fox, P.J., and others. The Mid-Atlantic Ridge (31° S -34° S): temporal and spatial variations of accretionary processes, submitted to Mar. Geophys. Res.

\*Grindlay, N.R., P.J. Fox and K.C. Macdonald. Tectonic characteristics of ridge axis discordant zones in the South Atlantic, submitted to Mar. Geophys. Res.

Grindlay, N.R., P.J. Fox and K.C. Macdonald. Tectonic characteristics of ridge axis discordant zones in the South Atlantic, EOS trans AGU (abs), 69, 1424, 1988.

Grindlay, N. R., P.J. Fox, S.C. Cande, D. Forsyth, K.C. Macdonald, and P. Vogt. Ridge axis discordant zones in the South Atlantic: Morphology, structure, evolution and significance, EOS trans AGU (abs), 68, 1491, 1987.

Macdonald, K.C. The crest of the Mid-Atlantic Ridge: models for crustal generation processes and tectonics, The Geology of North America, DNAG Vol.M, 51-68, 1986.

Severinghaus, J.P., and K.C. Macdonald. High inside corners at ridge-transform intersections, Marine Geophysical Researches, vol. 9, 353-367, 1988.

Welch, S.M., K.C. Macdonald, S.P. Miller, P.J. Fox, and N.R. Grindlay. Magnetic analysis of slow spreading in the South Atlantic, EOS trans AGU (abs), 67, 1227, 1986.

Welch, S.M., Magnetic analysis of the Mid-Atlantic Ridge from 31°-34°S, (MS thesis, U.C.S.B., 1988).

\*These three articles will comprise a special issue of the journal Marine Geophysical Researches.

**Spreading rates, rift propagation, and fracture zone offset histories during the past 5 my on the Mid-Atlantic Ridge; 25°-27° 30' S and 31°-34° 30' S**

by

**S. M. Carbotte, S. M. Welch, and K. C. Macdonald**

**Marine Science Institute, University of California, Santa Barbara, CA., 93106**

submitted to  
Marine Geophysical Researches  
April 15, 1989



Accession For	
NTIS CRA&I	<input checked="" type="checkbox"/>
DTIC TAB	<input type="checkbox"/>
Unannounced	<input type="checkbox"/>
Justification	
By <i>pu NP</i>	
Distribution/	
Availability Codes	
Dist	Avail and/or Special
<i>A-1</i>	

**Abstract**

The southern Mid-Atlantic Ridge (MAR) is spreading at rates (34-38 mm/yr) that fall within a transitional range between rates that characterize slow and intermediate spreading center morphology. To further our understanding of crustal accretion at these transitional spreading rates, we have carried out analysis of magnetic anomaly data from two detailed SeaBeam surveys of the southern MAR between 25°-27°30'S and 31°-34°30' S. Using two-dimensional Fourier inversions of the magnetic data we establish the history of spreading for the past 5 my and the evolution of offset of the southern MAR at the both short and long-offset ridge-axis discontinuities in the area. The spreading histories of adjacent ridge segments differ in terms of the sense and amount of asymmetric spreading within each. These differences have given rise to changes in the offset lengths of the bounding ridge axis discontinuities. Short offsets of the MAR simultaneously changed length by approximately 10 km from 1 my to 4 my ago. During this same time period, offset of the MAR at larger offset fracture zones remained comparatively constant. Total opening rates within our northern survey area decreased during this time period, and we find evidence for rift propagation at 1.8 -2.5 my within both areas. A shift in plate motion circa anomaly 3 may have given rise to these changes. However, the pattern of offset variation we see is not simply related to the geometry of the plate boundary in these regions which precludes a simple relationship between plate motion changes and plate boundary response. We document a case of rapid (minimum 60 mm/yr) rift propagation, occurring between 2.5 and 1.8 my, associated with transition of the Moore transform fault to an oblique trending ridge-axis discontinuity. Total opening rates for adjacent segments differ by 10 % on average, and interval opening rates within a ridge segment differ from one part of the segment to another, implying significant non-rigid plate behavior. Magnetic polarity transition widths from our inversion studies may be used to infer a zone of crustal accretion which is 3-6 km wide, within the inner floor of the rift valley. A systematic increase of transition width with age would be expected if deeper crustal sources dominate the magnetic signal in older crust but this is not observed. We present initial results from three-dimensional analysis which shows magnetization highs at both large

and short offset discontinuities. Within the central anomaly the highs are up to 15 Amps/m compared with a background of approximately 8-10 A/m and they persist for at least 2.5 my. The highs may be caused by eruption of highly fractionated strongly magnetized basalts at ridge axis discontinuities with both large and small offsets.

### Introduction

Until the late 1970's, our understanding of how new oceanic crust is formed at divergent plate boundaries was interpreted largely from data collected along widely-spaced tracks with poor navigational control. Based on these data, crustal accretion was interpreted as a predominantly two-dimensional phenomena. The advent of high-resolution mapping systems and precision navigation, allowed for detailed surveys of several portions of the world mid-ocean ridge system. These studies have revealed considerably greater variability and complexity in ridge structure than was initially assumed, and from them, a three-dimensional model of crustal accretion has emerged. Understanding what controls variability in ridge structure has been key to understanding crustal generation at spreading centers.

First order variability in spreading center morphology depends upon total opening rate. At the fast spreading rates characteristic of the East Pacific Rise ( $>90$  mm/yr), a broad axial ridge or high marks the locus of crustal accretion, whereas at the slow spreading rates of the northern Mid-Atlantic Ridge (MAR) ( $<30$  mm/yr), a 1-2 km deep rift valley is nearly ubiquitous (Macdonald, 1982). At faster spreading (30-80 mm/yr), a very broad range in axial rift valley depths is found (Macdonald, 1986), and it appears that a critical transition between slow and intermediate spreading center morphological types lies within this range of spreading rates. The southern MAR is spreading at rates that lie at the lower end of this 'transitional range' (35-40 mm/yr). Until very recently no detailed studies of the southern MAR had been made, and we have had sparse information about what ridge crest morphology characterizes this critical part of the spreading rate spectrum.

During late 1984, early 1985, researchers at URI and UCSB conducted two Seabeam cruises aboard the R/V Thomas Washington to a section of the MAR from  $30^{\circ}$ - $38^{\circ}$ S. Dense and continuous coverage of the ridge axis was obtained from  $31^{\circ}$ - $34^{\circ}$ 30' S (Fig. 1). This was one of the largest detailed ridge surveys ever completed, and the first high-resolution bathymetric survey carried out in the South Atlantic. Two additional Seabeam expeditions to the South Atlantic were made during Nov/Dec 1986 and Feb/March 1987 aboard the R/V Robert Conrad (Fig. 1). These cruises, which represent a joint URI, NRL, LDGO, UCSB mapping effort, focused on a portion of the MAR from  $25^{\circ}$ - $27^{\circ}$ 30' S. During all four cruises, Seabeam bathymetric data, underway magnetic, gravity and seismic data were collected. In this paper we present results from two-dimensional analysis of the magnetic data collected during both ridge crest surveys as well as preliminary results from three-dimensional analysis for regions with dense magnetic data coverage. We have determined the detailed history of spreading and the evolution of all offsets of the MAR axis within both regions for the past approximately 5 my. We have been particularly interested in the behavior of small offsets of the spreading axis located within these survey areas and how this behavior compares with that of larger offset transform faults. We document independent spreading histories for individual ridge segments which have given rise to changing offset along the short discontinuities while longer discontinuities have remained comparatively constant in length. Detailed analysis of the gravity and bathymetric data collected in conjunction with the magnetic data has been carried out by other workers. Kuo and Forsyth (in press) present a three-dimensional analysis of the gravity data from the  $31$ - $34^{\circ}$ 30'S area. A detailed analysis of the morphology of the short offset discontinuities within both areas is presented in Grindlay et al. (this issue). Fox et al. (this issue) present a detailed discussion of bathymetric data from the  $31$ - $34^{\circ}$ S area as it pertains to segmentation of the southern MAR. In the following section, we briefly describe the morphology of the two regions.

### Morphology

Prior to our Seabeam work at 25-27°30' S and 31-34°30' S, virtually all detailed surveys of the MAR had taken place in the North Atlantic (e.g., work in the FAMOUS area (Phillips and Fleming, 1978); TAG area (Rona and Gray, 1980)). The only detailed studies of the southern MAR were a bathymetric and magnetic survey for 6-8°S (Van Andel and Heath, 1970), and an extensive aeromagnetic survey of the ridge from 8-18°S described by Brozena (1986). GEBCO bathymetric maps for the South Atlantic were constructed from sparse wide-beam echo-sounding data and earthquake locations, and assumptions that the morphology of the southern MAR would be much like that established for the well-studied northern MAR. Fig. 2 shows bathymetric maps for 25-27°30'S and 31-34°30'S compiled from the Seabeam bathymetric data. For these areas, the location of the South American-African plate boundary on the GEBCO chart is, in some places, over 50 km different from the position of the plate boundary identified with the Seabeam data. Furthermore, the morphology of the MAR in these regions is quite different from that observed in the North Atlantic. In both surveys areas, the rift valley which is nearly ubiquitous in the North Atlantic, shallows and narrows along strike to a subtly rifted axial bulge (e.g., 33°00' S and 26°00'S). At the shallowest mid-segment areas, the rift valley is subdued and the cross-sections are similar to those of the intermediate spreading centers, e.g., the East Pacific Rise at 21° N (Normark, 1976) or the Galapagos spreading center (Klitgord and Mudie, 1974). Also within both areas, in addition to classic ridge-perpendicular transform faults, the ridge is offset by short oblique-trending discontinuities of the ridge axis which correspond to first and second order discontinuities respectively in the classification of Macdonald et al., (1988). The absence of throughgoing ridge-perpendicular structures makes the short-offset second-order discontinuities quite distinct from most of those observed in the North Atlantic (e.g., Fracture Zone A in the FAMOUS area, Detrick et al., 1973) but similar to oblique shear zones like the Kurchatov offset (Searle and Laughton, 1977). Within this paper we will refer to first order discontinuities i.e. transform faults and their off-axis trace as fracture zones. For second order discontinuities we will use the term 'discordant zone' to refer to the combined on/off-axis trace. For the southern MAR, the active portion of the discordant zone will be referred to as an 'oblique shear zone' or 'en echelon jog' of the rift valley depending on morphology.

Within the survey area from  $31^{\circ}$ - $34^{\circ}30'$ S (Fig. 2a), the MAR is offset at the Cox and Meteor transform faults, and at four second order discontinuities located at  $31^{\circ}15'$ S,  $31^{\circ}25'$  S,  $32^{\circ}30'$  S and  $33^{\circ}30'$  S (Grindlay et al., this issue; Fox et al., this issue). These six discontinuities, all of which are right stepping offsets, subdivide the MAR into six ridge segments. Throughout this paper, we will refer to these segments as labelled in Fig. 2a; 1 through 6 consistent with other papers on the area, 'S' indicates the southern survey area. The Cox and Meteor transform faults, offset the ridge by 92 and 69 km respectively; at the  $32^{\circ}30'$ S and  $33^{\circ}30'$ S discontinuities the MAR axis is displaced by 25 and 30 km respectively. At the  $31^{\circ}15'$  S and  $31^{\circ}25'$  S discordant zones, the MAR is offset 14 km in total, 10 km of which is associated with the  $31^{\circ}15'$  S discordant zone. The axial trace of the  $31^{\circ}25'$ S discordant zone is negligible and we do not identify separate ridge segments on either side of it. At both transform faults in the survey area, we see narrow deep valleys oriented  $080^{\circ}$  that continue off axis within the inactive portion of these fracture zones. At the  $31^{\circ}15'$  S and  $33^{\circ}30'$  S discordant zones however, the MAR is offset by oblique trending basins, arranged en echelon at  $31^{\circ}15'$ S and  $\sim 45^{\circ}$  oblique to the MAR axis at  $33^{\circ}30'$ S, within which plate motion is largely accommodated by extension (Grindlay et al., this issue). At the resolution of Seabeam, there is no evidence for throughgoing ridge-perpendicular faults between the offset portions of the MAR. Although offset of the MAR at  $32^{\circ}30'$ S is comparable to that at the other second order discontinuities in the region, here we see a shallow throughgoing trough that may mark a zone of focussed strike-slip motion.

The Moore discontinuity, located within the  $25$ - $27^{\circ}30'$  S area, is at present, an oblique shear zone similar to the second order discontinuities within the southern survey area (Fig. 2b). Left-lateral displacement of the MAR at the Moore discontinuity has evolved from over 100 km during the Eocene, when it was a transform fault or first order discontinuity, to 9.5 km at the present (Cande et al., 1988). The Rio Grande transform fault, located 100 km north of the Moore shear zone, offsets the MAR by 41 km in a right step. The Moore and Rio Grande offsets subdivide the MAR in this region into three ridge segments labelled 1N to 3N (Fig. 2b); 'N' indicates the segment is located within the northern survey area.

## Magnetic Data

A compilation of the total field magnetic data for both survey areas is included in Fig. 3. All data were collected with a surface-towed proton precession magnetometer. For the 25-27°30' S area, tracklines 100-200 km long and spaced 6-8 km apart, provide dense magnetic coverage to anomaly 3' for much of the survey. Magnetic coverage in the southern survey area was obtained out to anomaly 3' time along tracks spaced ~15 km apart and ~150 km long. Average track spacing near the ridge axis is 4-6 km for both surveys, providing virtually continuous coverage in these regions. Survey lines are oriented both perpendicular (~E-W) and parallel (~N-S) to the ridge. Navigation, based on transit satellites and GPS when available, provides absolute positional accuracy of 250-500 m for these surveys. During Seabeam post-processing, positional accuracy is improved by shifting tracks in order to minimize cross-over errors for overlapping bathymetric swaths. After these navigation corrections, maximum cross-over errors in the total field magnetic data are < 10 nT.

The magnetic anomalies in our South Atlantic data (Fig. 3) can be identified with considerably greater ease than in the North Atlantic. Although spreading rates are less than twice those of the slow spreading North Atlantic, much of the detail we see in magnetic data from the fast spreading EPR can be identified. For example, the Jaramillo, an event rarely recognizable in North Atlantic magnetics is present along most profiles in both South Atlantic areas. Interestingly, anomalies are noticeably easier to identify within the 25-27°30' S area than from 31-34°30' S although spreading rates at 31-34°30' S are only 2-3% slower.

In order to improve the accuracy of spreading rate determinations, we have carried out two-dimensional inversions of the observed magnetic anomaly data along selected lines. We have used the two-dimensional Fourier inversion method of Parker and Huestis (1974). This method is an iterative procedure in which the observed anomalous field along a chosen profile is inverted in the presence of bathymetry to obtain a magnetization solution. The method removes from the observed data skewness, and the complicating effects of topography. Assumptions inherent in the technique are that the magnetization of the source layer is constant with depth and is oriented parallel to an axial

geocentric dipole field, that the upper surface of the magnetized source layer is the observed bathymetry, that this layer is of constant thickness, and has a geometry that only varies in a direction perpendicular to the ridge (i.e. is two-dimensional). To generate geologically reasonable solutions (one in which positive and negative anomalies away from anomaly one are approximately equal in amplitude), this modelling method makes use of the annihilator; the magnetization distribution for a given topography that will produce no external field. Any multiple of the annihilator can simply be added to the magnetization solution as needed to balance positive and negative anomaly amplitudes with no change in the computed field.

Magnetization solutions obtained for selected lines within each survey area are shown in Fig. 4. Only lines greater than 50 km in length were selected. Lines less than 10 km from a fracture zone were excluded from the analysis as the assumption of a two-dimensional geometry for the source layer is questionable in these regions. Prior to inversion, the magnetic field and Seabeam center beam bathymetric data along each profile were projected onto a ridge-perpendicular trend and resampled at 500 m intervals. The magnetization solutions in Fig. 4 have been back projected approximately onto the original tracklines by stretching the projected bathymetric profile to match the observed center beam data. For all inversions, a 1 km source layer thickness was assumed. The International Geomagnetic Reference Field 1980 (Peddie, 1982) was removed from the data for the northern area. The regional field, approximated by a best fit least-squares line was subtracted from each profile in the southern area. No annihilator was needed to obtain reasonable solutions for any of the profiles shown.

Bandpass filtering of the magnetization solution must be carried out after each iteration of the inversion procedure, as the inversion operator amplifies the short and long wavelengths of the magnetization spectrum. A bandpass filter with a cosine taper at the short wavelength end from 2.5 - 5.0 km and 3.0 to 6.0 km was used for the southern and northern areas respectively. For data from the northern area, a filter cut-off of 2.5 km allowed spurious short wavelength variation to remain in the solutions, and a longer cut-off wavelength of 3.0 km was required. The need for more filtering of the northern data possibly reflects reduced signal to noise ratio with proximity to the magnetic

equator due to both the greater frequency of magnetic storms, and the reduced field amplitude measured at the earth's surface. The long wavelength filter parameters were set at the profile length (~150 km) for data from the southern area. In the northern area, long-wavelength filtering using an cosine taper from 100 km improved the quality of the solutions for lines greater than 100 km in length and resulted in no long-wavelength filtering of the shorter lines.

### Spreading Rates

Using the reversal time scale of Ness et al. (1980), anomalies are identified from the magnetization solutions and spreading rates measured perpendicular to the ridge for each anomaly interval. We assume that the beginning and end of all anomaly intervals except anomaly 2 and the Jaramillo, correspond with the location of half the peak to trough distance defining the edges of the identified anomaly. For anomaly 2 and the Jaramillo, due to their short duration, we assume the peak amplitude associated with these anomalies corresponds to the middle of these epochs. Rates are not calculated for anomaly intervals less than 0.25 my in duration. Interval half opening rates, averaged over all magnetization profiles within each ridge segment are indicated in Fig. 4. These spreading rates represent the average rate along the length of the ridge segment for the duration of the anomaly interval. Due to the short length of segment 3S, and its resultant proximity to a fracture/discordant zone along its length, two-dimensional analysis is not appropriate for this segment. As a result, we do not present spreading rates for ridge segment 3S, and the evolution of the 32°30' S offset is included with that of the Cox fracture zone. Sources of error in spreading rates measurements include navigation, uncertainties in the raw magnetic data, the reversal time scale, and in anomaly identification and measurement. Assuming anomaly identifications are correct and rigid plate behavior, errors estimated by the average standard deviation of interval spreading rates are +/- 2 mm/yr. The range in standard deviations for interval half rates is large (0.1 to 5.1 mm/yr), the largest standard deviations correspond to anomaly intervals during which we can document intra-segment rift propagation as will be discussed below.

Half spreading rates, determined for the total time elapsed from each reversal to the present, are given in Table 1. The locus of present-day crustal accretion, or the neovolcanic zone, is identified from the bathymetry and local highs in the magnetization distribution. Errors associated with these measurements are smaller than for interval half rates as we are averaging over successively larger time periods ( $\pm 0.5$  mm/yr one standard deviation).

Variation with time in interval half spreading rates is shown in Fig. 5. For each ridge segment, these rates vary from one anomaly interval to the next by 3-4 mm/yr on average, and as much as 10 mm/yr between some time periods. On the time scale of the individual anomaly intervals measured over (0.8 my average duration), spreading within each ridge segment has generally been asymmetric and the sense of asymmetry has not remained constant. However, for half spreading rates averaged over time periods greater than  $\sim 1$  my in duration, the same sense of asymmetry has been maintained within the entire northern area and within ridge segments 1S, 4S, and 5S (Table 1). Within the northern area, the sense and degree of asymmetric spreading across adjacent ridge segments has been that required to reduce offset of the MAR at both discontinuities (11 km at the Moore and 8.5 km at the Rio Grande fracture zones), and within the southern area, to increase offset at the  $31^{\circ}15'S$  discordant zone to 14 km, reduce offset at  $33^{\circ}30'S$  by 13 km, and maintain the offset lengths of the Cox and Meteor transform faults (Fig. 6).

Total opening rates for each anomaly interval are plotted in Fig. 7. Within all ridge segments, rates for successive intervals do not vary monotonically. However, from  $25-27^{\circ}30'S$ , full spreading rates overall, decreased between anomalies 4' and 2 time by 20-30%. Full rates since the Jaramillo have increased. A similar pattern is seen only for segment 2S within  $31-34^{\circ}30'S$ , although data coverage is less extensive within this area. Brozena (1986), using the time scale of LaBrecque et al. (1977), reports a decrease in spreading rates for 8-18 S, of more than 25% over a similar time period from anomaly 4 to 2, and acceleration since 2 my. When evaluating changes in total opening rates, it is important to consider that correlated changes in opening rates may actually reflect errors in the anomaly time scale. Differences between the LaBrecque et al. (1977) timescale and that of Ness et al. (1980) used in this study are small for 0-5 my.

Within each anomaly interval, full spreading rates for adjacent ridge segments differ by 3.7 mm/yr on average ( $\sim 10\%$ ), and during several time periods by more than 6 mm/yr (Fig. 7). Full spreading rates along the length of a spreading center are expected to decrease with decreasing distance to the pole of rotation for the two bounding plate. Using the Minster and Jordan (1978) pole of rotation for the South American/African plates, we expect spreading rates within our survey areas to decrease by  $\pm 0.1 - 0.2$  mm/yr over  $1^\circ$  of latitude. This variation is one order of magnitude smaller than the variation we see in interval spreading rates. Errors in interval spreading rates are large ( $\pm 2$  mm/yr one standard deviation), however, for several time periods the variation we see between adjacent segments is well outside these errors (e.g., segment 2N compared with 3N for intervals 2-2' and 3-3'). Such large differences in full spreading rates across adjacent ridge segments suggests intraplate deformation (e.g., intra-segment rift propagation or non-rigid behavior) during these time intervals. In contrast to these results for interval full rates, for rates averaged beyond anomaly 2 (Table 1), differences between adjacent ridge segments are less than 2.0 mm/yr (average difference 0.8 mm/yr) indicating that over these longer time scales the South American-African plates behave rigidly.

#### Transition Widths

Magnetic polarity transition widths, corresponding to the distance over which 90% of the change in magnetic polarity occurs (Atwater and Mudie, 1973) were measured from magnetization solutions for both survey areas. Polarity transitions are recorded within a finite width of ocean crust which reflects primarily effects of crustal extension, spreading throughout the time it takes for the field to reverse, and crustal accretion and alteration processes. Crustal accretion processes that give rise to finite transition widths include lava flows extending significant distances from their feeder dikes and burying older flows, the intrusion of dikes over a finite distance from the spreading center, and accretion of the gabbroic layer. We measured transition widths from magnetization solutions projected perpendicular to the ridge, and only for widely spaced reversals. For shorter magnetic

events, the magnetized layer produced may not be uniformly magnetized at any time during the event and a better estimate of transition widths are obtained from looking at anomaly shape, and amplitude compared with adjacent anomalies (Atwater and Mudie, 1973; Macdonald, 1977).

The mean transition widths are 4.0 km ( $\pm 1.4$  km one standard deviation), and 3.7  $\pm 1.5$  km for the 25-27°S and 31-34°S areas respectively (Table 2). Although we were expecting that transition widths within the northern area might be slightly narrower than in the southern area, given that anomalies are comparatively easier to identify, we in fact measured slightly wider transitions in this area. The difference between the two areas is however, small and probably not significant. Transition widths are shorter for the beginning of the central anomaly within the northern area, which may in fact, reflect the greater clarity of the anomalies generally.

Transition widths vary from one interval to the next (Table 2), but not in any systematic manner. We do not see any overall increase with age as might be expected from progressive sea-floor weathering of the magnetized layer. The highest transition widths measured are within the 25-27°S area for the end of 3' on both flanks of the ridge, the beginning of 3 on the east flank, and the end of 2' on the west flank within both areas. Larger transition widths on average during these intervals could reflect times of intraplate rift propagation (see discussion).

We can obtain an estimate for the width of the zone of crustal emplacement from measured transition widths by subtracting the width of crust produced during spreading throughout the reversal, and the amount of crustal stretching due to extension. Assuming it takes approximately 10,000 yrs for the field to reverse, at a half spreading rate of 17.5 mm/yr, 175 m of crust would be created. Assuming extension rates in the South Atlantic comparable to those in the North Atlantic FAMOUS area (~ 15% average for both flanks, Macdonald and Luyendyk, 1977), over a 4 km strip of crust, ~600 m of the width would be due to extension. Subtracting then 775 m from the measured transition widths we obtain averages of 3.3 km and 2.9 km for the two survey areas, which presumably reflect the width of the zone of crustal formation. There is some debate as to whether the measured transition width corresponds to one half the width of the crustal emplacement zone or is equal to it

(Atwater and Mudie, 1973; Macdonald, 1977; Shouten and Denham, 1979). Regardless, we can estimate an upper bound on the average width of the crustal emplacement zone of 6.5 km and 5.9 km.

Blakely and Lynn (1977) measured transition widths from surface tow magnetic data collected over ridges spreading at different rates, and concluded that transition width increases with increasing spreading rate. In contrast, Sempere et al. (1987), based on an analysis of Deep Tow data, found that transition widths may decrease slightly with increasing spreading rate. They concluded however, that the more significant change in transition width with spreading rate is a reduction in the range of widths measured with increasing spreading rate. Although it may be inappropriate to compare transition widths determined from Deep Tow data with those from surface tow data due to the differing resolution of the two data types, the range in transition widths we measure (1-8 km) and the average transition width (3.1 km) are comparable to that found in the FAMOUS area in the North Atlantic using Deep Tow data (Macdonald, 1977). Miller (1977) carries out a comparison, based on spectral analysis, of upward continued Deep-Tow data with surface tow data and finds an excellent match for wavelengths greater than 4 km. The transition widths we measure are close to this critical wavelength and hence comparison with North Atlantic Deep Tow-derived transition widths is not wholly inappropriate.

#### **High Amplitude Magnetic Anomalies**

In the anomalous magnetic field (Fig. 3) we see variation along strike in the magnitude of magnetic anomalies with the largest magnetic anomalies observed located at ridge-transform/shear zone intersections. Highly magnetized rocks have been dredged at propagating ridge tips and at ridge-transform intersections where they are assumed to reflect fractionation within the distal ends of a shallow magma chamber (Sinton et al., 1983; Sempere et al., 1988). We are currently carrying out three-dimensional analysis of the magnetic data in order to precisely locate these high amplitude anomalies and assess their possible association with a geochemical source. We use a three-dimensional approach because we are interested in magnetization variations adjacent to

fracture/discordant zones where topography is such that a two-dimensional assumption is inappropriate. The three-dimensional procedure we use is a direct extension of the two-dimensional Fourier inversion method of Parker and Huestis (1974) (see Macdonald et al., 1980 for details). We will present the bulk of our results in a later paper but include here a three-dimensional inversion solution for the Cox fracture zone and 33°30'S discordant zone (Fig. 8).

There are two features of particular interest in the magnetization distribution. One is that high magnetizations located adjacent to the 33°30'S oblique shear zone are as large as those found at the Cox transform fault. At both discontinuities, local magnetization highs reach 15 Amps/m compared with an 8-10 Amps/m average magnetization for the central anomaly. Variations in the magnetization solution may in fact reflect deviations in actual crustal thickness from the constant thickness assumed, e.g., high magnetizations could reflect local crustal thickening. It is unlikely however that the high magnetizations we observe at the ridge-discontinuity intersections are due to crustal thickening. Gravity modelling for 31°-34°30' S (Kuo and Forsyth, 1989) indicates the crust is actually 1-3 km thinner beneath the 33°30'S discordant zone, in which case, the amplitude of the magnetization highs observed represents a lower bound on actual magnitude.

A second interesting feature is that local magnetization highs are observed off-axis adjacent to both the Cox fracture zone and the 33°30' S discordant zone, indicating that these highly magnetized zones persist with age. Magnetizations locally up to 2-6 Amps/m greater than the average magnetization for the polarity interval can be identified in some places beyond anomaly 2'.

#### Intra-Segment Rift Propagation

A close look at magnetic anomalies indicates a rift propagation 'event' occurred within segment 2N 1.8 to 2.5 my ago (i.e., between anomaly 2 and 2'). For ~40 km north of the Moore discontinuity, the negative anomaly between anomaly 2 and 2' widens toward the fracture zone on both flanks of the ridge. Furthermore, anomaly 2' on the eastern flank is incomplete, and there are positive peaks within the 2-2' interval on the west flank that cannot be identified in the anomaly time scale. It appears then, that within this region, crust of anomaly 2' age has been transferred from the

east flank to the west. These observations all indicate rift propagation within segment 2N between anomaly 2 and 2' time. Corresponding to the time of this rift propagation 'event', the morphology of the Moore discontinuity changes abruptly ~ 40 km off-axis from a broad zone of ridge-parallel fabric at anomalous depths, to a classic ridge-perpendicular fracture zone valley (Fig. 2b; see Grindlay et al., this issue). The change in morphology is marked by a 7 km wide ridge on the west flank which rises 1000-1500 m, and a valley on the east flank both aligned approximately parallel to the present ridge axis. The ridge and corresponding valley that cross-cut the Moore fracture zone may be the bathymetric remnants of this rift propagation 'event'.

There are two possible scenarios for propagation within segment 2N. The valley on the east flank could be the fossil trace of propagation from the north within segment 2N that cut outside of the eastern rift valley wall, rafting it off to the west and shortening offset on the Moore discontinuity. In this scenario, the rafted rift valley wall would correspond to the ridge on the west flank. Alternately, the ridge on the west flank may be the remnant of propagation from segment 3N across the Moore fracture zone (Grindlay et al., this issue). We cannot determine a propagation rate for this event as we do not have direct evidence of the propagation (i.e. pseudofaults). However, from the N-S extent over which the end of anomaly 2' is disturbed, and assuming the event occurred between anomalies 2' and 2, we can determine a minimum propagation rate of 60 mm/yr, approximately 50% faster than the total opening rate at this time. At present, the Moore shear zone is located ~ 12 km north of its fracture zone trace prior to the end of 2' time, indicating that it has recently migrated north at a minimum rate of 5 mm/yr. The swath of sea floor disrupted by the Moore discontinuity since 2' is much wider than that prior to this time (Fig 2b), and the Moore shear zone may have since migrated both north and south within this zone. There is some evidence for intraplate deformation/propagation during this same time period north of the Rio Grande transform fault. Here we see a reentrant into oceanic crust between anomaly 2 and 2' age that is associated with large amplitude magnetic anomalies (Figs 2b and 3b).

Full spreading rates averaged over the ridge segment north of the Moore discontinuity are 6 mm/yr faster than south of it during 2-2' (Fig. 7). As noted earlier this difference is much greater

than the errors in our measurements and the change in spreading rate we expect to see with change in proximity to the plate pole of rotation. Simultaneous spreading within segment 2N, at the propagating rift in addition to at the prior location of spreading (hence an 'overlapping' geometry) could account for this difference in full spreading rates between segment 2N and 3N.

There are similar indications of rift propagation occurring between 2' and the Jaramillo in the vicinity of the  $33^{\circ}30'$  S discordant zone. Anomalies 2 and 2-2' north of this discontinuity are disturbed and hard to identify for roughly 35-40 km. Full spreading rates between 2 and 2' time are 10 mm/yr faster north of this discordant zone than south of it. Furthermore, there is a change in discordant zone morphology at  $\sim 2.5$  my from more narrowly focussed ridge-perpendicular structure to a broader zone of disrupted terrain (Grindlay et al., this issue). In the vicinity of the  $31^{\circ}15'$  S discordant zone, there is some evidence in the bathymetric data for rift propagation. Here we see a prominent north-south ridge of 0.72-0.94 my in age, that cross-cuts a ridge-perpendicular valley within the  $31^{\circ}15'$  S discordant zone, very similar in morphology to the ridge cross-cutting the Moore fracture zone. This ridge may be the morphological remnant of rift propagation from the north. Alternatively, this ridge may be a rift valley wall remnant which cross-cuts the  $31^{\circ}15'$  discordant zone due to a recent southward shift of the discontinuity. Although current offset at  $31^{\circ}25'$  S is negligible, there is a north-pointing v-shaped distribution of both bathymetric lows and magnetic highs (Figs. 2a and 3a) centered about  $31^{\circ}25'$  S indicating northward migration of this short discordant zone at a rate of  $\sim 20$  mm/yr over the past 2.5 my. Overall, the evidence for rift propagation within the southern area is not as compelling as that within the northern area. However, the clear evidence at the Moore discontinuity lends credence to the interpretation of similar features in the magnetic and bathymetric data of the southern area as intraplate rift propagation.

#### Changing offset distances at discontinuities

From the isochron locations shown in Fig. 4, we have reconstructed the history of offset of the MAR along each of the surveyed discontinuities (Fig. 9). As noted earlier, the evolution of the oblique shear zone at  $32^{\circ}30'$  S cannot be well resolved with two-dimensional analysis of our magnetic

data and we have included offset due to this feature with evolution of the Cox fracture zone. Similarly the evolution of the  $31^{\circ}25'$  S discordant zone cannot be distinguished from that of the  $31^{\circ}15'$  S discordant zone and we include offset at this discontinuity with the  $31^{\circ}15'$  discordant zone. The offset of isochrons at a ridge-axis discontinuity, measured on the east and west flanks of the ridge should be the same assuming rigid plate behavior. However, for several time periods, east and west offsets differ by more than 4 km (Fig. 9). The largest difference observed (12 km) is for the  $31^{\circ}15'$  S discordant zone at the beginning of anomaly 3. During this time, isochron offset on the east flank was close to 0 km but in the opposite sense to that observed at all subsequent times on both flanks, and to the sense of offset at this same time on the west flank. Although we do not have data beyond this time, it is likely that this behavior reflects the initiation of the  $31^{\circ}15'$  S discordant zone. The discrepancies between east and west isochron offsets at the Cox fracture zone are up to 4.5 km and probably reflect lack of control on the evolution of the  $32^{\circ}30'$  S discordant zone. Most other differences in east and west isochron offsets occur during time periods when the lengths of the ridge discontinuities were changing (see below) and may correspond to intraplate rift propagation and associated non-rigid behavior outlined earlier.

Average offset of isochrons for which we have data on both flanks of the ridge, are plotted for all discontinuities in Fig. 10. To emphasize how the lengths of these first and second order discontinuities have varied through time, the mean offset for each discontinuity has been removed and all are plotted together (Fig. 10). From these plots we see that all discordant zones within both survey areas and the Rio Grande fracture zone changed in length over approximately the same time period. Between 4 and 1 my, the Moore, Rio Grande, and  $33^{\circ}30'$  discontinuities shortened in length while offset of the MAR at the  $31^{\circ}15'$  discordant zone grew. At all four locations, the change in offset of the MAR was on the order of 10 km. Unlike these smaller-offset discontinuities, the length of the Cox- $32^{\circ}30'$  S fracture zone remained approximately constant. That the combined average offset at the Cox and  $32^{\circ}30'$  S discontinuities has remained constant implies that the  $32^{\circ}30'$  S discontinuity is actually a part of the greater Cox transform fault and hence it may be inappropriate to consider the short region (segment 3S) between these two discontinuities as an independent ridge segment. Its behavior

may be controlled primarily by tectonics within the Cox transform domain just as are the small pull-aparts which have briefly evolved into spreading centers near  $14^{\circ}\text{W}$  (Fox et al., this issue). At the Meteor fracture zone, we only have data beyond anomaly 2 for the east flank. Based on these data, the Meteor shortened and lengthened from 5 to 1 my, so that its present length is approximately the same as that 6 my ago. Offset of the MAR at the Moore discontinuity has been comparatively constant since and prior to the period of change from 2-4 my. The length of the  $31^{\circ}15'\text{S}$  discordant zone has also been essentially constant for the past 2 my. The rate of change in length at all discordant zones has been continuous at the scale of 0.8 my intervals at  $\sim 7$  km/my. This rate of change could easily be accomplished by small rift jumps within the 10-20 km wide inner rift valley floor.

### Discussion

What causes offset length variability?

The temporal instability of offset length at second order discontinuities may be a direct response to changes in plate motion or alternatively, adjacent ridge segments may have relatively independent spreading histories giving rise to offset variations. There are indications of a change in plate motion prior to the period of change in length of the discordant zones we have studied. Cande et al. (1988) determined one pole of rotation for the South American-African plates for the past 9 my. However, Grindlay et al. (this issue) have modelled isochrons and fracture zone orientations for  $31^{\circ}-34^{\circ}30'\text{S}$  and  $25^{\circ}-27^{\circ}30'\text{S}$  and find a best fit pole requires a slight change in plate orientation at anomaly 3 time ( $\sim 4.7$  my). Van Andel and Moore (1970) found a discontinuity in spreading rates at  $7^{\circ}-8^{\circ}\text{S}$  near anomaly 3 time. Offset of the MAR at  $31^{\circ}15'\text{S}$  appears to have initiated just prior to anomaly 3 time. Rift propagation may accompany plate reorganization (e.g. Hey et al., 1986). Brozena (1986) reports a period of ridge/fracture zone modification within  $8^{\circ}-18^{\circ}\text{S}$  between 4 and 3 my that includes rift propagation into 8 my crust. More recent propagation, during anomaly 2'-2, occurred at the Moore discontinuity and within segment 4S. Although the timing of all the events outlined above are not identical, they are roughly synchronous with the period of change in discordant zone offset from

4my to 1 my, and a causal relationship is implied i.e., plate motion changes may give rise to variation in the offset lengths of ridge axis discontinuities.

The evolution of fracture zones within 8-18°S reported by Brozena (1986), is remarkably similar to that found for our study area (Fig. 11). Short offset fracture zones within this area systematically shortened or lengthened within the past 10 my (e.g., Fig. 11, fracture zones C, B', and A). Change in the length of each discontinuity was on the order of 10 km, and was contemporaneous with changes in total opening rates. The similarity in the magnitude of fracture zone length change within 8-18°S and our survey areas to the south suggests coupling between these ridge segments and readjustment of the plate boundary along this length to a similar driving force. Fracture zones within 8-18°S were changing length well before the period of change we see in our survey areas. However, this difference may reflect a finite response time of ridge segments to changes in plate motion. Given the geometry of the plate boundary at 8-18°S, the offset variation observed since anomaly 4 time is that expected for a clockwise rotation of the spreading axis. One clockwise rotation will not however, account for the evolution of the fracture zones and discordant zones within either the 25-27°30'S or 31-34°30'S survey areas. The 33°30' S and 31°15'S discordant zones are both right stepping, but one has grown while the other has decreased in length. The Rio Grande and Moore discontinuities are right and left stepping respectively, yet both have shortened in length. The geometry and evolution of these two offsets is such that continued reduction in length will eventually result in a throughgoing MAR and evolution toward such a minimum energy configuration may be a mechanism contributing to temporal variability in the offset length of some discordant/fracture zones (Lachenbruch, 1976).

Brozena (1986) concludes that the plate boundary from 8-18°S has evolved in response to shifts in plate motion with the fragmentation and rotation of ridge segments between fracture zones. There is evidence for a shift in plate motion since ~ 5 my (anomaly 3 time) and we do see subsequent offset variation of approximately the same magnitude at several locations. However, as one rotation of the spreading axis would not generate the offset variability seen at 25-27°30' S and 31-34°30' S, we conclude that individual ridge segments may respond independently to changes in plate motion giving rise to discordant/fracture zone length variability.

Also of interest is the apparent difference in the length stability of first and second order discontinuities. Assuming rigid plate behavior, changes in plate motion would be expected to be accommodated by systematic shortening/lengthening of transform faults. As the age contrast in oceanic lithosphere across second order discontinuities is minimal, it is reasonable to expect that deformation associated with a reorganization of the plate boundary could more easily be accommodated across these features than large offset transform faults. This expectation is supported by the greater length stability observed for the long transform faults (> 80 km) both at 31-34°30' S and at 8-18°S (Figs. 10 and 11). Over the time period studied, the transform fault at 12°S (presently 82 km in length), and the Cox transform fault have changed little in length (+/-3 km). The Meteor transform fault, which has changed length but at present (69 km) has roughly the same length as 6 my ago, may lie within some transitional range between transform faults with considerable length stability (>80 km) and those (<50 km) that readily change length over time. (It is important to note here, that although these data indicate large offset fracture zones are more stable on the time scale of 5-10 my, over longer time periods this stability is not maintained. The Moore fracture zone has evolved from an offset length of over 100 km during the Eocene, similar to the present-day lengths of the larger offset transform faults studied.)

Why is the magnetic signal so large at small discontinuities?

Oblique shear zones located within our study area are associated with surprisingly large magnetic and structural signals; comparable in magnitude to those observed at transform faults. Our three-dimensional analysis of the magnetic data (Fig. 8) shows that magnetization highs located at the 33°30'S discordant zone are as large as those observed at the Cox ridge-transform intersection. Fox and Gallo (1984) suggest that much of the change observed in ridge morphology as a transform fault is approached can be explained in terms of the 'cold edge effect' generated by the age contrast in crust across the transform fault. Clearly at the oblique shear zones in the South Atlantic, this effect should be reduced and we would expect to see a more subdued bathymetric expression than at transform faults. We do not see this. Indeed the nodal basins at the 33°30' shear zone are deeper than

the deepest parts of the Meteor transform fault (Grindlay et al. in prep). The high inside corners located at this discordant zone are as large as those observed at either the Cox or Meteor transform faults (Severinghaus and Macdonald, 1988). Furthermore, crust is disturbed over a wider swath of sea floor at all second order discontinuities than at the 69 km long Meteor transform fault. The traces of second order discontinuities located on fast spreading ridges (i.e. overlapping spreading centers on the East Pacific Rise) are also associated with surprisingly large disruptions of the magnetic anomalies and bathymetry given the very small age offset ( $< 0.1$  my) across them (Macdonald et al., 1988).

The southern MAR appears segmented on two distinct scales, one defined by transform faults (first order discontinuities) spaced more than 100 km apart, and a second shorter segmentation interval of 50-100 km marked by the occurrence of discordant zones (second order discontinuities). Several authors have suggested that MAR segmentation on the finer scale may reflect segmentation of mantle upwelling (Crane, 1985; Whitehead et al., 1984). Macdonald et al. (1984) suggest that the morphology and existence of overlapping spreading centers on the East Pacific Rise results from along axis variation in the magmatic budget. They propose a model in which overlapping spreading centers are located at the distal ends of centers of magma supply from which magma migrates laterally along axis. Presumably, the distal ends of these upwelling centers receive a reduced magma supply giving rise to a colder thermal regime and possibly thinner crust. Similar along axis variation in magmatic budget may account for the large magnetic, geochemical and morphologic signals at second order discontinuities of the southern MAR. A reduced magma supply near the end points of each segment may result in short-lived transient magma chambers whose eruptive products become highly fractionated and strongly magnetized (eg. Sinton et al., 1983).

#### **The independence of spreading histories for adjacent ridge segments**

Our study of the magnetic data indicate independent spreading histories for adjacent ridge segments in terms of the sense and degree of asymmetric spreading and differences in total opening rates for adjacent ridge segments. This relative independence of spreading may reflect significant

decoupling in the magmatic source region for adjacent ridge segments. This view is supported by the work of Kuo and Forsyth (1989) from their determination of the mantle Bouguer anomaly for the 31-34°30'S area. To emphasize deviations from normal oceanic lithospheric structure, they have subtracted from the mantle Bouguer anomaly the effects of density variations in the upper mantle due to a passive flow model of spreading. The resulting residual anomalies show anomaly highs associated with the traces of the three discordant zones at 31°15' S, 32°30' S, and 33°30' S, indicating crustal thinning and/or lower mantle temperatures in these regions. The residual anomaly is most pronounced for the 33°30' S discordant zone, and they infer that, for the past 4 my, crust produced at this discontinuity is 1-3 km thinner than adjacent seafloor. In addition, they find a distinct "bull's eye" mantle Bouguer low centered on the shallow part of ridge segment 4S, which may reflect a local plume-like region of mantle upwelling or significant crustal thinning away from this region. Both of these results suggest that magma supply, which controls crustal thickness, is variable along this portion of the southern MAR and in particular, is significantly reduced at second order discontinuities. The morphology of the southern MAR rift valley within segment 2N shallows and narrows along strike similar to the shallowing within segment 4S. The v-shaped distribution of off-axis highs centered about the shallowest part of the ridge suggests this shallow region has persisted and has migrated along the strike of the ridge. Petrologic studies of axial basalts dredged from segment 2N indicate a deep central supply beneath this ridge segment, although they do not support along axis melt migration from a central supply toward the ends of this ridge segment (Batiza et al., 1988).

Schouten and White (1980), based on a study of variable offset discontinuities in the North Atlantic, suggest that these discontinuities separate the northern MAR into distinct spreading cells which respond independently to changes in relative plate motion and which remain stable in location over long time periods (at least 15 my). They postulate a thermal memory, associated with anomalous crust generated at fracture zones, that maintains the stable system of spreading cells even though offset at the bounding discontinuities is highly variable and can disappear altogether. In contrast to Schouten and White (1980), our data show that small-offset discontinuities can migrate slowly along

strike ( e.g., recent migration at the Moore and 31°25' discordant zones), although other discordant zones studied have remained spatially stable (e.g., at 33°30' S and 32°30' S).

#### **Causes of intrasegment propagation**

Intrasegment rift propagation at the Moore discontinuity is associated with change in morphology from well defined ridge-perpendicular structure to a wider diffuse zone of more oblique-trending and ridge-parallel fabric. Propagation occurred when the length of the Moore discontinuity was ~15 km, corresponding to an age contrast in lithosphere across this feature of < 1.0 my. Propagation occurred through the 31°15' S shear zone when its offset was ~14 km and at 33°30' S when its length was ~37 km. Presumably as age contrast across a discontinuity decreases the probability of propagation across it into the thin weak lithosphere on the opposite side increases. Phipps Morgan and Parmentier (1985) suggest that rift propagation is driven by gravitational forces associated with elevation gradients along the ridge axis. These elevation gradients may reflect along axis magma supply (higher regions corresponding to upwelling centers) implying rift propagation due to along-axis magmatic variability. Alternatively, rift propagation may occur in response to changes in plate motion. There is some evidence as outlined earlier, for a change in plate motion circa anomaly 3. Propagation 'events' occurred more recently and were simultaneous at 33°30' S and at the Moore discontinuity. Propagation at 31°15' S however, was not contemporaneous with these events, and both the 31°25' S and Moore discordant zones have migrated north along axis more or less continuously since anomaly 2. During a period of fracture zone/ridge reorientation from anomaly 3 to 2 time, Brozena (1986) reports a ridge jump or propagation into 8 my old crust across the fracture zone located at 17° S. This propagation required the establishment of a new transform fault within cold thick lithosphere ~50 km north of its former location and Brozena (1986) concludes this reorganization of the plate boundary must have been a response to a forcing mechanism like a change in plate motion. Based on the temporal relationship between several of the propagation 'events' outlined above, it is likely that intrasegment propagation within our study area is related to

changes in plate motion. However, magmatic variability in the rate of magma supply and a reduced age contrast across a ridge discontinuity are also indicated as possible causes.

#### **Rigid vs non-rigid behavior**

On a regional scale and over long time periods, the southern MAR plate boundary clearly behaves rigidly. Full spreading rates within 8-18°S and 25-27°30' S, spanning 20° show the same pattern of change through time for the past 8 my. Discordant zones along this boundary have simultaneously changed length along at least 10° of the ridge (from 25-27°30' S and 31-34°30' S). These changes may have occurred in response to a minor change in pole of opening for the southern MAR circa anomaly 3 time. On the time scale of polarity epochs and spatial scale of ridge segments however, our data implies significant non-rigid behavior at the southern MAR. Significant differences in total interval opening rates between adjacent ridge segments (10% on average, Fig. 7) imply non-rigid behavior, as do differences in interval half spreading rates within a ridge segment, reflected in the deviation of isochrons in Fig. 4 from straight and parallel lines (on the order of 10%). The largest differences observed in both interval half rates within a segment (e.g. up to 100% along the end of anomaly 2' isochron within segment 2N) and total opening rates between segments ( e.g. 20% between segments 2N and 3N for anomaly 2-2') correspond to the period of rift propagation at the Moore and 33°30' S discontinuities. However, those differences (on the order of 10 %) not clearly related to propagation events imply intraplate deformation. Le Douaran et. al. (1982) find changes in interval total opening rates along the northern MAR from 14° to 35°N that exceed the changes predicted by the Minster and Jordan (1978) pole for the North American-African plates. When they average over longer time periods than an anomaly interval these changes in total opening rates along the ridge diminish to fit the rigid plate model. They interpret their results, which are similar to ours, as reflecting non-rigid behavior occurring on the time scale of polarity epochs. It seems unlikely that far field stresses predicted from the slab pull hypothesis could be variable enough in time and space to account for this result. Perhaps a more likely explanation for these variations is a local source of increased total opening rate within an individual spreading segment either by means of crustal

extension due to faulting, variable resistance to spreading due to frictional or visco dynamic effects, or due to variable rates of magma supply and volcanism. These processes might vary on the time scale of 0.8 my (the average duration of the magnetic anomaly intervals examined in this study) or less and on the spatial scale of a ridge segment (Pockalny et al., 1988). The degree of non-rigid behavior is not unreasonable. For example, if all of the non-rigid behavior is accommodated by amagmatic extension, only 10% extension is needed in most cases. These rates of extension are within the bounds of studies in the FAMOUS area (Macdonald and Luyendyk, 1977), the Kane area (Pockalny et al., 1988; Karson et al., 1987) and the Josephine ophiolite (Norrell and Harper, 1988).

### Conclusions

Interval spreading rates, which reflect the stability through time of the spreading process, indicate that spreading within each ridge segment has been asymmetric with the sense of asymmetry often changing from one interval (~0.8 my duration) to the next. Averaged over longer time periods (>1.0 my) however, the sense of asymmetry has generally remained the same. Full interval spreading rates for adjacent ridge segments differ by 10 % on average. These differences, which exceed our measurement errors and are substantially more than the expected change with changing proximity to the pole of rotation for the South American and African plates, may reflect non-rigid behavior. Total opening rates from 25-27°30' S have decreased by 20-30% from anomaly 4' to 2 time. Full rates since the Jaramillo have increased. We see this same pattern for only one ridge segment within 31-34°30' S, although our data coverage here is less extensive. The changes in spreading rates we see may be of global significance or may point to significant errors in the anomaly time scale.

Magnetization highs of comparable magnitude are located at both the large offset Cox fracture zone and short offset 33°30' S discordant zone-ridge intersections. These magnetization highs persist off axis and can be traced in places beyond anomaly 2'.

Within the past 10.0 my, the Moore transform fault has evolved from a classic ridge-perpendicular feature with an offset of over 25 km to an oblique-trending second order ridge-axis

discontinuity 9.5 km in length. The change occurred between 2.5 and 1.8 my and involved a rift propagation 'event' which transferred crust of anomaly 2-2' time from the east to west flank of the ridge. Since that time, the Moore discontinuity has migrated north approximately 12 km. Although less clear, there is evidence for rift propagation 'events' during the same time interval in the vicinity of the 33°30'S discontinuity and since anomaly 2 time at the 31°15'S discontinuity.

Discordant zones within both survey areas have systematically lengthened or shortened by 10 km during the time interval from 1 my to 4 my while larger-offset fracture zones have remained comparatively constant in length. Changing offset along these short-offset discontinuities may be a mechanism by which the plate boundary responds to changes in plate motion. However, the sense in which the length of each offset has evolved (i.e. lengthening or shortening) is not simply related to the sense of offset (i.e. right or left lateral) across each discontinuity, and could not reflect one simple adjustment of the entire plate boundary in this region to a change in the direction of plate opening. Individual ridge segments within our study area have independent spreading histories in that the amount and sense of asymmetric spreading and total opening rates for adjacent ridge segments differ. Independent spreading histories may reflect significant decoupling in the mantle source region for these ridge segments and we conclude that ridge segments may respond independently to changes in plate motion giving rise to discordant zone length variability.

#### Acknowledgments

We thank S. P. Miller for assistance with the magnetic modelling. P. Vogt, S. C. Cande and P. J. Fox conducted the 1986/87 Seabeam surveys, and we thank them for comments and discussion. We thank N. Grindlay for providing the shifted Seabeam bathymetric compilations. We also thank L. J. Perram, D. Blackman and other students who provided their assistance at sea. A. Padgett and W. Borst drafted the figures. This study was supported by grants from the Office of Naval Research (contracts N00014-84-K-0523 and N00014-87-K-0152)

## References

- Atwater, T. M. and Mudie, J. D., 1973, Detailed Near-Bottom Geophysical Study of the Gorda Rise, *J. Geophys. Res.* 78, 8665-8686.
- Batiza, R. Melson, W. G., and O'Hearn, T., 1988, Simple Magma Supply Geometry Inferred Beneath a Segment of the Mid-Atlantic Ridge, *Nature* 335, 428-431.
- Blakely, R. J., and Lynn, W. S., 1977, Reversal Transition Widths and Fast Spreading Centers, *Earth Planet. Sci. Lett.* 33, 321-330.
- Brozena, J. M., 1986, Temporal and Spatial Variability of Seafloor Spreading Processes in the Northern South Atlantic, *J. Geophys. Res.* 91, 497-510.
- Cande, S. C., LaBrecque, J. L., and Haxby, W. F., 1988, Plate Kinematics of the South Atlantic: Chron C34 to Present, *J. Geophys. Res.*, 93, 13,479-13,492.
- Crane, K., 1985, The Spacing of Rift Axis Highs: Dependence upon Diapiric Processes in the Underlying Lithosphere?, *Earth Planet. Sci. Lett.* 72, 405-414.
- Detrick, R. S., Mudie, J. D., Luyendyk, B. P., and Macdonald, K. C., 1973, Near Bottom Observations of an Active Transform Fault (Mid-Atlantic Ridge at 37°N), *Nature* 246, 59-61.
- Fox, P. J., et al., The Mid-Atlantic Ridge (31 S - 34 S): Temporal and Spatial Variations of Accretionary Processes, in prep. for this issue, *Marine Geophys. Res.*
- Fox, P. J., and Gallo, D. G., 1984, A Tectonic Model for Ridge-Transform-Ridge Plate Boundaries: Implications for the Structure of Oceanic Lithosphere, *Tectonophysics* 104, 205-242.
- GEBCO - General Bathymetric Chart of the Oceans, South Atlantic Chart, 1978, Canadian Hydrographic Service, Ottawa, Ont.
- Grindlay et al., in prep for this issue, *Marine Geophys. Res.*
- Heirtzler, J. R., 1985, *Relief of the Surface of the Earth, Report MGG-2*, published by National Geophysical Data Center, Boulder, Co.
- Hey, R. N., Kleinrock, M., Miller, S. P., Atwater, T., and Searle, R. C., 1986, Seabeam/Deep Tow investigation of an active Oceanic Propagating Rift System, *J. Geophys. Res.* 91, 3369-3393.
- Karson, J. A., Thompson, G., Humphris, S. E., Edmond, J. M., Bryan, W. B., Brown, J. R., Winters, A. T., Pockalny, R. A., Casey, J. F., Campbell, A. C., Klinkhammer, G., Palmer, M. R., Kinzler, R. J., Sulanowska, M. M., 1987, Along-Axis Variations in Seafloor Spreading in the MARK Area, *Nature* 328, 681-685.
- Klitgord, K. D., and Mudie, J. D., 1974, The Galapagos Spreading Center: A Near Bottom Geophysical Survey, *Geophys. J. R. Astron. Soc.* 38, 536-586.
- Kuo, B.-Y., and Forsyth, D. W., 1989, Gravity Anomalies of the Ridge-Transform System in the South Atlantic Between 31 and 34.5 S: Upwelling Centers and Variations in Crustal Thickness, *Marine Geophys. Res.* (in press).
- Lachenbruch, A. H., 1976, Dynamics of Passive Spreading Centers, *J. Geophys. Res.* 81, 1883-1902.

- LaBrecque, J. L., Kent, D. V., and Cande, S. C., 1977, Revised Magnetic Polarity Time Scale for the Late Cretaceous and Cenozoic Time, *Geology* 5, 330-335.
- Le Douaran, S., Needham, H. D., and Francheteau, J., 1982, Pattern of Opening Rates Along the axis of the Mid-Atlantic Ridge, *Nature* 300, 254-257.
- Macdonald, K. C., 1977, Near-Bottom Magnetic Anomalies, Asymmetric Spreading, Oblique Spreading, and Tectonics of the Mid-Atlantic Ridge near lat 37° N, *Geol. Soc. Am. Bull.* 88, 541-555.
- Macdonald, K. C., and Luyendyk, B. P., 1977, Deep-tow Studies of the Structure of the Mid-Atlantic Ridge Crest near 37° N, *Geol. Soc. Am. Bull.* 88, 621-636.
- Macdonald, K. C., Miller, S. P., Huestis, S. P., and Speiss, F. N., 1980, Three-Dimensional Modelling of a Magnetic Reversal Boundary from Inversion of Deep-Tow Measurements, *J. Geophys. Res.* 85, 3760-3780.
- Macdonald, K. C., 1982, Mid Ocean Ridges: Fine Scale Tectonic, Volcanic and Hydrothermal Processes within the Plate Boundary Zone, *Ann. Rev. Earth and Plan. Sci. Lett.* 10, 155-190.
- Macdonald, K. C., Sempere, J.C. and Fox, P. J., 1984, East Pacific Rise from Siqueiros to Orozco Fracture Zones: Along-Strike Continuity of Axial Neovolcanic Zone and Structure and Evolution of Overlapping Spreading Centers, *J. Geophys Res.* 89, 6049-6069.
- Macdonald, K. C., 1986, The Crest of the Mid-Atlantic Ridge: Models for Crustal Generation Processes and Tectonics, *The Geology of North America M*, 51-68.
- Macdonald, K. C., Fox, P. J., Perram, L. J., Eisen, M. F., Haymon, R. M., Miller, S. P., Carbotte, S. M., Cormier, M.-H., and Shor, A. N., 1988, A new View of the Mid-Ocean Ridge from the Behavior of Ridge-Axis Discontinuities, *Nature* 335, 217-225.
- Miller, S. P., 1977, The Validity of the Geologic Interpretation of Marine Magnetic Anomalies, *Geophys. J. R. Astron. Soc.* 50, 1-22.
- Minster, J. B., and Jordan, T. H., 1978, Present-day Plate Motions, *J. Geophys. Res.* 83, 5331-5354.
- Ness, G., Levi, S., and Couch, R., 1980, Marine Magnetic Anomaly Timescales for the Cenozoic and Late Cretaceous: A Precip, Critique, and Synthesis, *Rev. Geophys. Space Phys.* 18, 753-770.
- Normark, W. R., 1976, Delineation of the Main Extrusive Zone of the East Pacific Rise at Lat. 21°N, *Geology* 4, 681-685.
- Norrell, G. T., and Harper, G. D., 1988, Detachment Faulting and Amagmatic Extension at Mid-Ocean Ridges: the Josephine Ophiolite as an Example, *Geology* 16, 827-834.
- Parker, R. L., and Huestis S. P., 1974, The Inversion of Magnetic Anomalies in the Presence of Topography, *J. Geophys. Res.* 79, 1587-1593.
- Phillips, J. D., and Fleming, H. S., 1978, Multi-Beam Sonar Study of the Mid-Atlantic Rift Valley 36-37°N: FAMOUS, *Geological Society of America*, MC-19.
- Phipps Morgan, J., and Parmentier, E. M., 1985, Causes and Rate-Limiting Mechanisms of Ridge Propagation: A Fracture Mechanics Model, *J. Geophys. Res.* 90, 8603-8612.

- Pockalny, R. A., Detrick, R. S., and Fox, P. J., 1988, Morphology and Tectonics of the Kane Fracture Zone from Seabeam Bathymetry Data, *J. Geophys. Res.* 93, 3179-3193.
- Peddie, N. W., 1982, International Geomagnetic Reference Field 1980, *Geophysics* 47, 841-842.
- Rona, P. A., and Gray, D. F., 1980, Structural Behavior of Fracture Zones Symmetric and Asymmetric about a Spreading Axis: Mid-Atlantic Ridge (latitude 23°N to 27°N), *Geological Society of America Bull.* 91, 485-494.
- Schouten, H., and Denham C. R., 1979, Modeling the Oceanic Magnetic Source Layer, in *Deep Drilling Results in the Atlantic Ocean: Ocean Crust, Maurice Ewing Ser.*, vol. 2, ed. by M. Talwani, C. G. Harrison, and D. E. Hayes, 151-159.
- Schouten, H., and White, R. S., 1980, Zero-Offset Fracture Zones, *Geology* 8, 175-179.
- Searle, R. C., and Laughton, A. S., 1977, Sonar Studies of Mid-Atlantic Ridge and Kurchatov Fracture Zone, *J. Geophys. Res.* 82, 5313-5328.
- Sempere, J.-C., Macdonald, K.C., and Miller, S. P. 1987, Detailed Study of the Brunhes/Matuyama Reversal Boundary on the East Pacific Rise at 19°30'S: Implications for Crustal Emplacement Processes at an Ultra Fast Spreading Center, *Marine Geophys. Res.*, 9, 1-23.
- Sempere, J.-C., Meshkov, A., Thommeret, M., Macdonald, K. C., 1988, Magnetic Properties of Some Young Basalts from the East Pacific Rise, *Marine Geophys. Res.* 9, 131-146.
- Severinghaus, J. P., and Macdonald, K. C., 1988, High Inside Corners at Ridge-Transform Intersections, *Marine Geophys. Res.* 9, 353-367.
- Sinton, J. M., Wilson, D. S., Christie, D. M., Hey, R. N., and Delaney, J. R., 1983, Petrologic Consequences of Rift Propagation on Oceanic Spreading Ridges, *Earth Planet. Sci. Lett.* 62, 193-207.
- Van Andel, T. H., and Heath, G. R., 1970, Tectonics of the Mid-Atlantic Ridge, 60-80 South Latitude, *Marine Geophys. Res.* 1, 5-36.
- Van Andel, T. H., and Moore, T. C., 1970, Magnetic Anomalies and Seafloor Spreading Rates in the Northern South Atlantic, *Nature* 226, 328-330.
- Whitehead, Jr., J. A., Dick, H. J. B., and Schouten, H. 1984, A Mechanism for Magmatic Accretion Under Spreading Centers, 312, 146-147.

## Figure Captions

**Figure 1.** Location of the detailed ridge crest surveys superimposed on shaded relief seafloor map (Heirtzler, 1985).

**Figure 2.** Seabeam bathymetry for a) 31-34°30' S and b) 25-27°30' S. All ridge segments are labelled as referred to in the text. Bathymetric data has been gridded at 1 km grid spacing and recontoured. Contour interval 250 m, grey level change 500 m. See Fox et al., this issue and Grindlay et al., this issue, for complete bathymetric maps and discussion of their significance. Note the variation in fracture/discordant zone morphology in these areas.

**Figure 3.** Magnetic anomaly field for a) 31-34°30' S and b) 25-27°30' S. The anomalous field is contoured at 100 nT intervals. Negative anomalies are shaded. Track line control is indicated with small dashes at contour crossings. To obtain the anomalous field, a best fit plane to the regional field is removed for the 31-34°30' S area. For the 25-27°30' S area, a best fit plane to the IGRF 1980 is removed.

**Figure 4.** Magnetization solutions for a) 31-34°30' S and b) 25-27°30' S. Small numbers give average interval half spreading rate within a ridge segment, as determined from magnetization solutions projected perpendicular to the ridge axis. Solutions shown here are back-projected approximately onto the original track lines. Due to the short duration of the J to 1 interval, interval spreading rates given are from 2 to 1. Small dots show the location along each track, of all anomaly picks used for spreading rates determinations. Picks from magnetization solutions in addition to those shown here are included. Anomaly picks determine isochron locations, which are shown in medium line. Disruption of anomalies 2-2', and 2' within segment 2N reflects an intra-segment rift propagation 'event' that has left bathymetric remnants which cross-cut the Moore discordant zone. The deviation of other isochrons from straight and parallel lines may reflect non-rigid behavior within a ridge segment.

**Figure 5.** Histograms of interval half spreading rates for each ridge segment. Rates for the eastern flank of the MAR are shown with dashed line, and for the western flank, with solid line. Graphs show significant asymmetric spreading within each ridge segment, the magnitude and sense of which has varied over time. Differences in asymmetric spreading for adjacent ridge segments have given rise to variable offset on bounding discordant zones and indicate independent spreading histories for adjacent ridge segments.

**Figure 6.** Schematic diagram of the plate boundary showing average half spreading rates for the past ~ 4 my (i.e. since the end of anomaly 3 time) for all ridge segments except 6S. Rates for segment 6S are for ~ 2 my (i.e. since anomaly 2 time), due to more limited data coverage. Averaged over these time periods, spreading within ridge segments 1S, 4S, and 5S and all segments in the 25-27°30' S area, has been asymmetric with the same sense of asymmetry maintained. Note that the sense of asymmetry has been that required to reduce offset of the MAR along both fracture zones within the northern area, reduce offset at 33°30' S, increase the offset length of the 31°15' S discordant zone, and maintain the offset lengths of the Cox and Meteor transform faults.

**Figure 7.** Histograms showing variation with time in full interval spreading rates for each ridge segment. Although rates for successive intervals do not vary monotonically, we see a general pattern of total opening rates decreasing from 4' to 2 time by 20-30% for ridge segments 2N, 3N and 2S. We do not see this pattern for other ridge segments, although data coverage is less extensive. Of particular note are the large differences during some anomaly intervals in full rates for adjacent ridge segments. The largest differences may correspond to times of intra-segment propagation, however the smaller more pervasive differences imply a degree of intraplate deformation.

**Figure 8.** Three-dimensional inversion solution for the Cox fracture zone and  $33^{\circ}30'S$  discordant zone. Contours of magnetization are every 1 Amps/m. Small arrows identify local magnetization highs which are found at ridge-discardant/fracture zone intersections. Note that the magnitude of these highs is the same at both discontinuities although ridge offset at these discontinuities are much different. These magnetization highs also persist off-axis adjacent to the discordant/fracture zone traces.

**Figure 9.** Offset of isochrons at each ridge-axis discontinuity plotted as a function of time. Data from the east and west flanks of the ridge are plotted separately. Isochron offset lengths on each side of the ridge, which should be the same assuming rigid plate behavior, differ by 1 to 12 km. East and west differences at the Cox- $32^{\circ}30'S$  fracture zone may reflect lack of control on the  $32^{\circ}30'S$  discordant zone. Differences at the Moore and  $33^{\circ}30'S$  discordant zones may reflect intrasegment propagation and those at  $31^{\circ}15'S$  may reflect initiation of this offset. Isochrons were located using a best fit line to anomaly picks with a minimum rotation between adjacent lines.

**Figure 10.** Comparison of isochron offset histories for a) short-offset discontinuities and b) the larger offset fracture zones. For each discontinuity, the offset of isochrons on both flanks of the ridge are averaged, and the mean offset removed. Plots show that short-offset discontinuities have changed in length by approximately the same amount (10 km) over approximately the same time period (1 my to 4 my) while the Cox and Meteor fracture zones have remained comparatively constant in length. Changing offset at second-order discontinuities may be a mechanism by which the plate boundary responds to changes in plate motion.

**Figure 11.** Fracture zone offset vs time for fracture zones located between  $8-18^{\circ}S$  (from Brozena, 1986). As we observe in our survey areas to the south, short-offset discontinuities (FZ A, FZ C, and FZ B') have changed length while the larger offset FZ B has maintained its length. Fracture zones have changed length over a longer time period than observed in our area (8 my compared with 4 my), but the magnitude of offset changes are comparable. Due to the geometry of the plate boundary in the regions studied, and due to some discrepancy in timing, we cannot simply attribute fracture zone offset variability along this entire length of the southern MAR ( $8-34^{\circ}30'S$ ) to a change in the plate pole of rotation, although the consistent magnitude of offset change and the simultaneity of change within our southern areas do support a causal relationship.

**Table 1** Half spreading rates within each ridge segment, for total time elapsed from each reversal to present. Rates indicate constant asymmetric spreading with the sense of asymmetry maintained for rates averaged beyond the Jaramillo.

**Table 2.** Transition widths measured for widely spaced reversals. 'n' indicates the number of magnetization solution profiles measured for each reversal average. Average of the interval transition widths and one standard deviation are given for each survey area.

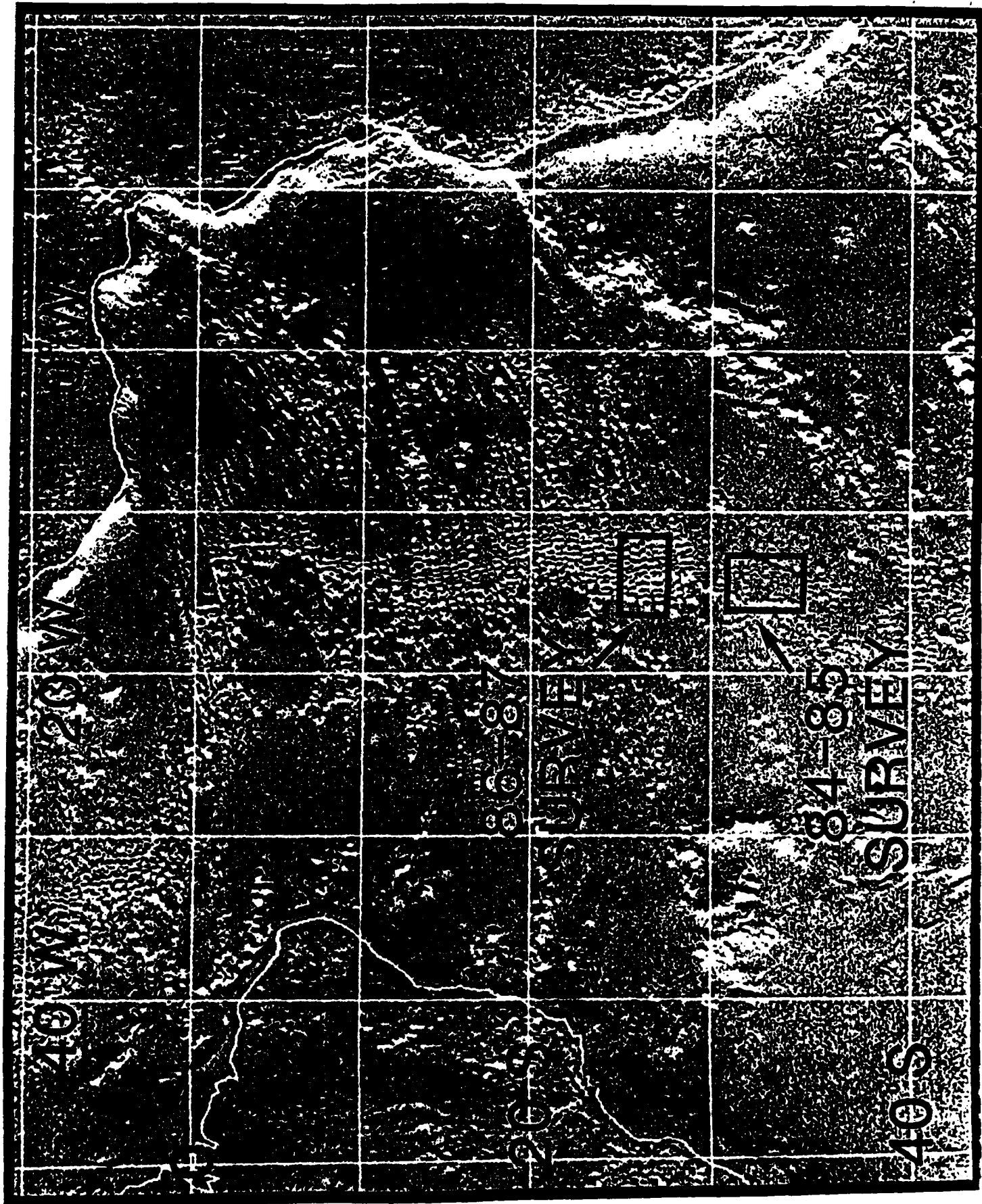


Fig. 1

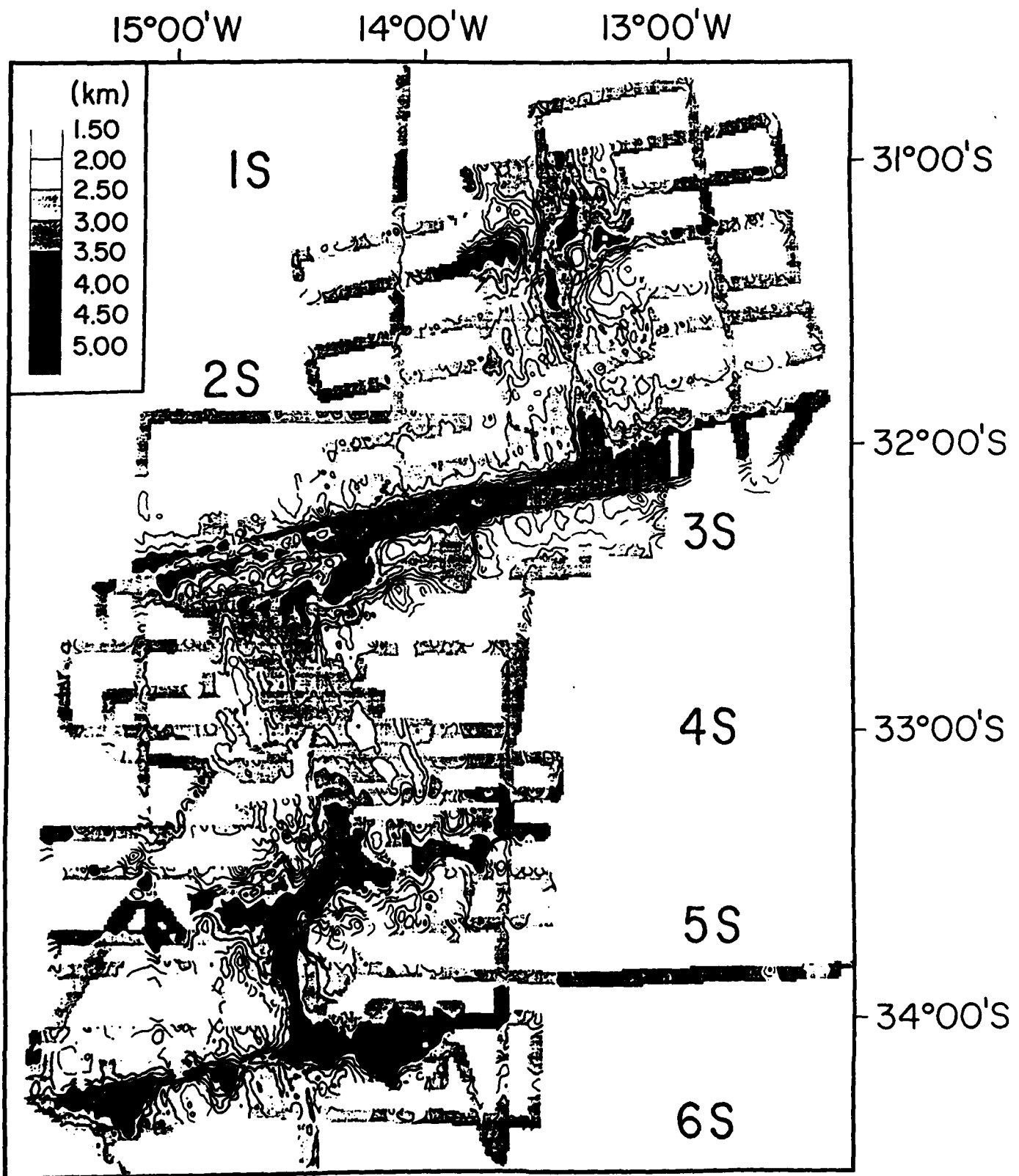


Fig. 2a

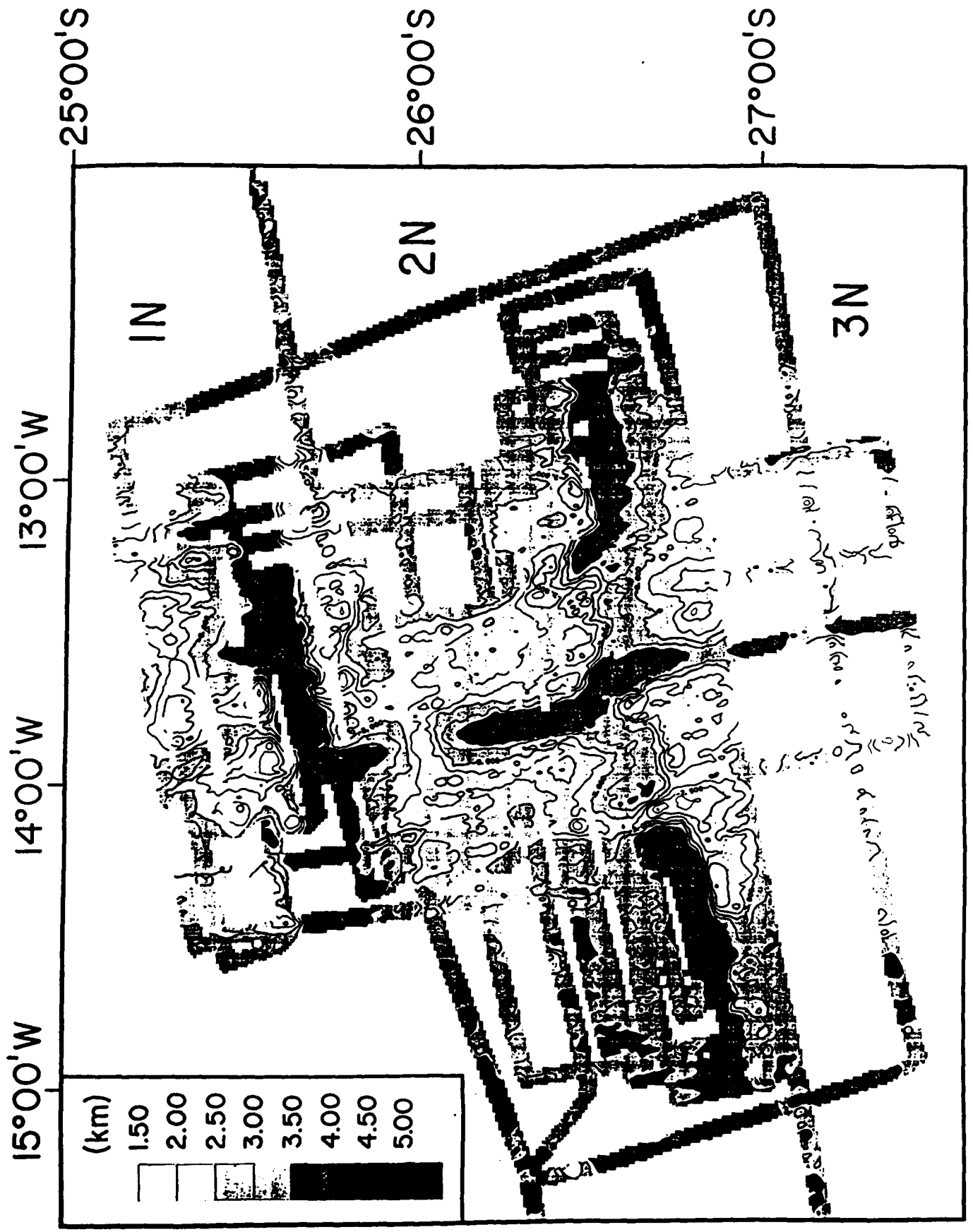


Fig. 2b

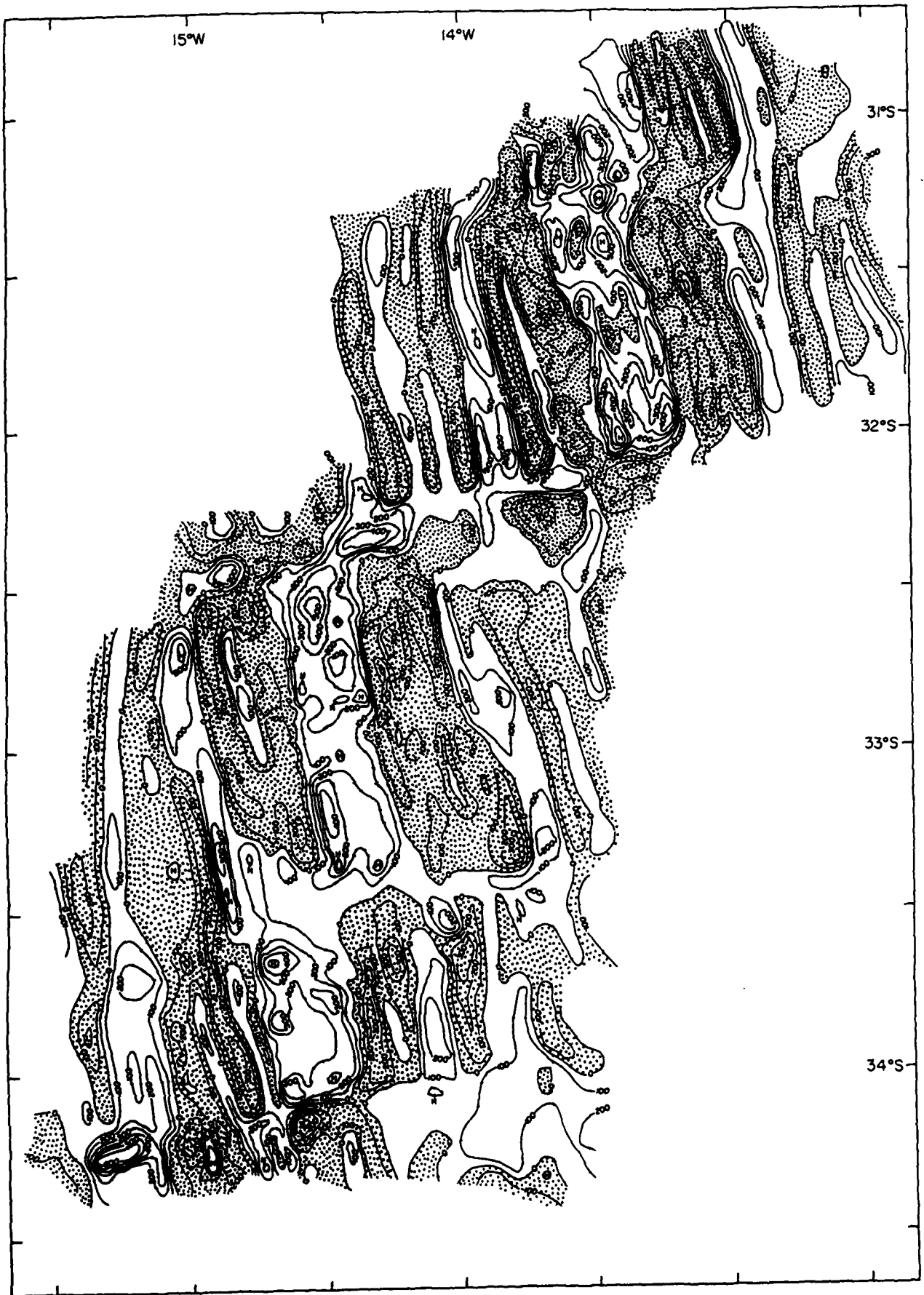


Fig. 3a

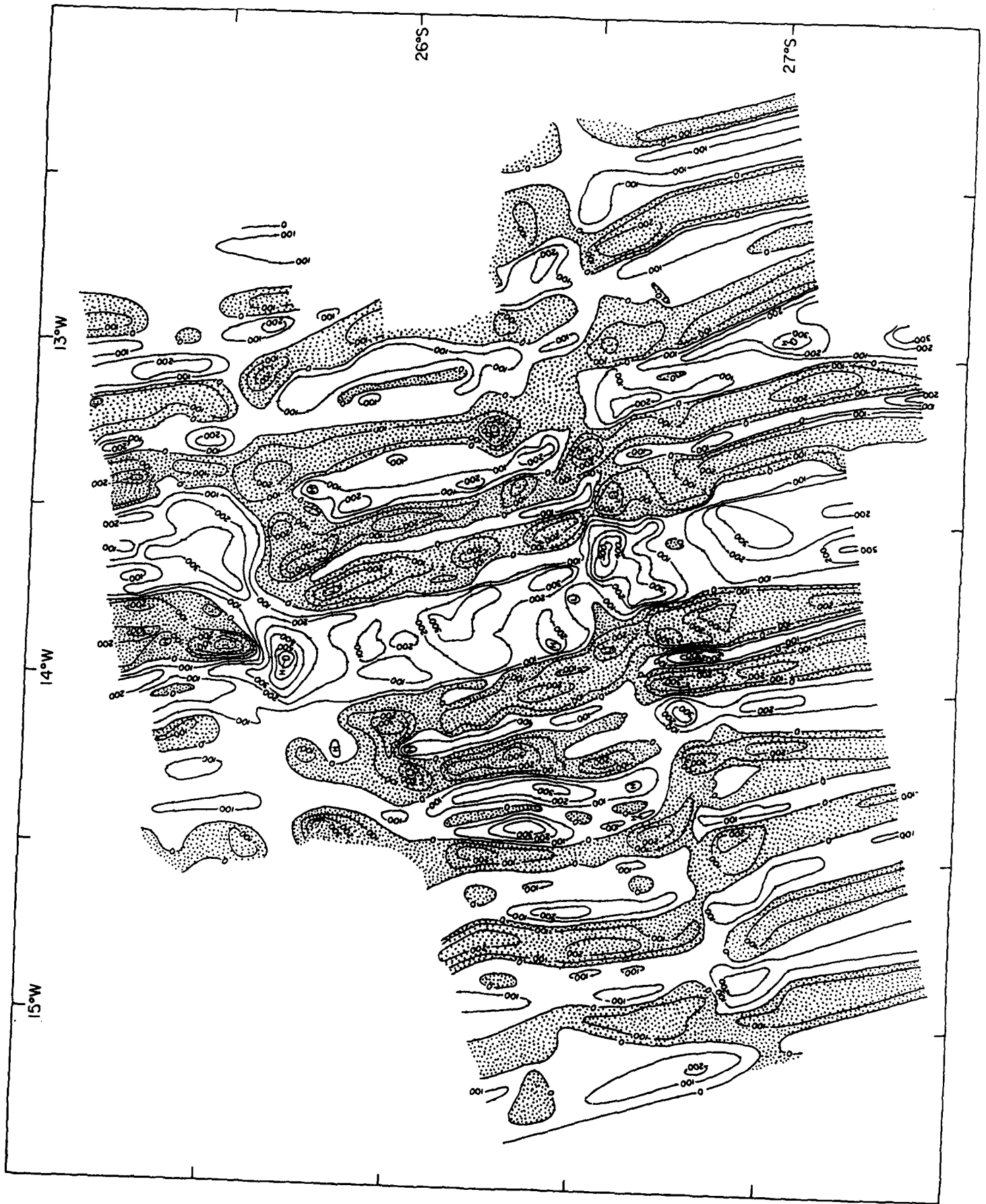


Fig. 3b

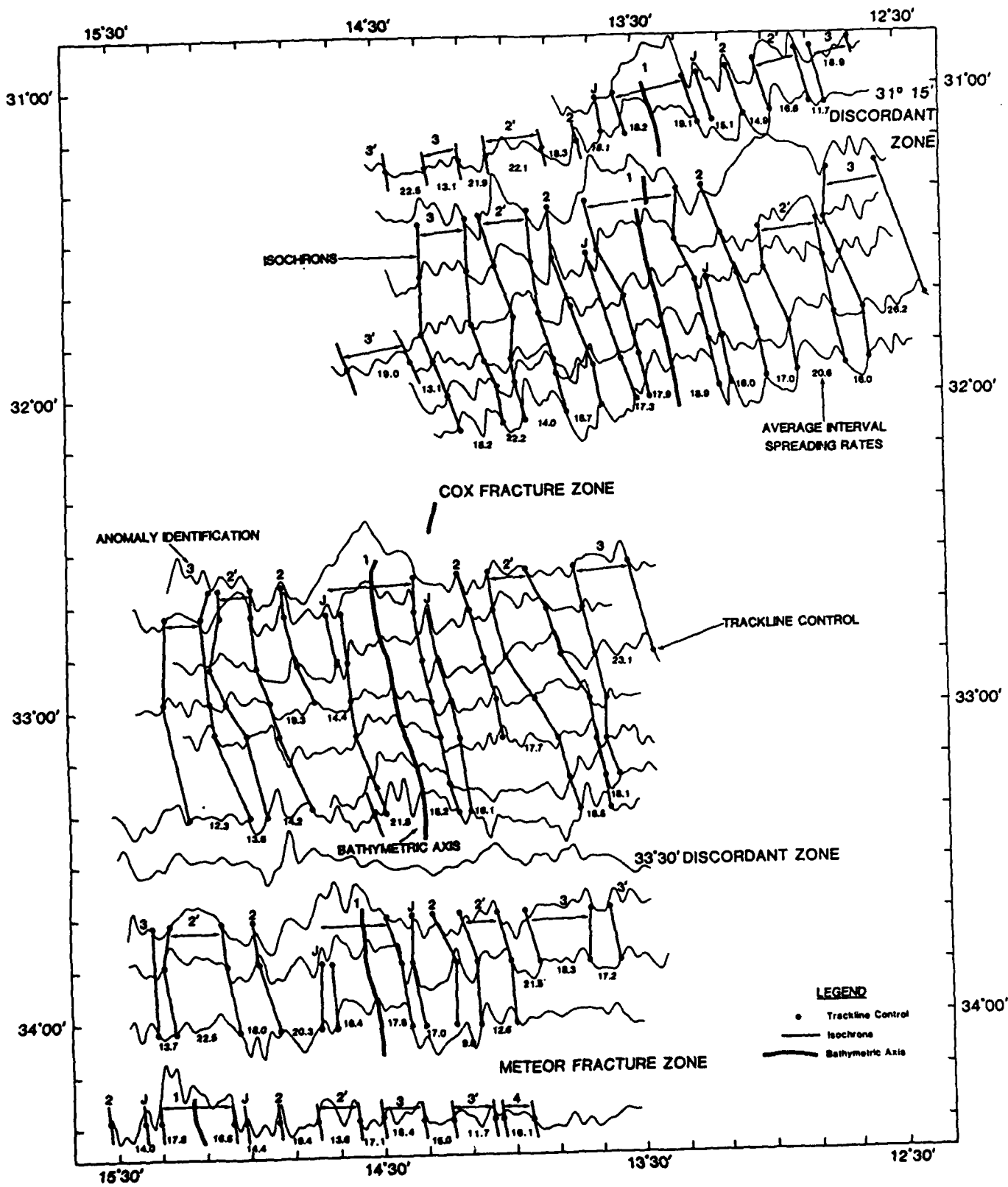
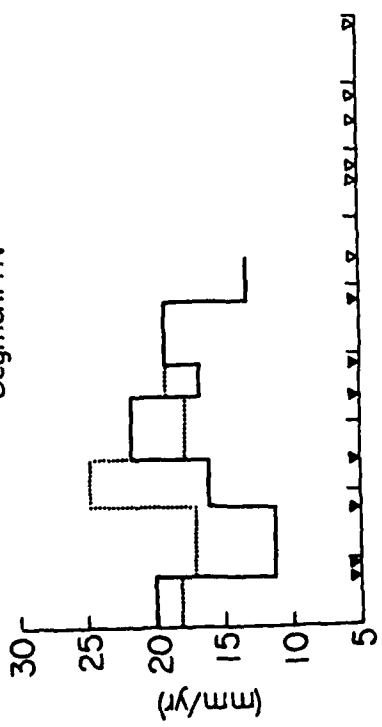


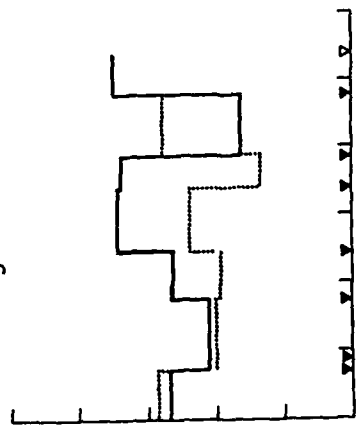
Fig. 4a



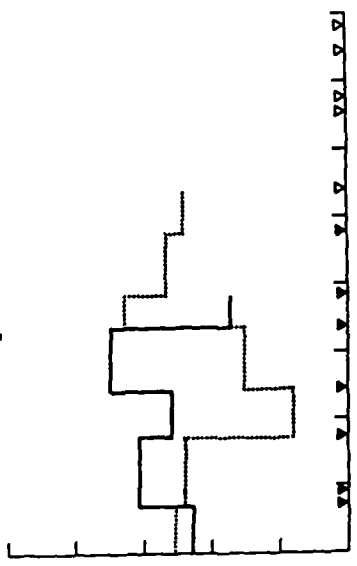
Segment 1 N



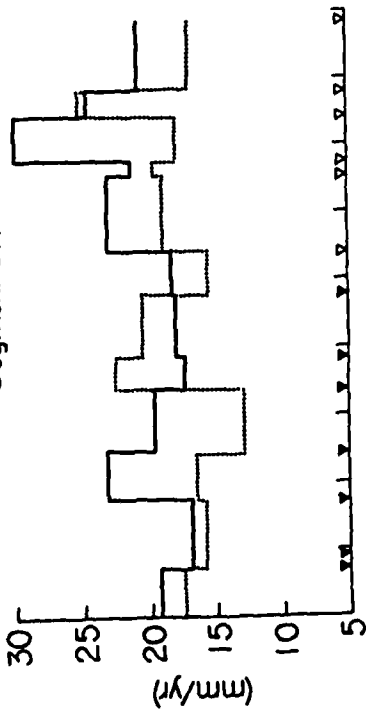
Segment 1 S



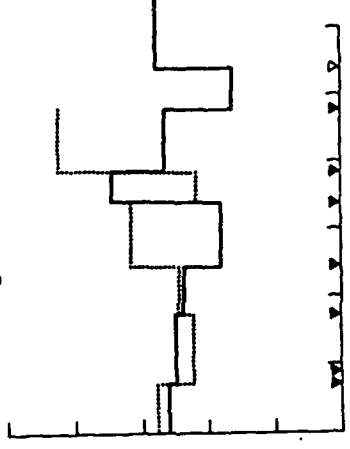
Segment 5 S



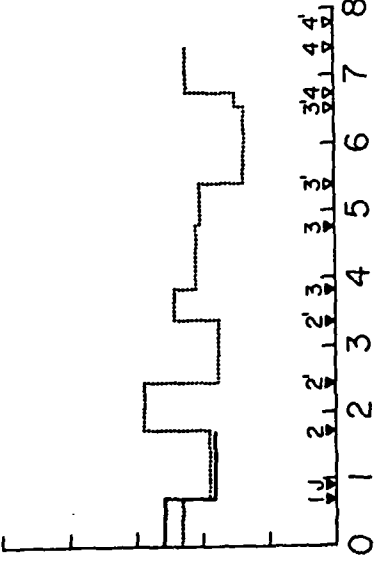
Segment 2 N



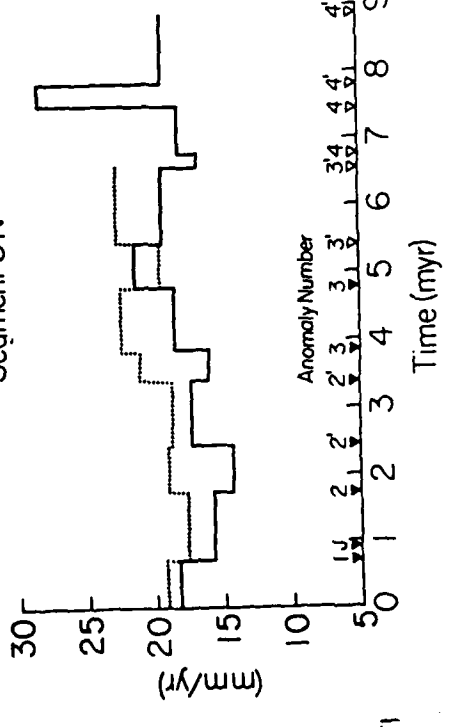
Segment 2 S



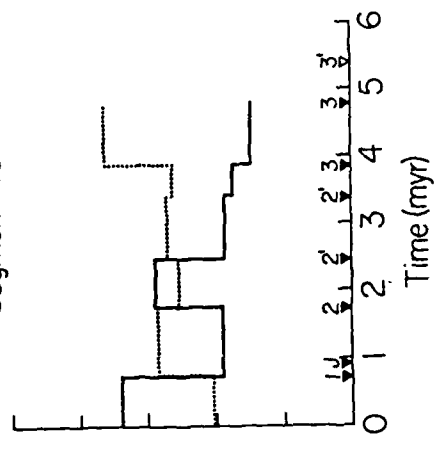
Segment 6 S



Segment 3 N



Segment 4 S



..... EAST  
 ——— WEST

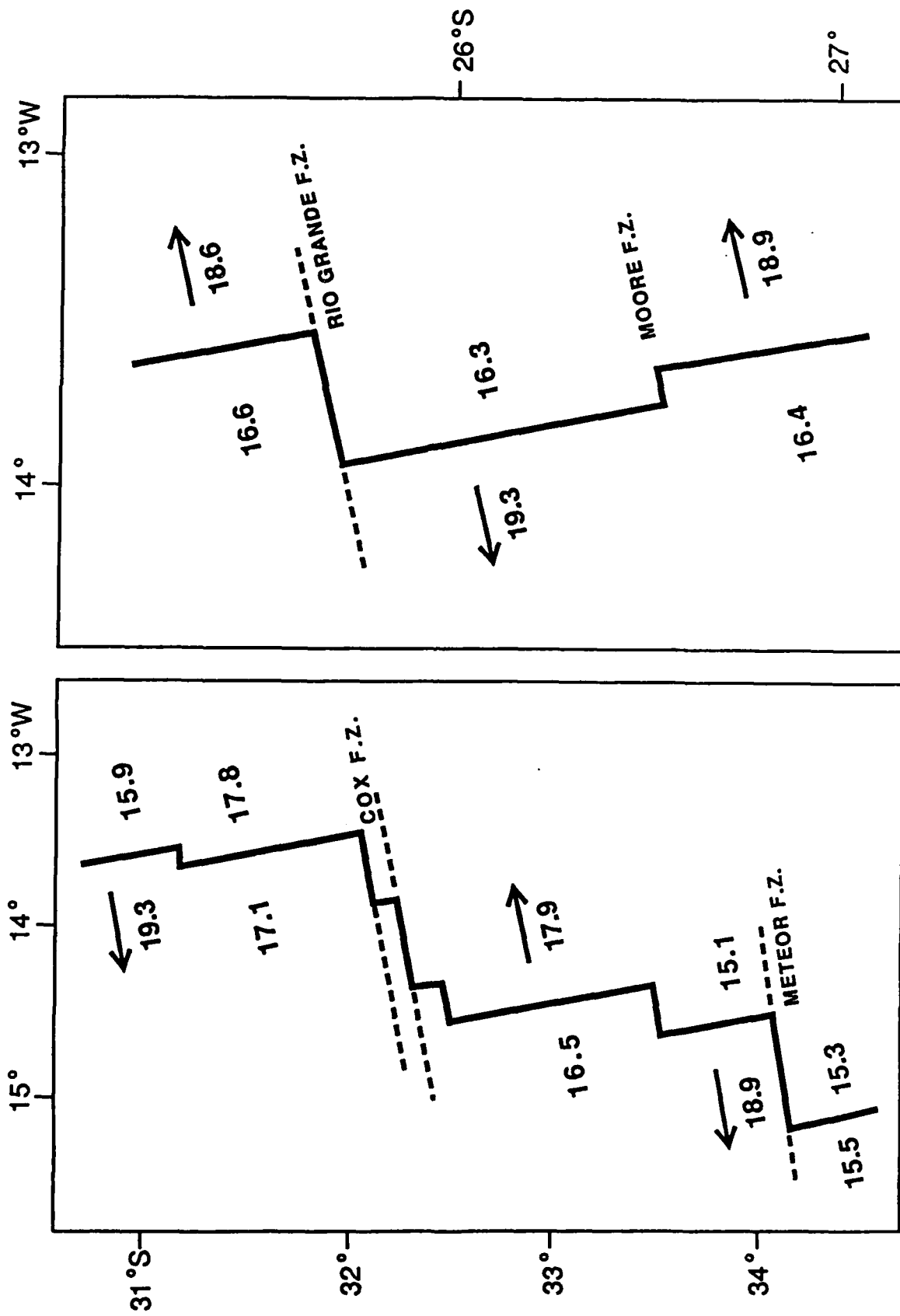


Fig. 6

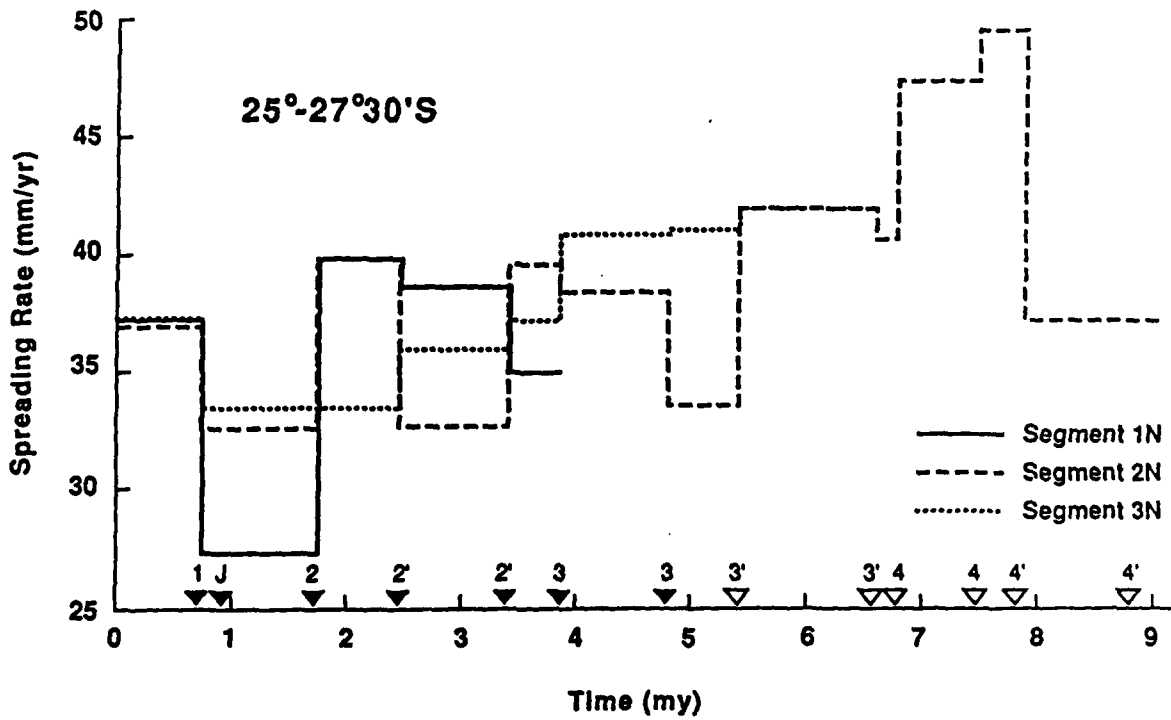
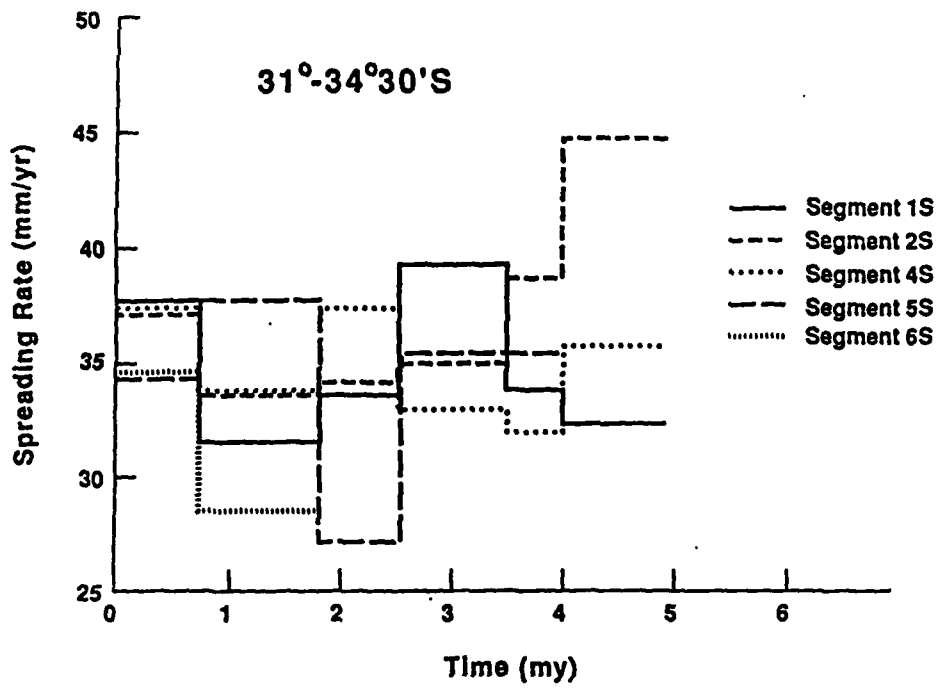


Fig. 7

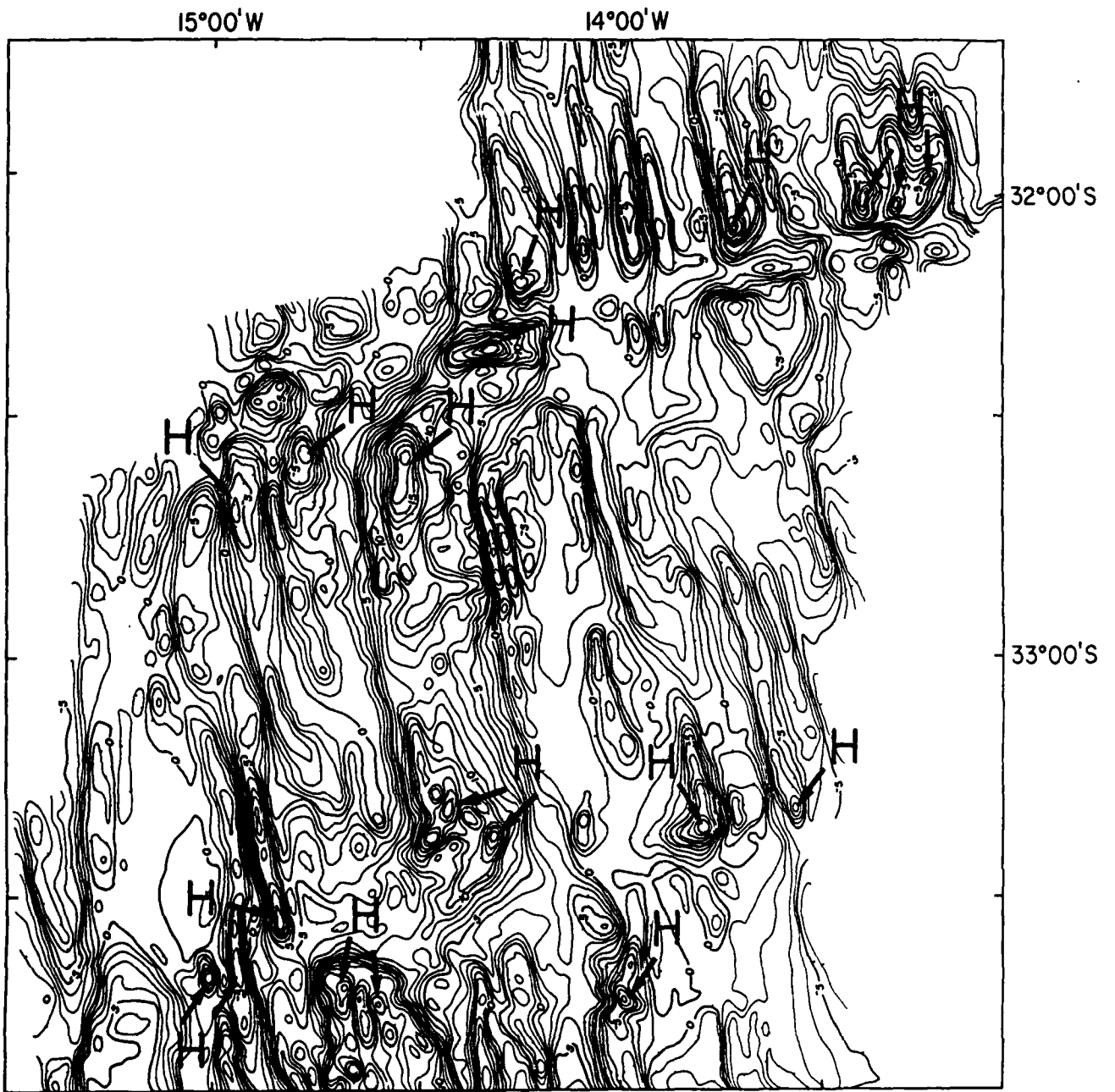
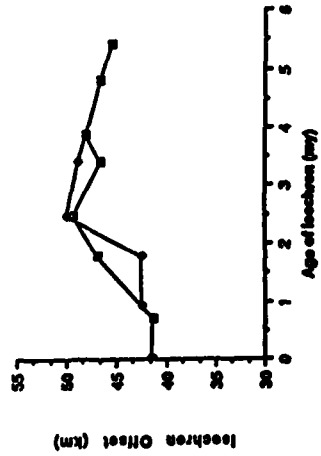
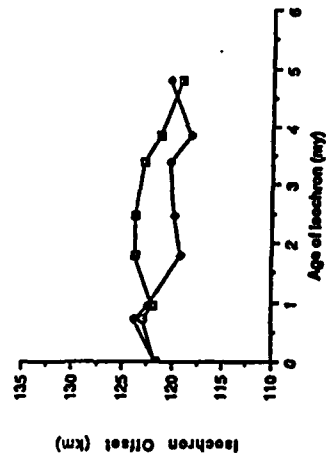


Fig. 8

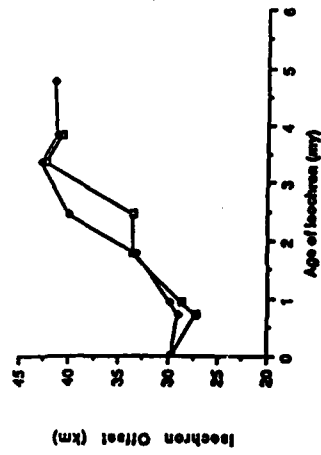
Rio Grande Fracture Zone



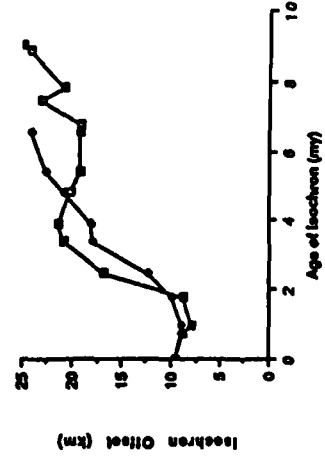
Cox Fracture Zone



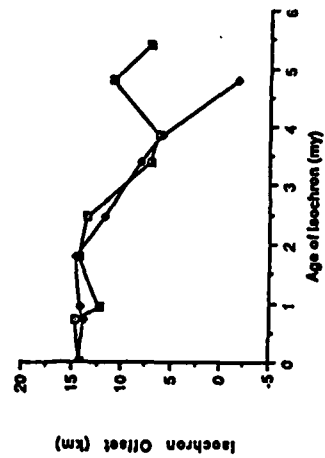
33 30' S Discordant Zone



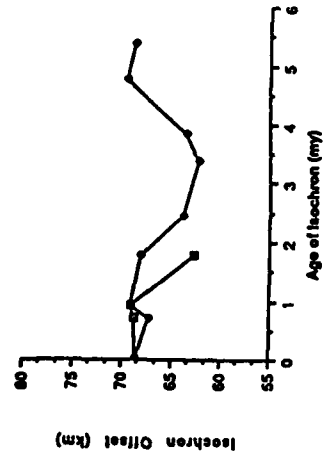
Moore Discordant Zone



31 15' S Discordant Zone

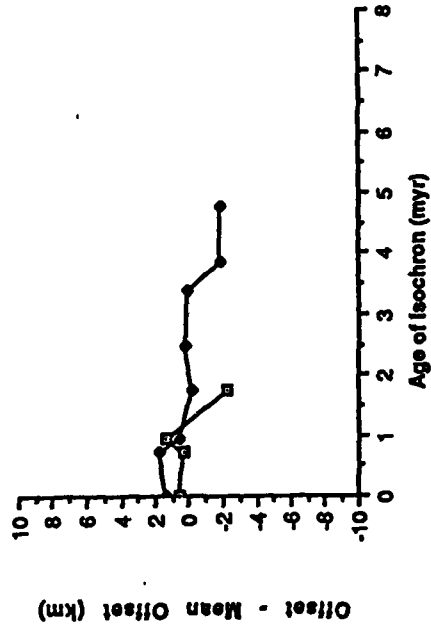


Meteor Fracture Zone



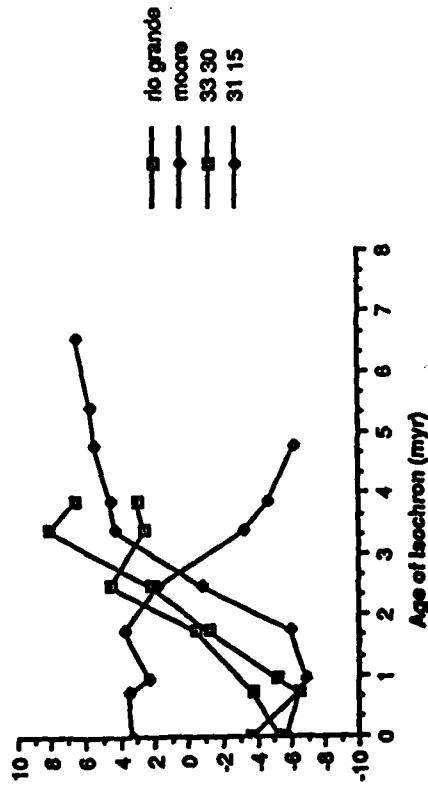
west  
east

Variation in Isochron Offset



10b

Variation in Isochron Offset



10a

Fig. 10

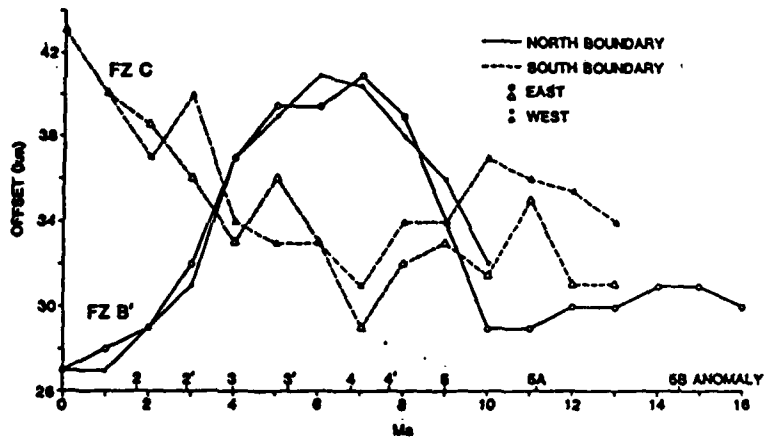
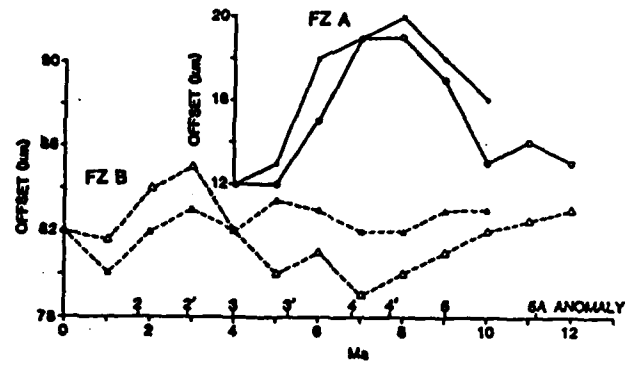


Fig. 11



Table 2 - Transition Widths

Isochron	25°-27°30' S				31°-34°30' S			
	west	n	east	n	west	n	east	n
beginning 3'	4.1	5	3.3	3				
end 3'	5.2	7	4.9	5	3.8	2	3.9	3
beginning 3	3.4	7	5.6	7	3.0	9	3.4	7
beginning 2'	3.0	8	4.0	8	3.8	15	3.3	16
end 2'	4.5	7	4.0	9	4.9	15	3.9	15
beginning 1	3.0	8	2.9	8	3.7	15	3.5	15
Average for each survey			4.0				3.7	
Standard deviation			1.4				1.5	

# High Inside Corners at Ridge-Transform Intersections

JEFF P. SEVERINGHAUS and KEN C. MACDONALD

*Dept. of Geological Sciences and Marine Sciences Institute, U.C. Santa Barbara, CA 93106, U.S.A.*

(Received 1 March, 1988)

**Keywords:** mid-ocean ridge, spreading centers, tectonics of spreading centers, transform faults, tectonics of transform faults, seafloor topography, median valley, axial valley, origin of topography, ridge-transform intersections, topography due to strike-slip faults, lithospheric flexure, asymmetry in topography of the median valley, tectonics.

**Abstract.** A large topographic high commonly occurs near the intersection of a rifted spreading center and a transform fault. The high occurs at the inside of the 90° bend in the plate boundary, and is called the 'high inside corner', while the area across the spreading center, the 'outside corner', is often anomalously low. To better understand the origin of this topographic asymmetry, we examine topographic maps of 53 ridge-transform intersections. We conclude the following: (1) High inside corners occur at 41 out of 42 ridge-transform intersections at slow spreading ridges, and thus should be considered characteristic and persistent features of rifted slow spreading ridges. They are conspicuously absent at fast spreading ridges or at spreading centers that lack a rift valley. (2) High inside corners occur wherever an axial rift valley is present, and an approximate 1:1 correlation exists between the relief of the rift valley and the magnitude of the asymmetry. (3) Large high inside corners occur at both long and short transform offsets. (4) High inside corners at long offsets decay off-axis faster than predicted by the square root of age cooling model, precluding a thermal-isostatic origin, but consistent with dynamic or flexural uplift models.

These observations support the existing hypothesis that the asymmetry is due to the contrast in lithospheric coupling that occurs in the active transform versus the inactive fracture zone. Active faulting in the transform breaks the lithosphere along a high angle fault, permitting vertical movement of the inside corner block, whereas the inactive fracture zone forms a weld that couples the outside corner to the adjacent block, preventing it from rising. Large asymmetry at very short transform offsets appears to be caused by the added effect of a second uplift mechanism. Young lithosphere in the rift valley couples to the older plate, and when it leaves the rift valley it lifts the older plate with it. At very short offsets, this 'coupled uplift' acts upon the high inside corner; at long offsets, it may upwarp the older plate or its expression may be muted.

## 1. Introduction

At rifted, slow-spreading mid-ocean ridges the rift

mountains adjacent to the active transform are consistently 0.5 to 1.5 km higher than the rift mountains adjacent to the inactive fracture zone (Figures 1, 2). This topographic asymmetry contrasts sharply with the elevation symmetry predicted by the depth-age relation (Parsons and Sclater, 1977). Others have also noted this asymmetry (Searle and Laughton, 1977; Karson and Dick, 1983; Fox and Gallo, 1984; Kuo *et al.*, 1984; OTTER, 1984; Parmentier and Forsyth, 1985; and Collette, 1986), yet its origin remains obscure (Parmentier and Forsyth, 1985).

In most cases the inside corner has the form of a large submarine mountain peak, reaching the shallowest depths of any point on the ridge. In other cases, the inside corner is not a peak, but rather a broad topographic high. In both cases a topographic asymmetry occurs, because the outside corner consistently has anomalously low elevation. Relief between the summit of the inside corner and the adjoining nodal basin commonly exceeds 4000 m. The summit generally occurs 15–20 km from the spreading center and 10–15 km from the center of the transform fault. Figure 2 shows several examples.

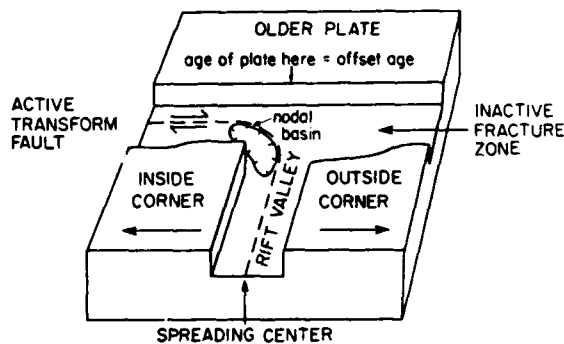


Fig. 1. Nomenclature used at a ridge-transform intersection. At fast spreading ridges the axial rift valley is replaced by an axial high.

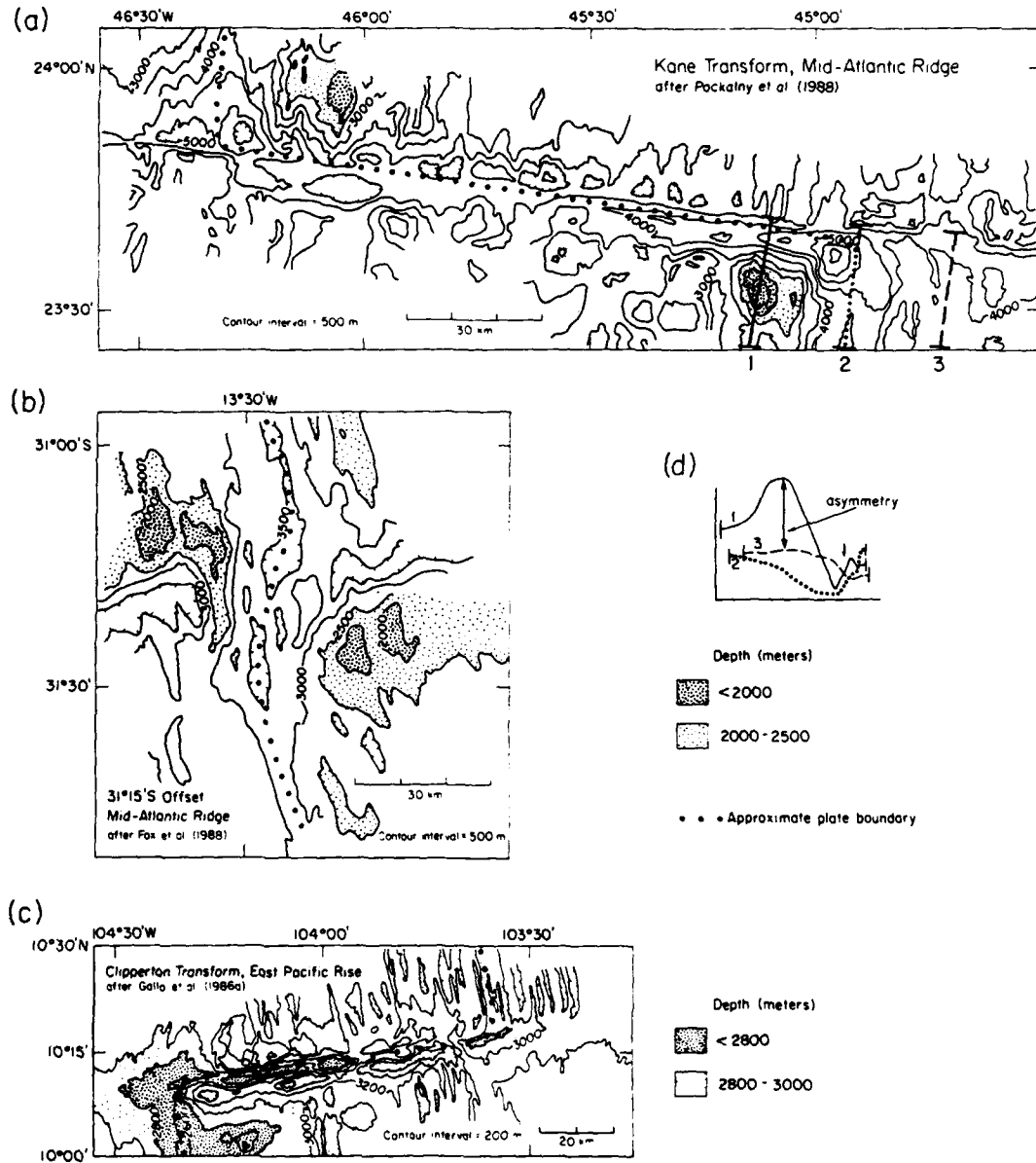


Fig. 2. Examples of ridge-transform intersections. (a) Rifted, slow spreading, long transform fault, high inside corner prominent. (b) Rifted, slow spreading, short transform fault, high inside corner prominent. (c) Nonrifted, fast spreading, no high inside corner. As shown in (d), asymmetry is calculated by measuring the maximum difference between depth profiles located on the crest of the rift mountains. Arrow marks transform trace.

In this study we place constraints on the origin of high inside corners by studying and comparing available topographic maps of ridge-transform intersections. We establish their size, shape, evolution off-axis, and variation against three parameters: spreading rate, trans-

form offset length, and rift valley relief. We find that the relationships among these variables favor the hypothesis that asymmetry is due to the interplay between bonding across the fracture zone and vertical movements associated with the origin of the axial rift valley.

## 2. Measurement Methods

We studied bathymetric maps covering 53 ridge-transform intersections (Figure 3), 38 of which are high resolution maps made with multi-beam sonar systems (e.g., Seabeam) with a contour interval of 100 m or less. The remainder are high quality maps made with conventional single-beam sonar. Ridge segments shorter than 40 km in length were excluded from study, because the perturbing effects of transforms on ridge morphology overlap. For each site studied we measured asymmetry, average asymmetry, rift valley relief, transform offset length and transform offset age (Table I).

Asymmetry is measured by constructing two depth profiles parallel to the spreading axis on either flank of the spreading axis. The profiles are positioned on crust of approximately equal age along the highest topography that occurs at a distance of 15 to 25 km from the axis. The profiles lie along narrow, linear, axis-parallel ridges, which generally correspond to the crest of the rift mountains at rifted spreading centers. The profiles are then projected onto a plane

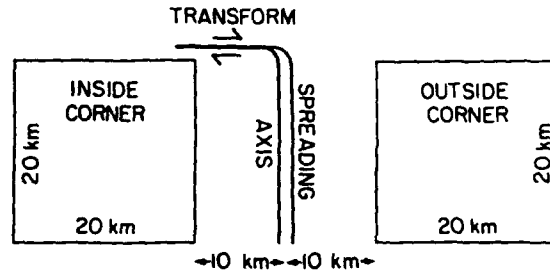


Fig. 4. Method of calculating average asymmetry. Elevations within the two squares are averaged and the difference of the two averages is taken. Squares are positioned as close to the transform valley as is possible without including major portions of the transform valley.

parallel to the spreading axis for comparison. Asymmetry is taken as the maximum elevation difference between the profiles (Figure 2a, d). This technique is approximate, as the topographic noise at slow spreading ridges is large. As a check on this method, average asymmetry is measured (Figure 4).

Rift valley relief is measured by comparing the average elevation of the rift mountains (measured

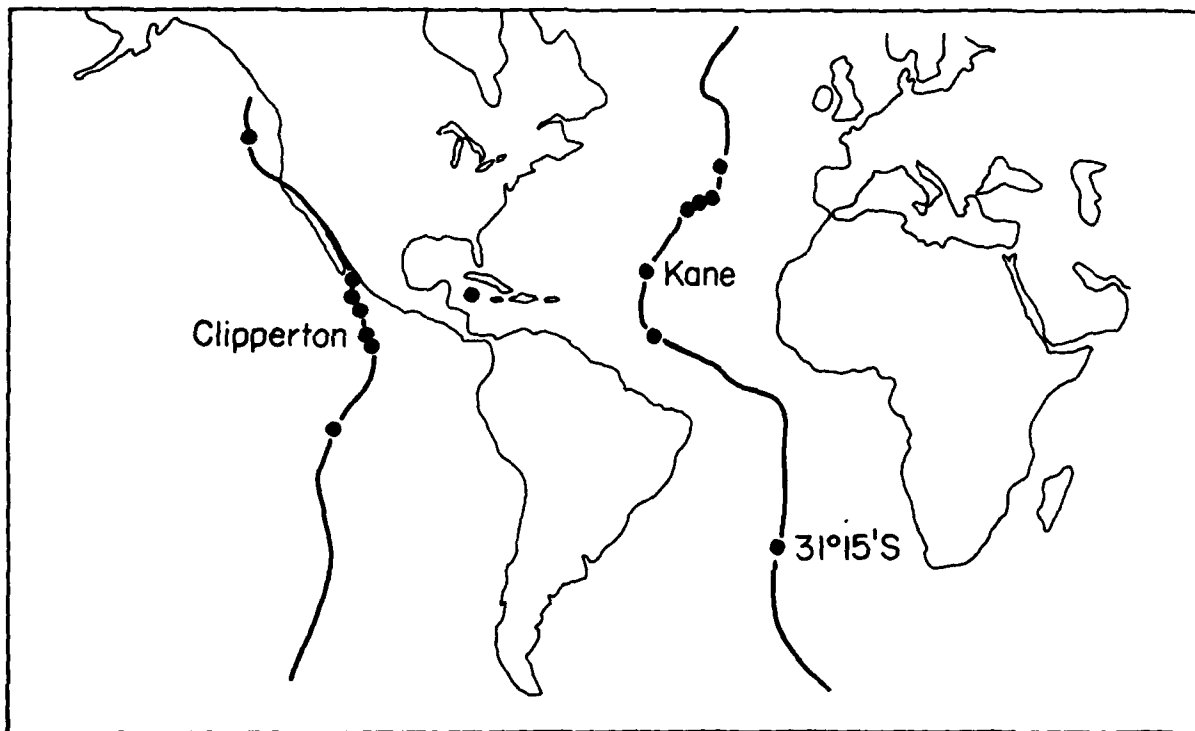


Fig. 3. Locations of the 53 ridge-transforms intersections studied. Where many occur close together, not all are shown.

TABLE I  
Ridge-transform intersections studied and data collected

Name	Latitude	1/2 spr. rate (mm yr <sup>-1</sup> )	Asymmetry (km)	Av. Asymmetry (km)	Rift valley relief (km)	Offset (km) (m.y.)		Reference
Mid-Atlantic Ridge:								
Kurchatov	N 40 30 N	12	1.0	0.60	0.8	18	1.5	Searle and Laughton, 1977
Kurchatov	S 40 30 N	12	0.9	0.45	1.3	18	1.5	Searle and Laughton, 1977
Pico	S 37 40 N	10	0.9	*	0.9	40	4.0	Phillips and Fleming, 1978
Unnamed	N 37 15 N	10	0.7	0.26	0.9	45	4.5	Phillips and Fleming, 1978
FAMOUS A	N 37 00 N	10	-0.5	0.15	1.0	20	2.0	Phillips and Fleming, 1978
FAMOUS A	S 37 00 N	10	0.5	0.24	1.0	20	2.0	Phillips and Fleming, 1978
FAMOUS B	N 36 35 N	10	0.9	0.44	1.0	22	2.2	Phillips and Fleming, 1978
FAMOUS B	S 36 35 N	10	0.5	0.14	1.1	22	2.2	Phillips and Fleming, 1978
FAMOUS C	N 36 15 N	10	1.2	0.37	1.1	18	1.8	Phillips and Fleming, 1978
FAMOUS C	S 36 15 N	10	0.5	0.13	1.2	18	1.8	Phillips and Fleming, 1978
FZ F	S 35 40 N	11	0.5	*	0.9	45	4.1	Fox and Gallo, 1984
Oceanographer	E 35 00 N	11	0.8	*	0.9	128	11.6	Fox and Gallo, 1984
Oceanographer	W 35 00 N	11	1.2	*	0.8	128	11.6	Fox and Gallo, 1984
FZ I	N 34 30 N	11	0.8	*	0.8	40	3.6	Fox and Gallo, 1984
TAG unnamed	N 26 15 N	13	0.4	0.20	1.2	5	0.4	Rona and Gray, 1980
TAG unnamed	S 25 40 N	13	1.2	0.70	1.0	20	1.5	Rona and Gray, 1980
TAG unnamed	N 24 50 N	13	1.6	0.95	1.0	30	2.3	Rona and Gray, 1980
TAG unnamed	S 24 40 N	13	0.5	0.40	1.0	30	2.3	Rona and Gray, 1980
TAG unnamed	S 24 40 N	13	0.5	0.40	1.9	30	2.3	Rona and Gray, 1980
Kane	E 23 40 N	14	2.5	1.00	1.4	150	10.7	Pockalny <i>et al.</i> , 1988
Kane	W 23 40 N	14	1.2	0.80	1.9	150	10.7	Pockalny <i>et al.</i> , 1988
Unnamed	N 23 08 N	14	1.5	0.25	1.4	5	0.4	Pockalny <i>et al.</i> , 1988
Unnamed	S 23 08 N	14	1.8	0.65	1.5	5	0.4	Pockalny <i>et al.</i> , 1988
Vema	E 10 45 N	12	1.5	0.90	1.6	320	26.7	Macdonald <i>et al.</i> , 1986
Vema	W 10 45 N	12	1.6	0.80	1.6	320	26.7	Prince and Forsyth (in press) 1988
Rio Grande	E 25 40 S	19	1.3	*	1.0	40	2.1	Grindlay <i>et al.</i> , 1987
Rio Grande	W 25 40 S	19	1.1	*	1.0	40	2.1	Grindlay <i>et al.</i> , 1987
Moore	E 26 35 S	19	0.9	*	1.2	12	0.6	Grindlay <i>et al.</i> , 1987
Moore	W 26 35 S	19	0.7	*	1.2	12	0.6	Grindlay <i>et al.</i> , 1987
Unnamed	N 31 15 S	18	0.7	0.55	1.4	15	0.8	Fox <i>et al.</i> , 1985
Unnamed	S 31 15 S	18	1.0	0.58	0.9	15	0.8	Fox <i>et al.</i> , 1987
Cox	E 32 10 S	18	0.8	0.40	0.9	120	6.7	Grindlay <i>et al.</i> , 1985
Cox	W 32 10 S	18	0.8	0.21	0.4	120	6.7	Grindlay <i>et al.</i> , 1985
Unnamed	N 33 30 S	18	0.8	0.28	0.4	25	1.4	Fox <i>et al.</i> , 1985
Unnamed	S 33 30 S	18	1.0	0.43	1.5	25	1.4	Fox <i>et al.</i> , 1985
Meteor	E 34 10 S	18	1.5	*	1.5	80	4.4	Grindlay <i>et al.</i> , 1985
Meteor	W 34 10 S	18	1.3	*	1.4	80	4.4	Grindlay <i>et al.</i> , 1985
Norda	N 37 20 S	17	1.1	*	1.6	20	1.2	Fox <i>et al.</i> , 1985
Norda	S 37 20 S	17	1.2	*	1.2	20	1.2	Fox <i>et al.</i> , 1985
Caribbean:								
Oriente	W 19 00 N	10	2.4	0.83	1.5	>1000	>40	Holcombe <i>et al.</i> , 1973
Cayman Rise	N 18 15 N	10	1.3	0.55	1.5	20	2.0	CAYTROUGH, 1979
Cayman Rise	S 18 15 N	10	1.7	1.00	1.5	20	2.0	CAYTROUGH, 1979
Swan	E 17 40 N	10	1.6	0.18	1.5	>600	>40	CAYTROUGH, 1979
Eastern Pacific:								
Blanco	W 44 30 N	29	0.2	*	-0.3	340	11.7	Crane <i>et al.</i> , 1985
Tamayo	E 23 00 N	30	0.3	0.08	0.3	80	2.7	Francheteau <i>et al.</i> , 1979
Tamayo	W 23 00 N	30	-0.2	-0.18	-0.3	80	2.7	Francheteau <i>et al.</i> , 1979
Rivera	W 20 00 N	34	0.2	0.10	0.1	444	13.1	Mammerickx <i>et al.</i> , 1978
Orozco	E 15 30 N	45	0.1	-0.10	0.0	50	1.1	Madsen <i>et al.</i> , 1986
Orozco	W 15 30 N	45	0.3	*	-0.5	50	1.1	Madsen <i>et al.</i> , 1986
Clipperton	E 10 15 N	55	-0.1	-0.3	-0.2	85	1.5	Gallo <i>et al.</i> , 1986a
Clipperton	W 10 15 N	55	-0.1	-0.1	-0.4	85	1.5	Gallo <i>et al.</i> , 1986a
Siqueiros	W 08 30 N	69	-0.1	-0.15	-0.3	113	1.6	Rosendahl, 1980
Garret	E 13 30 S	80	-0.1	-0.10	-0.2	130	1.6	Gallo and Fox, submitted, 1988
Garret	W 13 30 S	80	-0.2	*	-0.2	130	1.6	Gallo and Fox, submitted, 1988

\*Insufficient map coverage.

15–25 km off-axis) with the elevation of the axis. In order to avoid measuring rift valley relief as compounded by the effects of high inside corners, rift valley relief is measured at a point 30 km distant

from the transform or mid-way between transforms, whichever is closer.

We calculate offset age by dividing offset length by local spreading rate. Spreading rate is obtained from

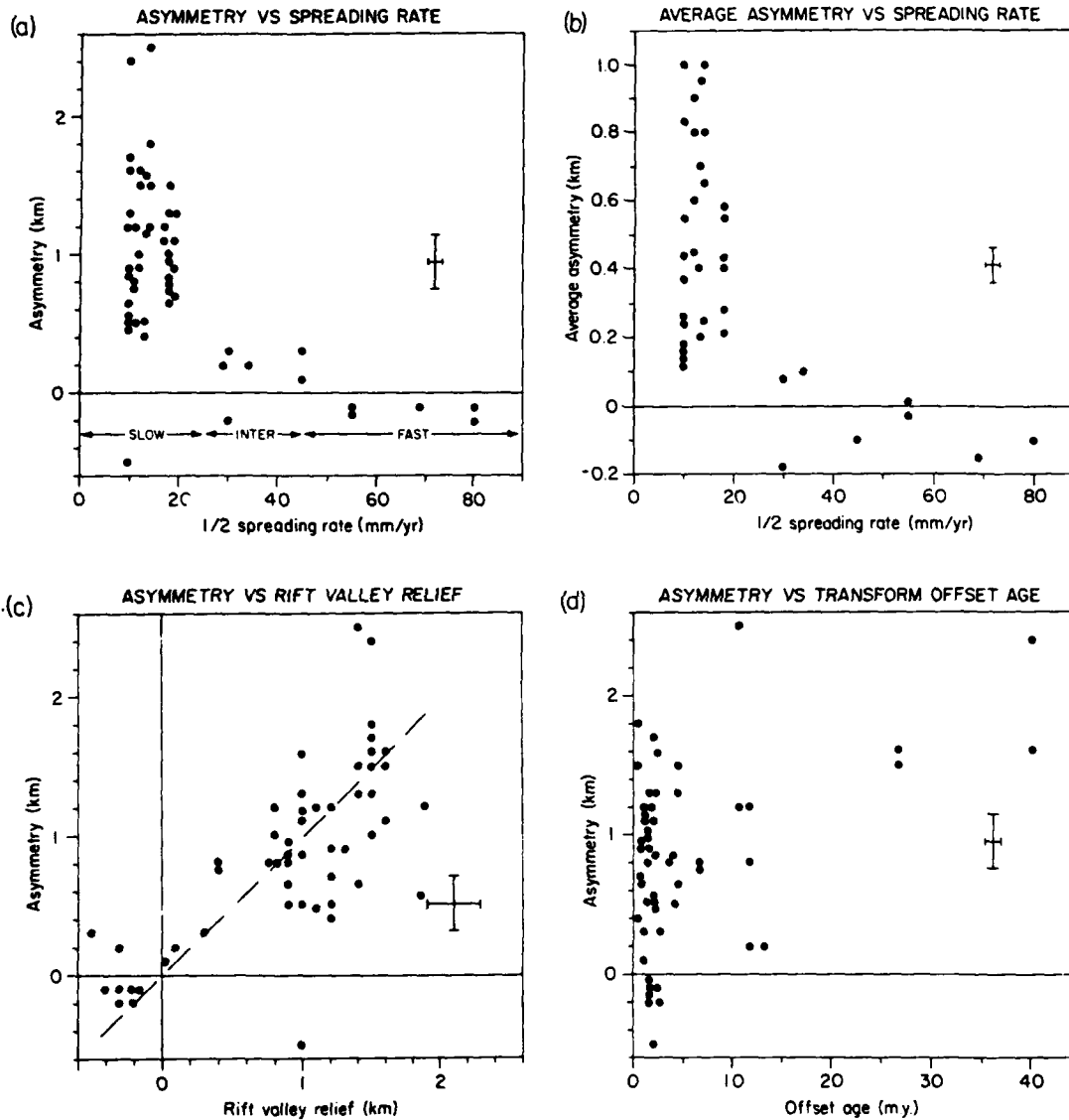


Fig. 5(a). Asymmetry as a function of half spreading rate. High inside corners are common at slow spreading ridges but do not occur at fast spreading ridges. In fact, inside corners may be slightly lower than outside corners at fast spreading ridges, corresponding to a negative asymmetry. Approximate, subjective error bars shown. (b) Average asymmetry as a function of spreading rate. This quantity probably underestimates true asymmetry because deeps are averaged in, and thus should be considered a lower bound. Note that scale of ordinate is larger than in parts a, c, and d. (c) Asymmetry plotted against rift valley relief. Dashed line is a 1:1 correlation. The correlation suggests that high inside corners are linked to the processes creating the rift valley. Stray points in the second quadrant are the Orozco Transform and FAMOUS Transform A East, both offsets that have unusual morphologic complexities. (d) Plot of asymmetry as a function of transform offset age. Wide scatter of this plot indicates that no simple relationship exists between magnitude of asymmetry and transform age offset. However, very large offsets (e.g., Kane, Oceanographer, Vema) do tend to have large high inside corners (see Figure 11).

published sources or from magnetic anomaly data where published values are not available.

### 3. Asymmetry, Spreading Rate, Rift Valley Relief, and Offset Age

High inside corners occur at 41 of the 42 ridge-transform intersections studied at slow spreading rates (Figure 5a). Asymmetry ranges from 0.5 to 2.5 km at slow spreading ridges, but decreases to zero with increasing spreading rate. Ridges spreading at intermediate rates have small positive asymmetries, while there is no significant elevation anomaly at fast spreading rates. Average asymmetry shows the same pattern, with smaller amplitude, and a slightly negative asymmetry at fast spreading rates is seen (Figure 5b).

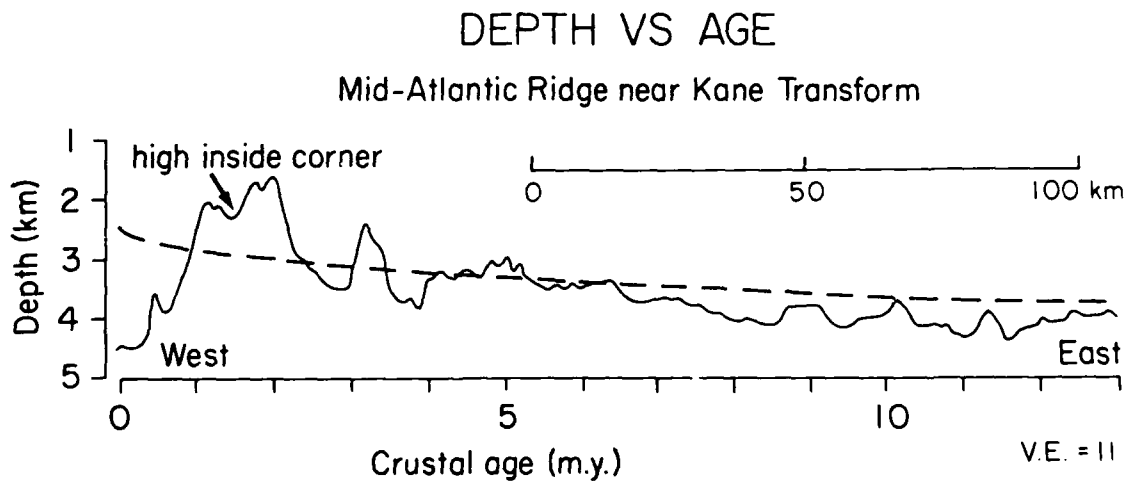
A good correlation exists between asymmetry and the relief associated with rift valleys (Figure 5c). We interpret this correlation as evidence that the high inside corner is linked in a basic way to the uplift that creates the rift valley walls.

Surprisingly, no obvious correlation exists between the magnitude of asymmetry and offset age, as shown by the wide scatter in Figure 5d. Note that both large and small transform offsets can have large

asymmetry. A similar graph of asymmetry versus offset length also showed wide scatter. Given the observed increase in the depth of the nodal basin with offset age reported by Fox and Gallo (1984), we had suspected that asymmetry might increase with offset age. We find instead that large asymmetry can occur even at very small offsets, some of which are no larger than the width of the rift valley (e.g., 31°15' S Mid-Atlantic Ridge, Figure 2b).

### 4. Evolution of High Inside Corners with Age

High inside corners at large-offset transforms appear to subside more rapidly than would be expected from thermal contraction as the lithosphere cools. If the gross spreading center topography is approximately steady state, then a depth profile can be viewed as a record of seafloor elevation through time (Figure 6). Note that subsidence is much faster than the square root of age curve given for reference. Six of the seven high inside corners at large-offset transforms with sufficient Seabeam coverage show a similar pattern of rapid subsidence (Kane E, Kane W, Meteor E, Meteor W, Oriente, and Swan do; Cox E does not). At short offsets, where off-axis evolution of the inside corner is along an inactive fracture zone, subsidence of the



From map of Pockalny et al. (1988)

Fig. 6. Depth profile parallel to and ~20 km north of Kane Transform Fault, passing through northern high inside corner. Dashed line is cooling model ( $z = 2.8 + 0.35t^{1/2}$  where  $z$  = depth in km and  $t$  = age in m.y. (Parson and Sclater, 1977)). Intercept on the depth axis is arbitrarily chosen: the shape of the curve is significant rather than the absolute value of the curve. A half spreading rate of  $14 \text{ mm yr}^{-1}$  (Purdy et al., 1978) was used to convert distance to age. The sharp drop-off of the high inside corner compared to the predicted subsidence due to cooling argues against a thermal-isostatic origin for the high inside corner.

inside corner may be slower (e.g., Kurchatov Fracture Zone, Searle and Laughton (1977)).

At many large-offset transforms subsidence of the high inside corner is not monotonic; as it passes the opposite spreading axis a second, smaller topographic high appears (e.g., Figure 2a). In some cases this high takes the form of a prominent 'transverse ridge', while in other cases it is a local topographic high or is poorly expressed. It occurs at five of the six large-offset transform sites with sufficient Seabeam coverage (Kane E, Kane W, Meteor W, Cox E, Cox W; not pronounced at Meteor E). Abrams *et al.* (1988) have documented this topographic feature at the eastern intersection of the Kane Fracture Zone with the Mid-Atlantic Ridge. They demonstrate with

gravity and seismic studies that it is uplifted but relatively normal oceanic crust, and model it as flexure of a lithosphere with 4 km elastic thickness. That this high amounts to a 'rejuvenation' or second phase of uplift is supported by submersible observations of fresh talus and other signs of renewed activity in this area (Karson and Dick, 1983).

### 5. Tilting

The topography of the outside corner slopes gently towards the inactive fracture zone at 40 out of the 42 slow spreading sites (Swan and FAMOUS A East are the exceptions). An important observation is that the ridge-parallel abyssal hills topography continues

FAMOUS Ridge Segment AB, Mid-Atlantic Ridge  
after Phillips and Fleming (1978)

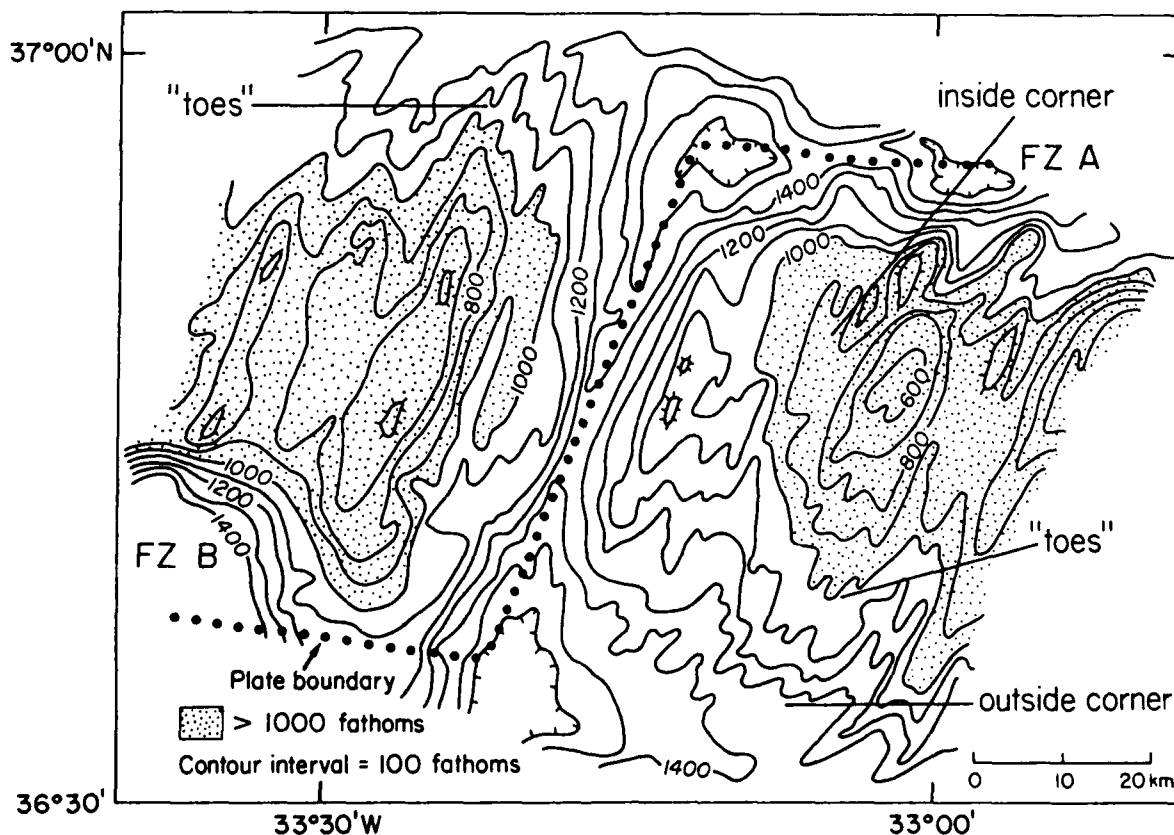


Fig. 7. FAMOUS Fracture Zones A and B, exhibiting the typical morphology of outside corners at slow spreading ridges. The outside corner slopes toward the inactive fracture zone, and the ridge-parallel abyssal hills on the sloping surface result in contour lines with the appearance of 'toes'. In contrast, the inside corner is bounded by a steep scarp. Tilting of the outside corner about a horizontal axis parallel to the transform is inferred to occur, possibly involving lithospheric flexure.

undisturbed down this slope well into the fracture zone. Because of this fact, this gently sloping surface (about 2°) appears to be the result of tilting or flexure of the outside corner block, rather than failure on transform-parallel faults. Contour lines on the surface interact with the corrugated abyssal hills topography to create the appearance of 'toes' (Figure 7), a pattern like that seen on a partially immersed, tilted piece of corrugated tin. In contrast, the inside corner is bounded by a sharp, steep scarp facing the transform, and the abyssal hills appear to be disrupted by a set of transform-parallel faults.

Because the slope of the outside corner exceeds the slope of the rift valley floor as the rift valley deepens toward the transform, the slope of the outside corner cannot be purely inherited from the initial slope of the crust when it was formed. Rather, this difference in slope implies several degrees of rotation about a horizontal axis parallel to the transform. Where transforms are closely spaced (~50 km), the tilting appears to involve the entire block between transforms, as was also reported by Searle (1979).

## 6. Discussion

The occurrence pattern of high inside corners argues that they are characteristic, persistent features of slow spreading ridges. Wherever there is a rift valley, they occur. The ubiquity of high inside corners suggests that they are steady state features; if they appeared and disappeared with time one would expect to see some ridge-transform intersections without them. Deffeyes (1970) and Atwater and Mudie (1973) made a similar argument for the steady state nature of the rift valley. Thus we assume in this discussion that the high inside corner and rift valley are steady state features.

High inside corners are unlikely to be of volcanic constructional origin because they lack fresh pillows or other signs characteristic of seamounts, and expose a variety of highly tectonized plutonic and ultramafic rocks (Karson and Dick, 1983; Bryan and Moore, 1977; CAYTROUGH, 1979). A purely thermal-isostatic origin is also unlikely because high inside corners appear to decay faster than predicted by a square root of age cooling model. Their faulted boundaries and rapid decay, as well as the correlation between rift valley relief and inside corner height all suggest that high inside corners are caused by the

same forces that give rise to the axial rift valley. Interestingly, inside corners are the locus of intense microseismicity (Rowlett, 1981; Rowlett and Forsyth, 1984).

### 6.1. DECOUPLING

Our observations provide new and compelling support for the 'decoupling' hypothesis advanced by previous workers (Searle and Laughton, 1977; Karson and Dick, 1983; Kuo *et al.*, 1984; Collette, 1986). In the interest of clarity, this model is briefly reiterated. This model holds that the elevation asymmetry between inside and outside corners is due to the contrast in plate coupling between the active transform and the inactive fracture zone. The actively slipping transform decouples the plates, allowing the inside corner to rise in response to the forces that create the uplifted rift valley walls, while the inactive fracture zone forms a weld that prevents the outside corner from rising in response to the same forces (Figure 8).

Three observations support this model. First, the consistent tilting of the outside corner toward the inactive fracture zone is what would be expected if the outside corner were coupled to the older plate and prevented from rising. Second, the decoupling model is consistent with the observation that the correlation between asymmetry and rift valley relief is approximately 1:1. Rift valley relief is a measure of the uplift experienced by the lithosphere. If decoupling were to allow this amount of uplift to occur on the inside corner while coupling prevented it on the outside corner, the size of the resulting asymmetry would approximately match the relief of the rift valley.

Third, slow spreading ridge-fault-fault triple junctions provide a test of the decoupling model (Figure 9a). Because both corners are bounded by active strike slip faults, both corners should be topographically high, if decoupling by strike slip is the cause for high inside corners. The single example of an outside corner that does not slope toward the fracture zone is the Swan Transform/Mid-Cayman Rise intersection (Figure 9b). Instead, the outside corner here is anomalously shallow, slopes away from the fracture zone, and locally is higher than the older plate, contrary to the pattern elsewhere. Regional seismicity patterns suggest that this intersection may

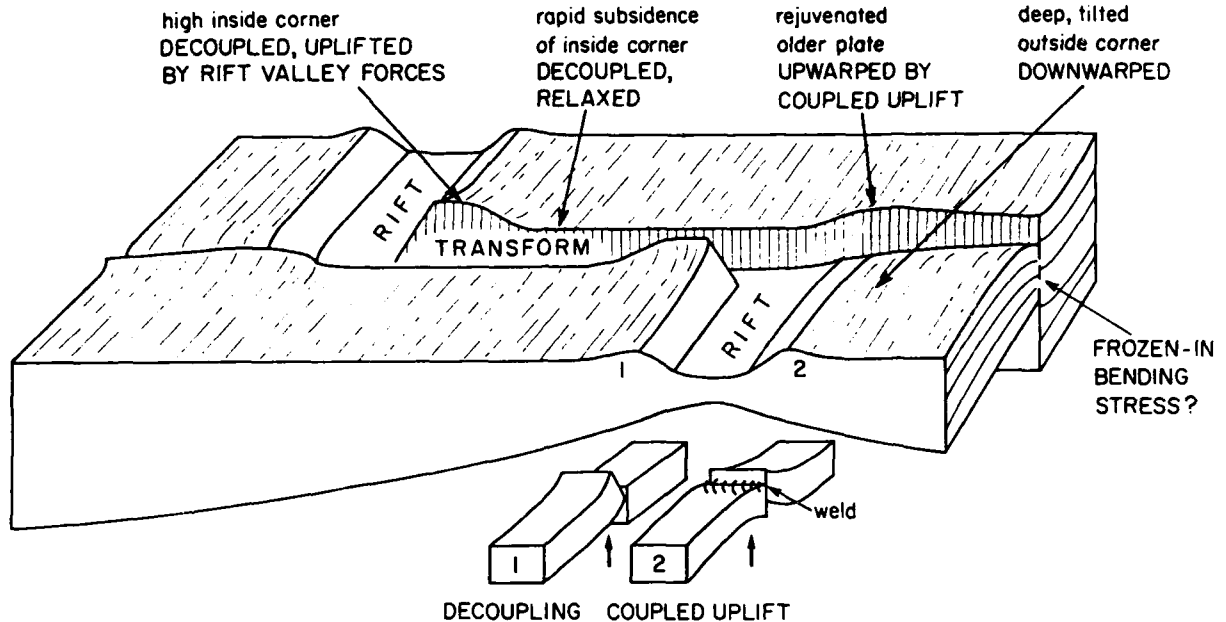


Fig. 8. Summary of the proposed mechanisms for the origin of high inside corners. Observations shown in lower case letters, and their interpretation in terms of the model shown in upper case letters. Transform faulting breaks the lithosphere along a near-vertical fault, permitting differential vertical movement. Vertical movements are a result of the forces that create the rift valley. Decoupling and coupled uplift result from the presence and absence, respectively, of lithospheric failure due to transform faulting. Heavy arrows symbolize the uplift force creating the rift valley walls.

be a ridge-fault-fault triple junction (Sykes *et al.*, 1982), thus supporting the decoupling model. However, the anomalous outside corner does not look like a normal high inside corner, and a transform valley only begins to appear to the east of the outside corner; these complexities remain unexplained by the decoupling model.

The decoupling model also predicts the presence of negative asymmetry (outside corners higher than inside corners) at fast spreading ridges. Where an axial high is present, the lithosphere only subsides. An offset juxtaposes the outside corner against older lithosphere that has already gone through much of its subsidence. When the two sides weld, the outside corner will be prevented from subsiding normally. The inside corner, being decoupled by active transform faulting, is free to sink. It is encouraging that slightly negative asymmetry is present at the fastest spreading centers (Figure 5a, b). A high outside corner formed in this manner represents the early stages of the flexural response to differential subsidence across a fracture zone described by Sandwell (1984).

## 6.2. COUPLED UPLIFT AT SHORT TRANSFORM FAULTS

The decoupling model does not appear to explain the large asymmetry observed at very small offsets (Figure 2b, 5d). A true transform fault is probably not present at the smallest offsets, and most of the high topography at small offsets is adjacent to the inactive fracture zone rather than the transform. Yet we observe asymmetry at these offsets that is as large as or larger than the asymmetry at large age offsets.

We propose a corollary to the decoupling hypothesis, called 'coupled uplift', which explains the large size of high inside corners at small offsets. This idea is similar to the explanation proposed by Searle and Laughton (1977) for the asymmetry of fracture zone topography at several North Atlantic ridge offsets. If we accept the premise that the outside corner is being held down by a weld to the older plate, then there must be an equal force acting to lift the older plate. This effect is illustrated in Figure 8, and is a simple explanation for the older plate rejuvenation described above for large offset transforms. At very short offsets, this upward warped older plate

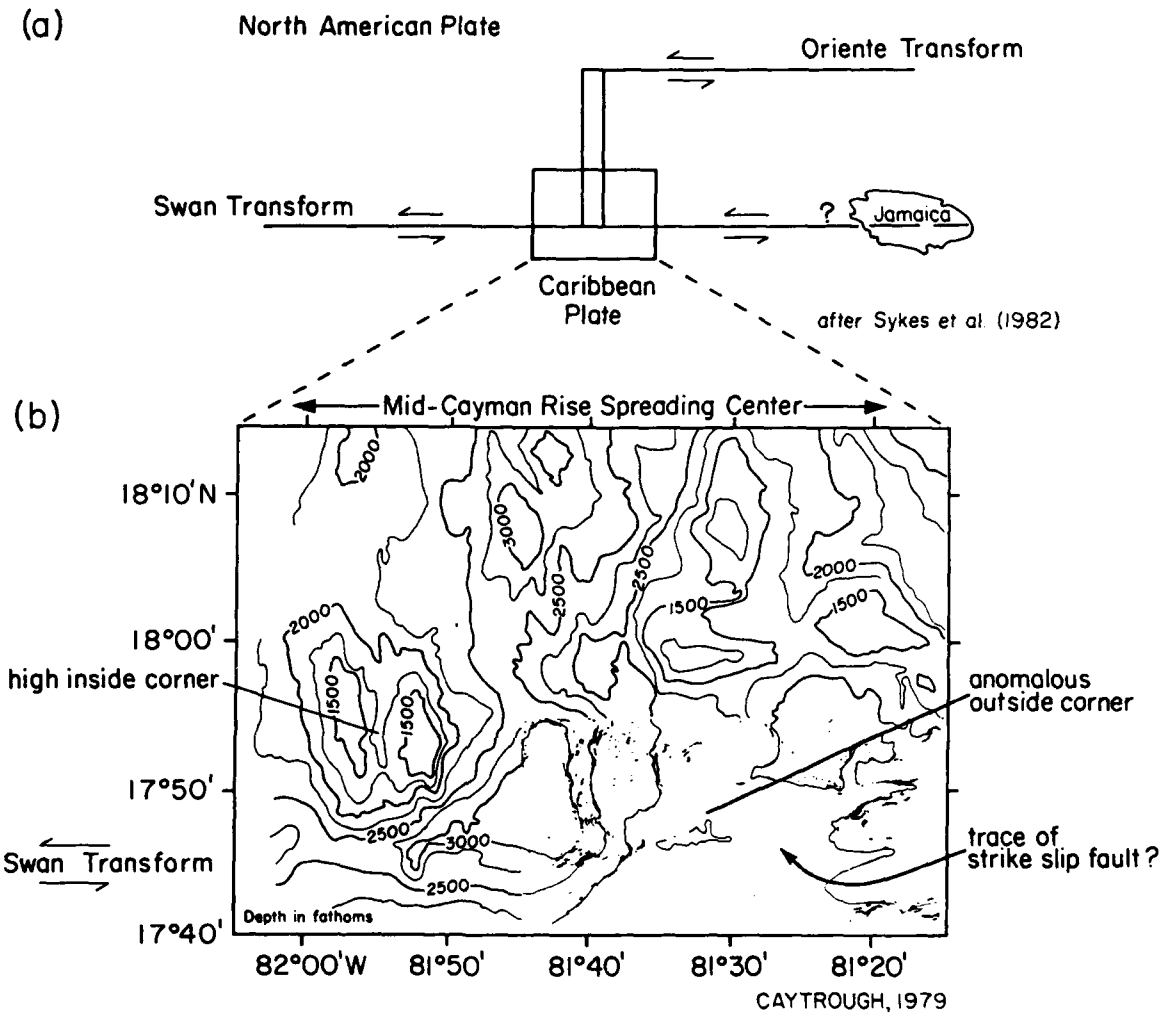


Fig. 9. (a) Probable Cayman Trough plate configuration deduced from regional seismicity, indicating that this intersection is a ridge-fault-fault triple junction, and that strike slip motion may occur between the outside corner and older plate. If the decoupling model is correct, such a triple junction should have *two* high inside corners. (b) Multi-beam bathymetry of the intersection of the Swan Transform with the Mid-Cayman Rise spreading center. Note the unusually shallow, north-sloping outside corner, and possible fault trace between outside corner and older plate. The association of strike slip motion with the single example of a high outside corner supports the decoupling model.

actually *is* the inside corner of the opposite ridge-transform intersection. Therefore, the inside corner at short offsets experiences uplift first due to decoupling, followed by or associated with a second phase of uplift due to 'coupled' uplift (Figure 10a). The summing of these two episodes of uplift can explain the large size of small offset high inside corners (Figure 10b).

An alternative explanation for the older plate rejuvenation is that spreading center magmas heat and

erode the older plate, leading to uplift (e.g., Gallo *et al.*, 1986b). While tenable at fast spreading ridges, we believe that this mechanism is unlikely to be applicable at slow spreading ridges in view of the reduced thermal budget of slow spreading ridges near transforms (Fox and Gallo, 1984). A third possibility, more difficult to evaluate, is that viscous head loss (e.g., Lachenbruch, 1973, 1976; Sleep and Biehler, 1970) occurs in rising asthenosphere as it shears against the vertical wall of the older plate,

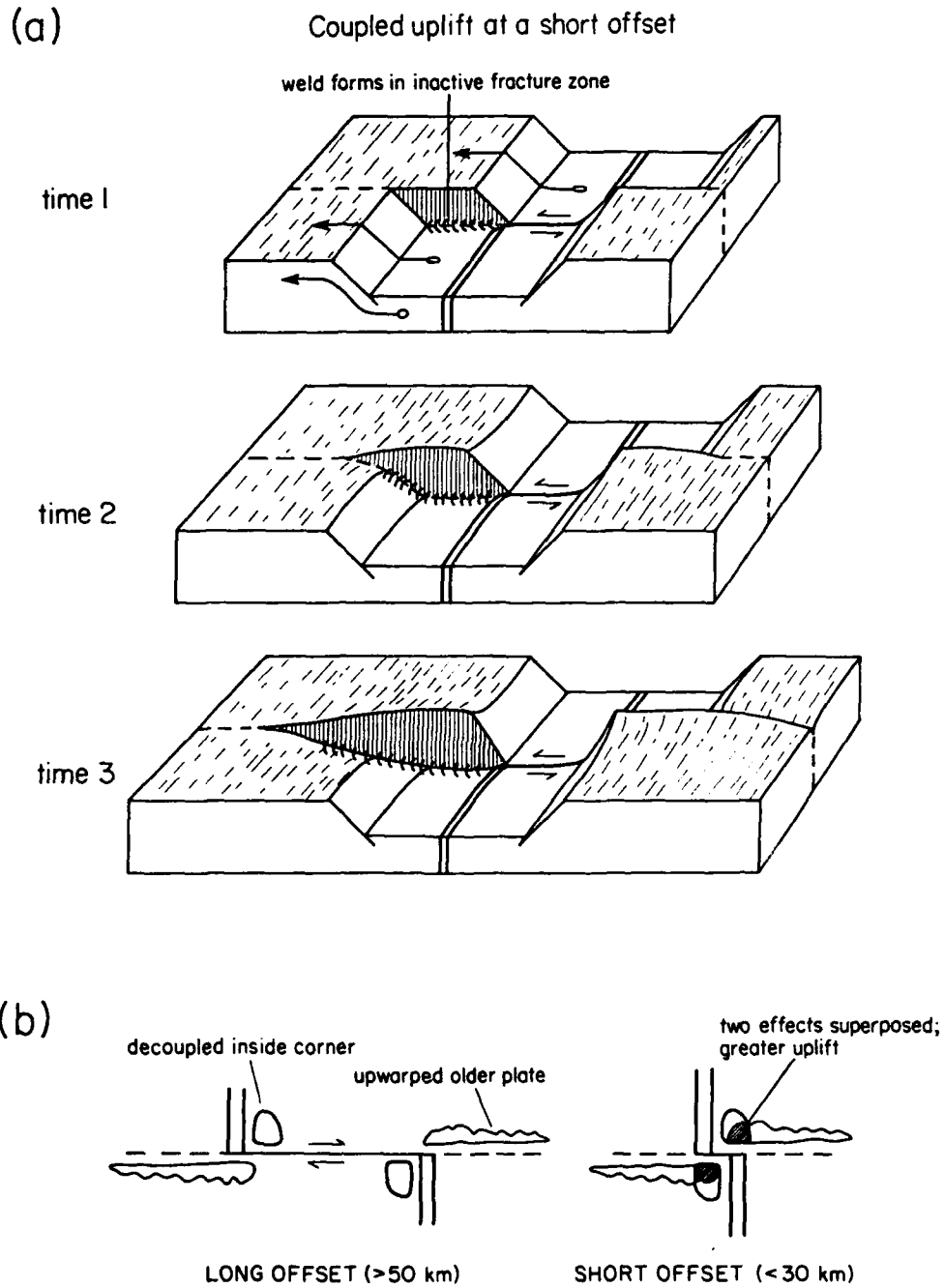


Figure 10. (a) Formation of high inside corners at a short offset by coupled uplift. The depressed block in the rift valley welds to the higher block on the other side of the fracture zone which has already been uplifted. As the lower block rises it lifts the higher one with it. (b) Schematic diagram demonstrating that effects of decoupling and coupled uplift are separate at large offset transforms, but are superposed at short offsets.

uplifting the older plate and creating the deep nodal basin.

Neither viscous head loss nor coupled uplift satisfactorily explains the absence of a prominent transverse ridge along the western limb of the Kane Fracture Zone (Abrams *et al.*, 1988). This absence, and the uneven occurrence of an upwarped older plate at long offset transforms, may be due to the relatively high flexural rigidity of the older plate, causing the expression of coupled uplift to be muted. Alternatively, the weld may be imperfect in some fracture zones.

It is still not clear why the high inside corner at long offsets is commonly a prominent peak rather than the same height as the rift mountains along strike; the decoupling model only explains the *difference* in elevation between inside and outside corners. We speculate that uplift increases along strike towards transforms, concomitant with the observed deepening of the rift valley toward transforms discussed by Parmentier and Forsyth (1985). Thus, as the forces that are responsible for the rift valley

increase with the increasing depth of the rift valley, so does the height of the inside corner (Figure 11).

An alternate explanation offered by Chen (1988) is that the high inside corner is caused by a twisting moment exerted along the transform fault which upwarps the inside corner. This twisting moment is caused by a linear increase in shear stress with depth along the transform fault (as predicted by Byerlee's law). This force may add to the force which we have proposed (that related to the origin of the rift valley) as they are not mutually exclusive. The twisting moment has the appeal of explaining why the inside corner at long offsets is a prominent peak rather than the same height as the rift mountains along strike; the upwarp caused by the twisting moment along the transform fault may add several hundred meters of relief to the inside corner (Chen, 1988). On the other hand this mechanism cannot be the only one causing uplift of the inside corner high, as it does not explain several important observations which are explained by our model. It does not explain the good correlation between rift valley relief and topographic asymmetry (i.e. height of the inside corner), nor can it explain the occurrence of a pronounced high inside corner at short offset transform faults. The asymmetry predicted by the twisting moment model is generally too small; it predicts several hundred meters at a long offset transform fault and much less at a short offset transform. In addition, the twisting mechanism predicts a high inside corner at fast-spreading, non-rifted ridge transform intersections; instead we see an inside corner low as predicted by our model.

In some places, the inside corner appears to be bordered by steep escarpments on at least three sides; two parallel to and facing the rift valley and transform fault as would be expected, but also a third escarpment parallel to and facing away from the transform fault. The former two escarpments have been interpreted to be normal faults by numerous investigators (e.g., Fox and Gallo, 1984; Macdonald *et al.*, 1986). We interpret this third set to be caused by normal faulting as well, resulting from differential uplift and possible flexure of the lithosphere. A simple calculation suggests that, for an elastic thickness of 8 km, the stresses involved in the flexing of the lithosphere near the inside corner are approximately 3 kilobars (Young's modulus =  $5 \times 10^{10}$  Pa). We assume for the purpose of this calculation that the difference in long wavelength curvature between

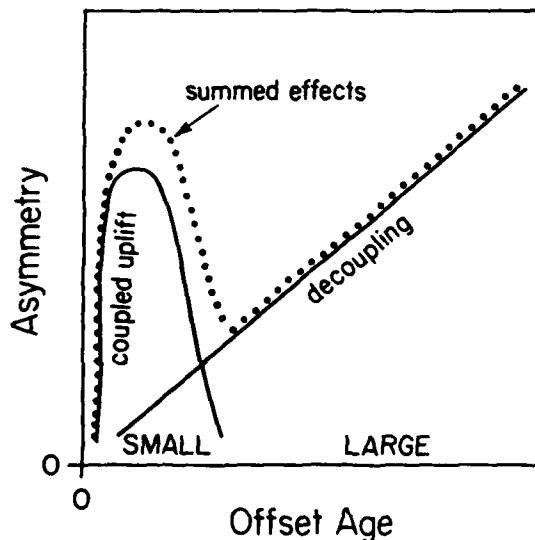


Figure 11. Postulated relative contribution of decoupling and coupled uplift to asymmetry at various offset ages, considering rifted spreading centers only. Zero offsets have no asymmetry, and offsets one-quarter to one-half rift valley width will begin to have coupled uplift. Coupled uplift ceases to affect inside corner as offset increases, because inside corner becomes distant from upwarped older plate. Decoupling grows due to greater rift valley relief resulting from the thermal effects of increasing age contrast across the fracture zone. The resulting bimodal curve may partially explain the scatter in Figure 5(d).

the inner floor of the rift and the rift mountains is caused by flexure). This is close to the yield strength of olivine for conditions appropriate to this problem (e.g., see Figure 15 in Tapponier and Francheteau, 1978), which suggests that the lithosphere if bent far enough may occasionally break near the high inside corner, creating normal faults that dip away from the transform fault.

### 6.3. IMPLICATIONS FOR SCARS MADE BY RIDGE OFFSETS

We hypothesize that inside corners at long offsets subside rapidly (Figure 6) because they are decoupled by the active transform. They are rejuvenated by coupled uplift as they pass the opposite spreading center, but then do not subside quickly because they are welded to the outside corner block of the now thick plate (Figure 8). The low elevation of the outside corner likewise should persist in inactive fracture zones because of the weld, leading to the characteristic asymmetric cross section of fracture zones formed at slow spreading ridges (Searle and Laughton, 1977; Collette, 1986).

If some bending stress is 'frozen in' in old fracture zones, the geoid anomaly will be enhanced over and above the anomaly that would be produced by non-stress-supported topography. Since coupled uplift at small offsets is capable of producing large flexure as well as large topographic asymmetry, we predict that the geoid anomalies over fracture zones caused by short transform offsets may be easily as large as those of fracture zones caused by long transform offsets. Indeed, Seasat-derived geoid anomalies over the scar from the small 33°30' S offset on the Mid-Atlantic Ridge are as large as those from the scars of the neighboring Cox and Meteor Transforms, which are long offsets (Gibert and Courtillot, 1988).

In this analysis we do not address the force causing uplift of the inside corner, but rather start with uplift as a given, taking the existence of the rift valley as proof that uplift does occur. We suggest that whatever mechanism creates the rift valley (and hence the rift mountains) also provides the uplift force for the high inside corner. Several competing hypotheses have been put forward for the origin of the rift valley: the viscous head loss model (Sleep, 1969; Lachenbruch, 1973, 1976; Parmentier and Forsyth, 1985), the steady state necking model (Tapponier and Francheteau, 1978), and the bending

moment model (Phipps Morgan *et al.*, 1987). All provide the needed uplift and are compatible with our hypothesis for the origin of high inside corners.

### 7. Conclusions

The conclusions reached in this paper represent three different levels of confidence. That high inside corners are characteristic, persistent features of rifted slow spreading ridges seems inescapable. Similarly, we can be certain that they do not occur at fast spreading ridges, and that their size is not a simple function of offset length. A second level of confidence concerns their origin. That high inside corners are caused by decoupling in the active transform is supported by three lines of evidence: the apparent tilting of the outside corner in contrast with the normal faulting of the inside corner, the good correlation between rift valley relief and the size of the asymmetry, and the presence of inferred strike slip faulting adjacent to the lone example of an anomalously tilted, high outside corner at the Mid-Cayman Rise spreading center. On a third level of confidence, we speculate that the large height of inside corners at small offsets can be explained by coupled uplift. The combined hypotheses may be summarized as follows: At slow spreading ridges the lithosphere is formed at a low elevation in the rift valley floor, and goes through uplift as it moves up the rift valley walls (Atwater and Mudie, 1973; Macdonald and Luyendyk, 1977). A transform offset will juxtapose a low block that is in the rift valley against a block that has already gone through its uplift. If these blocks weld to each other, when the lower block goes through its uplift it will lift the upper block with it – the coupled uplift – and make a high inside corner (at a short offset) or a rejuvenated older plate (at a long offset). In contrast, the decoupled inside corner is free to rise. Therefore we generalize that the decoupled inside corner reflects the 'equilibrium' elevation of the lithosphere, whereas the outside corner, rejuvenated older plate, and short offset inside corner reflect elevations that are influenced by coupling and the attendant flexure of the lithosphere.

### Acknowledgements

We thank John Bicknell, Y. J. Chen and P. J. Fox for helpful discussions, and P. J. Fox, N. R.

Grindlay, D. G., Gallo, and R. A. Pockalny for making available unpublished charts. The manuscript benefitted greatly from reviews by Roger Searle and Tanya Atwater. The figures were drafted by Antoinette Padgett, and Sam Welch helped with computer work. Support came from ONR contract N00014-87K-0152 and NSF grant OCE 86-09706.

## References

- Abrams, L. J., Detrick, R. S., and Fox, P. J., 1988. Morphology and Crustal Structure of the Kane Fracture Zone Transverse Ridge. *J. Geophys. Res.* **93**, 3195-3210.
- Atwater, T. M. and Mudie, J. D., 1973. Detailed Near-Bottom Geophysical Study of the Gorda Rise. *J. Geophys. Res.* **78**, 8665-8686.
- Bryan, W. B. and Moore, J. G., 1977. Compositional Variations of Young Basalts in the Mid-Atlantic Ridge Rift Valley near Lat. 36°49' N. *Geol. Soc. Amer. Bull.* **88**, 556-570.
- Caytrough, 1979. Geological and Geophysical Investigation of the Mid-Cayman Rise Spreading Center: Initial Results and Observations, in M. Talwani, C. G. Harrison, and D. E. Hayes (eds.), *Deep Drilling Results in the Atlantic Ocean: Ocean Crust, Maurice Ewing Series 2*. Amer. Geophys. Union, Wash., D.C., pp. 66-93.
- Chen, Y. J., 1988. A Mechanical Model for Producing the Topographic Feature of 'Inside Corner High' at a Ridge-Transform Fault Intersection. *Trans. Amer. Geophys. Union, EOS* **69**, 489.
- Collette, B. J., 1986. Fracture Zones in the North Atlantic: Morphology and a Model. *J. Geol. Soc. London* **143**, 763-774.
- Crane, K. L., Aikman, F., Embley, R., Hammond, S., Malahoff, A., and Lupton, J., 1985. The distribution of hydrothermal fields on the Juan de Fuca Ridge. *J. Geophys. Res.* **90**, 727-744.
- Deffeyes, K. S., 1970. The Axial Valley: A Steady State Feature in the Terrain, in J. Johnson and B.C. Smith (eds.), *Megatectonics of Continents and Oceans*. Rutgers Univ. Press, Brunswick, N.J., pp. 194-222.
- Fox, P. J. and Gallo, D. G., 1984. A Tectonic Model for Ridge-Transform-Ridge Plate Boundaries: Implications for the Structure of Oceanic Lithosphere. *Tectonophysics* **104**, 205-242.
- Fox, P. J., Grindlay, N. R., Macdonald, K. C., Bicknell, J., and Forsyth, D. W., 1985. The Morphotectonic Character of the Mid-Atlantic Ridge between 31 S and 34 S: Implications for Plate Accretion. *Trans. Amer. Geophys. Union, EOS* **66**, 1091.
- Francheteau, J., Choukroune, P., Rangin, C., and Seguret, M., 1979. Bathymetric Map of the Tamayo Transform Fault, in B. T. R. Lewis, P. Robinson et al., *Initial Reports of the Deep Sea Drilling Project, Leg 65*. U.S. Govt. Printing Office, Wash., D.C., color map supplement.
- Gallo, D. G. and Fox, P. J., 1988. A Seabeam Investigation of the Garret Fracture Zone: Constraints on the Tectonics of Very-Fast-Slipping Transforms. *Marine Geophys. Res.* (submitted).
- Gallo, D. G., Fox, P. J., and Macdonald, K. C., 1986a. A Sea Beam Investigation of the Clipperton Transform Fault: The Morphotectonic Expression of a Fast Slipping Transform Boundary. *J. Geophys. Res.* **91**, 3455-3467.
- Gallo, D. G., Fox, P. J., Madsen, J. A., Macdonald, K. C., and Forsyth, D. W., 1986b. Fast-Slipping Ridge-Transform Intersections: Morphotectonic Evidence for Thermal Rejuvenation of Old Lithosphere by Ridge Axis Processes. *Trans. Amer. Geophys. Union, EOS* **66**, 1092.
- Gibert, D. and Courtillot, V., 1988. Seasat Altimetry and the South Atlantic Geoid, I. Spectral Analysis. *J. Geophys. Res.* **92**, 6235.
- Grindlay, N. R., Fox, P. J., and Macdonald, K. C., 1985. A Sea Beam Investigation of Christmas and Easter Transform Faults: A Geophysical Investigation of Two Recently Discovered Offsets of the Southern Mid-Atlantic Ridge. *Trans. Amer. Geophys. Union, EOS* **66**, 1289.
- Grindlay, N. R., Fox, P. J., Cande, S. C., Forsyth, D., Macdonald, K. C., and Vogt, P., 1987. Ridge Axis Discordant Zones in the South Atlantic: Morphology, Structure, Evolution, and Significance. *Trans. Amer. Geophys. Union, EOS* **68**, 1491.
- Holcombe, T. L., Vogt, P. R., Matthews, J. E., and Murchison, R. R., 1973. Evidence for Sea-Floor Spreading in the Cayman Trough. *Earth Planet. Sci. Lett.* **20**, 357-371.
- Karson, J. A. and Dick, H. J. B., 1983. Tectonics of Ridge-Transform Intersections at the Kane Fracture Zone. *Marine Geophys. Res.* **6**, 51-98.
- Kuo, B.-Y., Morgan, W. J., and Forsyth, D. W., 1984. Asymmetry in Topography of the Crestal Mountains near a Ridge-Transform Intersection. *Trans. Amer. Geophys. Union, EOS* **65**, 274.
- Lachenbruch, A. H., 1973. A Simple Mechanical Model for Oceanic Spreading Centers. *J. Geophys. Res.* **78**, 3395-3417.
- Lachenbruch, A. H., 1976. Dynamics of a Passive Spreading Center. *J. Geophys. Res.* **81**, 1883-1901.
- Macdonald, K. C. and Luyendyk, B. P., 1977. Deep-Tow Studies of the Structure of the Mid-Atlantic Ridge Crest near Lat. 37 N.: Preliminary Observations. *Geol. Soc. Amer. Bull.* **88**, 621-636.
- Macdonald, K. C., Castillo, D. A., Miller, S. P., Fox, P. J., Kastens, K. A., and Bonatti, E., 1986. Deep-Tow Studies of the Vema Fracture Zone I. Tectonics of a Major Slow Slipping Transform Fault and its Intersection with the Mid-Atlantic Ridge. *J. Geophys. Res.* **91**, 3334-3354.
- Madsen, J., Fox, P. J., and Macdonald, K. C., 1986. Morphotectonic Fabric of the Orozco Transform Fault: Results from a Sea Beam Investigation. *J. Geophys. Res.* **91**, 3439-3454.
- Mammerickx, J., Reichle, M. S., and Reid, I. D., 1978. Bathymetry of the Rivera Fracture Zone. IMR Technical Report Series TR 62, Scripps Institution of Oceanography.
- OTTER, 1984. The Geology of the Oceanographer Transform: The Ridge-Transform Intersection. *Marine Geophys. Res.* **6**, 109-141.
- Parmentier, E. M. and Forsyth, D. W., 1985. Three Dimensional Flow Beneath a Slow-Spreading Ridge Axis: A Dynamic Contribution to the Deepening of the Median Valley Toward Fracture Zones. *J. Geophys. Res.* **90**, 678-684.
- Parsons, B. and Sclater, J. G., 1977. An Analysis of the Variation of Ocean Floor Bathymetry and Heat Flow with Age. *J. Geophys. Res.* **82**, 803-827.
- Phillips, J. D., and Fleming, H. S., 1978. Multi-beam Sonar Study of the Mid-Atlantic Ridge Rift Valley, 36-37 N. *Geol. Soc. Am. Map Ser. MC-19, 1-5*.
- Phipps Morgan, J., Parmentier, E. M., and Lin, J., 1987. Mechanisms for the Origin of Mid-Ocean Ridge Topography: Implications for the Thermal and Mechanical Structure of Accreting Plate Boundaries. *J. Geophys. Res.* **92**, 12 823-12 836.
- Pockalny, R. A., Detrick, R. S., and Fox, P. J., 1988. The Morphology and Tectonics of the Kane Transform from Sea Beam Bathymetry Data. *J. Geophys. Res.* **93**, 3179-3193.
- Prince, R. A. and Forsyth, D. W., 1988. Three Dimensional Modelling of Gravity Anomalies at the Vema Fracture Zone - Mid-Atlantic Ridge Intersection: Crustal Thickness and the Extent of Local Isostatic Compensation. *J. Geophys. Res.* (in press).

- Purdy, G. M., Rabinowitz, P. D., and Schouten, H., 1978, The Mid-Atlantic Ridge at 23° N: Bathymetry and Magnetics, in W. G. Melson, P. D. Rabinowitz *et al.*, *Initial Reports of the Deep Sea Drilling Project, Leg 45*, U.S. Govt. Printing Office, Wash., D.C., pp. 119-128.
- Rona, P. A. and Gray, D. F., 1980, Structural Behavior of Fracture Zones Symmetric and Asymmetric about a Spreading Axis: Mid-Atlantic Ridge (Latitude 23° N to 27° N), *Geol. Soc. Amer. Bull.* **91**, 485-494.
- Rosendahl, B. R., 1980, Bathymetry of the East Pacific Rise and the Siqueiros Fracture Zone, in B.R. Rosendahl, R. Hekinian *et al.*, *Initial Reports of the Deep Sea Drilling Project, Leg 54*, U.S. Govt. Printing Office, Wash., D.C., color map supplement.
- Rowlett, H., 1981, Seismicity at Intersections of Spreading Centers and Transform Faults, *J. Geophys. Res.* **86**, 3815-3820.
- Rowlett, H. and Forsyth, D. W., 1984, Recent Faulting and Microearthquakes at the Intersection of the Vema Fracture Zone and the Mid-Atlantic Ridge, *J. Geophys. Res.* **89**, 6079-6094.
- Sandwell, D. T., 1984, Thermomechanical Evolution of Oceanic Fracture Zones, *J. Geophys. Res.* **89**, 11 401-11 413.
- Searle, R. C., 1979, Side-Scan Sonar Studies of North Atlantic Fracture Zones, *J. Geol. Soc. London* **136**, 283-292.
- Searle, R. C. and Laughton, A. S., 1977, Sonar Studies of the Mid-Atlantic Ridge and Kurchatov Fracture Zone, *J. Geophys. Res.* **82**, 5313-5328.
- Sleep, N. H., 1969, Sensitivity of Heat Flow and Gravity to the Mechanism of Seafloor Spreading, *J. Geophys. Res.* **74**, 542-549.
- Sleep, N. H. and Biehler, S., 1970, Topography and Tectonics at the Intersections of Fracture Zones with Central Riffs, *J. Geophys. Res.* **75**, 2748-2752.
- Sykes, L. R., McCann, W. R., and Kafka, A. L., 1982, Motion of Caribbean Plate During Last 7 Million Years and Implications for Earlier Cenozoic Movements, *J. Geophys. Res.* **87**, 10 656-10 676.
- Tapponier, P. and Francheteau, J., 1978, Necking of the Lithosphere and the Mechanics of Slowly Accreting Plate Boundaries, *J. Geophys. Res.* **83**, 3955-3970.



# This publication is available in microform.

University Microfilms

International reproduces this  
publication in microform:  
microfiche and 16mm or  
35mm film. For information  
about this publication or any  
of the more than 13,000 titles

we offer, complete and mail the coupon to: University  
Microfilms International, 300 N. Zeeb Road, Ann Arbor,  
MI 48106. Call us toll-free for an immediate response:  
800-521-3044. Or call collect in Michigan, Alaska and  
Hawaii: 313-761-4700.

Please send information about these titles:

Name \_\_\_\_\_

Company/Institution \_\_\_\_\_

Address \_\_\_\_\_

City \_\_\_\_\_

State \_\_\_\_\_ Zip \_\_\_\_\_

Phone (     ) \_\_\_\_\_

University  
Microfilms  
International

The Geology of North America  
 Vol. M, The Western North Atlantic Region  
 The Geological Society of America, 1986

## Chapter 4

# *The crest of the Mid-Atlantic Ridge: Models for crustal generation processes and tectonics*

**Ken C. Macdonald**

*Department of Geological Sciences and Marine Science Institute, University of California at Santa Barbara, Santa Barbara, California 93106*

### HISTORICAL INTRODUCTION

By 1854, there were enough deep ocean soundings to allow M. F. Maury to draw the first bathymetric chart of the North Atlantic Ocean in 1855. He defined the great shoaling "middle ground" of the Atlantic basin, later to be known as the Mid-Atlantic Ridge (MAR). It is interesting to note that during the Challenger expedition (1872-1876), Sir Wyville Thomson predicted, on the basis of water temperatures alone, that the MAR is a nearly continuous topographic barrier dividing the Atlantic Ocean. In the 1950s, continuous echogram profiles revealed the presence of a deep median valley along the axis of the MAR (Heezen and others, 1959; Hill 1960). Seismicity (Gutenberg and Richter, 1954) and the occurrence of youthful basaltic lavas on the MAR (Shand, 1949) indicated that the median valley was a geologically active rift zone. Heezen (1960) first suggested that extension across the rift valley might be responsible for accretion of basaltic oceanic crust and the drift of the continents, but his contention that this rifting resulted from expansion of the earth was incorrect. High heat flow measured on the MAR (Bullard and Day, 1961) and large axial magnetic anomalies (Heezen and others, 1959) were added to seismicity and recent volcanism as enigmas associated with the rift valley.

In his seafloor spreading hypothesis Hess (1962) elegantly explained these puzzling observations in a unified model, and the bilateral symmetry of magnetic anomalies found on other mid-ocean ridges (Vine and Matthews, 1963; Vine, 1966) elevated seafloor spreading to a widely accepted theory. However, there were early indications that the MAR from 10 to 50°N was problematical. During the flurry of magnetic anomaly studies in the 1960s that demonstrated seafloor spreading in one ocean basin after another, magnetic anomalies over the "type" mid-ocean ridge in the northern Atlantic eluded a clear simple seafloor spreading interpretation, except over the Reykjanes Ridge.

There was little doubt, however, that the MAR had to be a major oceanic spreading center and that the median valley must mark the axis of spreading. To test this hypothesis, the first exten-

sive study of the MAR median valley was launched by Canadian investigators at 45°N based on Hill's (1960) earlier work in the area (Fig. 1). In the next several years, the ridge at 45°N was studied in unprecedented detail, including high density magnetic, gravity, and bathymetric surveys (e.g., Loncarevic and others, 1966; Loncarevic and Parker, 1971), seismic refraction (e.g., Keen and Tramontini, 1970), and extensive sampling and experimental work (e.g., Aumento, 1968; Barrett and Aumento, 1970; Irving, 1970). Numerous petrologic and geochemical studies yielded the first testable models for oceanic crustal formation (e.g., Cann, 1970; Aumento and others, 1971). At about the same time, significant but less intensive studies were carried out at 23°N (van Andel and Bowin, 1968) and at 43°N (Phillips and others, 1969).

In spite of these detailed and carefully designed studies, the geophysical structure, fine-scale tectonics and petrogenesis of the MAR remained obscure. For example, correlatable magnetic anomalies, the fundamental measure of seafloor spreading, were still poorly resolved, and even the most sophisticated techniques for analyzing magnetic data yielded only marginal results (Loncarevic and Parker, 1971). Many of the unanswered questions were addressed by more advanced technology that became available in the late 1960s and early 1970s. In the Trans-Atlantic geotraverse program (TAG), new efforts included long, high-resolution geophysical profiles followed by detailed narrow-beam mapping and sampling of the MAR from 24 to 27°N (Fig. 1). A dive program followed in 1982 using the research submersible ALVIN (Rona and others, 1982).

The most ambitious and comprehensive MAR program was project FAMOUS at 37°N (Heirtzler and Le Pichon, 1974). This program centered around the first use of manned submersibles in mid-ocean ridge exploration, but many other technologies were also used and tested during FAMOUS (French-American Mid-Ocean Undersea Study). These included deep-tow, ANGUS (Acoustically Navigated Geologic Underwater System), ocean bottom seismometer refraction, transponder navigated dredging, GLORIA long-range side-scan sonar, SASS multi-beam echosounding, LIBEC large area photography, and near-bottom mag-

netic and thermal measurements. Although the new techniques elucidated and more carefully defined many of the vexing problems concerning MAR tectonics, some of the old problems remained and many new ones arose as we investigated crustal generation processes on a finer scale. The MAR seemed fairly simple in the mid to late 1960s once it was recognized as a major plate boundary where the oceanic crust is accreted within and beneath the rift valley. Resolving the tectonics on the scale of terrestrial field investigations, however, proved to be a difficult and rewarding challenge.

In this chapter I shall discuss the detailed investigations of the MAR from 36 to 37°N carried out during the FAMOUS (1973-74) and AMAR (ALVIN Mid-Atlantic Ridge) (1978) ALVIN expeditions. In addition, reference will be made to work from 45°N, 26°N and 23°N, and to recent studies near the Oceanographer, Kane, and Vema fracture zones. The following topics will be discussed: (1) gross structure of the MAR, (2) tectonics and volcanism within the rift valley, (3) models for the axial

magma chamber, (4) disruption of spreading center processes by closely spaced transform faults.

## 1. GROSS STRUCTURE OF THE MID-ATLANTIC RIDGE

The large-scale geomorphology of oceanic spreading centers seems to be controlled primarily by total opening rate, which varies from about 1 to 16 cm/yr. At the slow total opening rates of 1 to 3 cm/yr characteristic of the MAR in the north Atlantic, a deep rift valley marks the spreading center (Figs. 2, 3). At spreading rates of 3 to 5 cm/yr (slow-intermediate transition), characteristic of the south Atlantic and parts of the Indian Ocean, an axial rift valley is well developed only near transform faults, shoaling significantly and almost disappearing between transform faults. The median valley is a "nested" rift, with an inner floor bounded by block-faulted inner walls (Needham and Francheteau, 1974). Beyond are faulted but relatively horizontal terraces bounded by the outer walls (Macdonald, 1975) (Fig. 4). The extremely rough and faulted topography created in the rift valley is largely preserved in the ocean basin, diminished only by sediment burial. At intermediate opening rates of 5 to 9 cm/yr, the rift valley, if present, is only 50 to 200 m deep. This shallow rift is

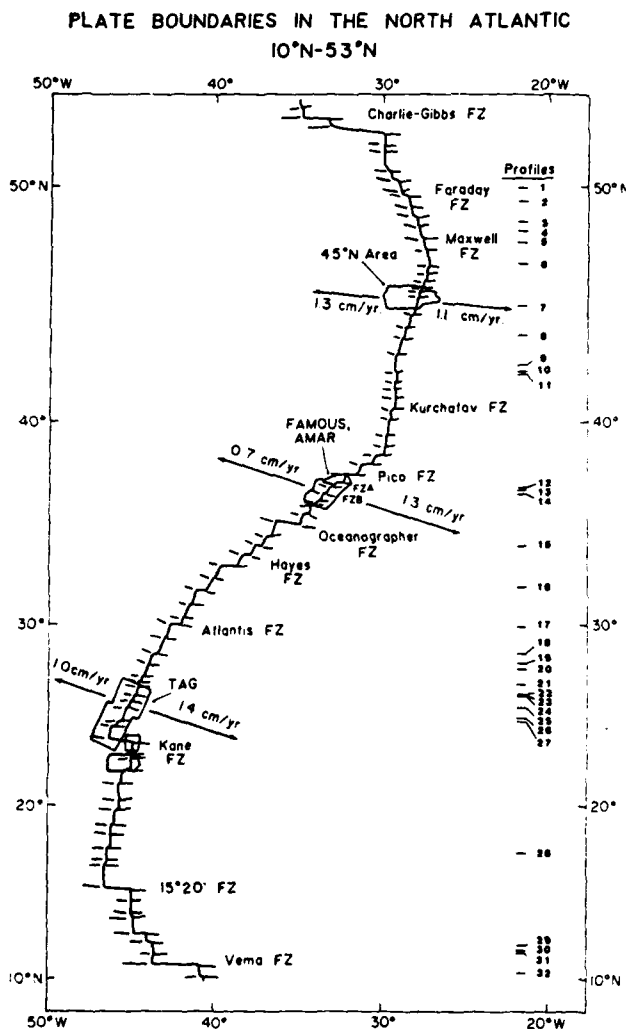


Figure 1. Detailed information of the Mid-Atlantic Ridge plate boundary based on detailed surveys (areas enclosed in boxes) and on GEBCO charts. Detailed study areas discussed in the text are shown with local spreading rates indicated. Fracture zones are shown in red. The latitudes of numbered median rift profiles in Figure 3 are indicated on the right. Notice how frequently the MAR is interrupted by transform faults. Many of the transform faults offset the ridge only a short distance (<30 km) and appear as bends in the overall trend of the MAR. Only the first 100-200 km of the fracture zone traces are shown in red. Many of the traces are not colinear with the associated transform faults suggesting minor shifts in the locations of the transform faults as shown in Figure 10D (see section 4 for discussion.)

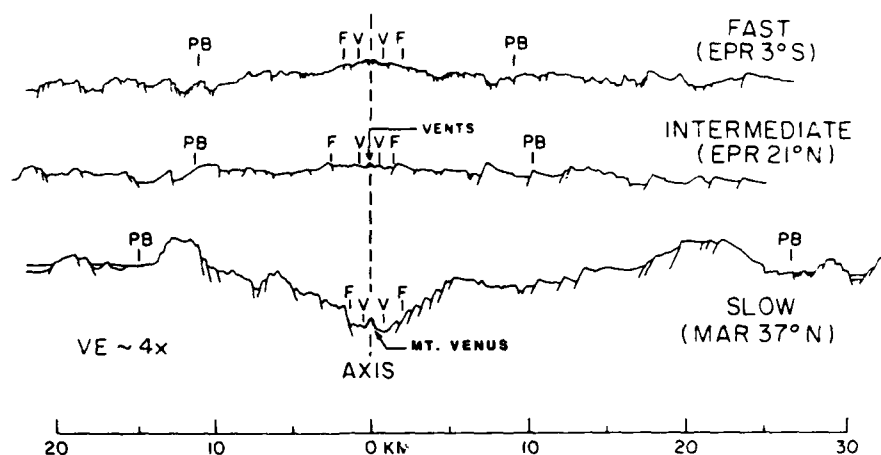


Figure 2. High resolution deep-tow profiles of the Mid-Atlantic Ridge rift valley in the FAMOUS area (bottom) with profiles of the intermediate and fast spreading parts of the East Pacific Rise for comparison. Neovolcanic zone bracketed by Vs, zone of fissuring by Fs, plate boundary zone (width of active fault zone) by PBs. Data from Macdonald and Luyendyk (1977), Lonsdale (1977), Normark (1976), and Shih (1980).

superposed on a broad axial high and the flanking topography is relatively smooth (Fig. 2). At fast spreading rates (greater than 9 cm/yr) there is no rift valley: instead a triangular, semi-circular or rectangular-shaped axial high is observed (e.g., EPR south of 15°N; Rea, 1978; Macdonald and others, 1984). The topography is relatively smooth with a fine-scale horst and graben structure.

Careful inspection of the regional bathymetry of the MAR (Plate 2) reveals that the rift valley is continuous except near major hot spots. The ubiquity of a rift valley on all non-hot spot slow spreading ridges suggests that it is a steady state structure (Fig. 5) (Deffeyes, 1970; but see Vogt, this volume, Ch. 24). If this is true, a problem arises in explaining the disappearance of the axially dipping regional slope of the rift valley as it is transformed into the horizontal undulating relief of the rift mountains (Harrison and Watkins, 1977; Verosub and Moores, 1981). One model is that the rift valley walls are tilted back to approximately horizontal in the rift mountains. The rift valley/rift mountain transition may be accomplished by a modest rotation (5–9°) of the entire rift valley half section as it passes into the rift mountains. A second model is that the rift valley is undone by “unfaulting” along pre-existing inward-facing faults (Harrison, 1974). Thus, as new normal faults are created near the center of the valley, relict normal faults are collapsed by reverse faulting at the valley edges. A third hypothesis is that the rift valley staircase is effectively over-printed by normal faults that dip away from the valley axis (Macdonald and Atwater, 1978a). These may be new fault planes or reactivated faults that previously had small offsets. All three processes must be acting in the rift mountains to maintain a steady state rift valley (Macdonald and Atwater, 1978a; Harrison and Stieltjes, 1977). These processes are related to a significant tilting of fault blocks away from the rift axis by at least 10–30° (Macdonald and Atwater, 1978b). This tilting is either manifested by flexure and resulting failure of the crust by

outward-dipping normal faulting, or by simple tilting of crustal blocks (Macdonald and Atwater, 1978b). These processes occur as far as 30 kilometers off axis, which accounts for the greater width of the plate boundary zone on slow spreading ridges (approximately 60 kilometers), compared with fast spreading centers (about 8–20 kilometers) (Shih, 1980).

There is still considerable debate over the size occurrence and mechanisms of Atlantic oceanic crust rotation. One hypothesis is that the rotations may be surprisingly large, and that significant outward tilting may be accomplished by rotation along listric normal faults that occur in the rift valley and rift mountains. A listric normal fault is one that is curved and concave upward, such that the fault dip is high or medium angle (greater than 45°) near the surface, decreasing to near horizontal at depth. However, it should be noted that there is little evidence from ophiolites for crustal tilts exceeding 60° as suggested by Verosub and Moores (1981).

Bathymetric profiles of the rift valley reveal that, while the valley is present nearly everywhere, its shape, depth and width may vary considerably (Fig. 3). Depth of the valley floor relative to the rift mountains may vary in the extreme, from 1.0 to 2.8 km, with a mean value of 1.4 km (Fig. 5). The width between the shallowest points of the bounding scarps generally varies from 20 to 40 km. The variation in depth to the floor of the rift valley is related to proximity to transform faults.

Any model for the creation of the MAR rift valley must account for its extraordinary depth and its disappearance at intermediate spreading rates. I have compiled data from the MAR, the East Pacific Rise, (EPR), the Indian Ocean Ridge, and the Pacific Antarctica Ridge to investigate the disappearance of the rift valley as a function of spreading rate (Fig. 5). It is almost always present (except for major hot spots) at spreading half-rates lower than 1.7 cm/yr. At spreading half-rates above 4.5 cm/yr.

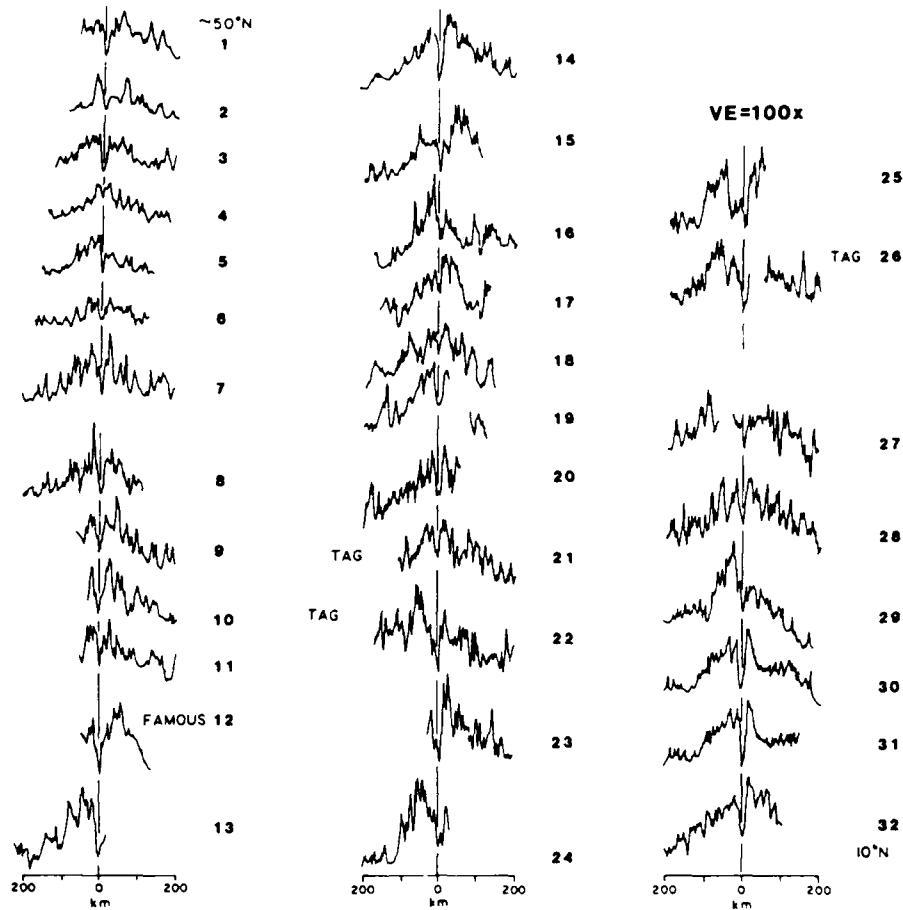


Figure 3. Profiles of the MAR rift valley from 10° to 50°N. All are surface vessel echo-sounding profiles except for profile 12 in the FAMOUS area (which is the same as the deep-tow MAR profile in Figure 2). Notice how the median rift valley is ubiquitous, its depth varying from 1.0 to 2.8 km. On profile 4 the valley is partially filled in by a seamount. The shape of the valley varies from a V-shaped to a U-shaped structure as discussed in the text.

an axial high is always present, while for half-rates between 1.7 and 4.5 cm/yr the axis may have either a rift valley or a gentle axial high with a very shallow summit rift zone (Figs. 2 and 5).

The transition from rift valley to axial high as a function of spreading rate is more gradual than one might conclude from the data in Figure 5. For spreading half-rates exceeding 1.7 cm/yr, a rift valley greater than 300 m deep occurs only within 20 km of a triple junction or transform fault intersection. A good example is the EPR near 23°N where a 600 m deep rift valley occurs 12 km away from the intersection of the EPR with the Tamayo Fracture zone. It is indistinguishable from the inner rift of the FAMOUS area (see Fig. 6 in Macdonald and others, 1979 and compare with Figures 2 and 3). Yet, only 30 km from the intersection, the EPR is marked by a clear axial high. In addition, many of the profiles in Figure 5 occur near ridge-transform intersections. Thus a model for rift valley dynamics must account for a gradual disappearance of the rift valley at spreading half-rates exceeding 1.7 cm per year,

and the persistence of a rift valley at rates up to 9.0 cm per year near transform fault or triple junction intersections.

There is a plethora of rift valley models. Of the kinematic models, there are several that explain rift valleys and axial peaks as caused by imbalances in the width of the crustal accretion zones versus the width of the lithospheric acceleration zones (Defeyes, 1970; Anderson and Noltmeyer, 1973; Nelson, 1981; Reid and Jackson, 1981). These models suggest that creation of the oceanic crust takes place over a wider region than the active tectonic zone, that is, an area wider than 60 km. This contradicts *Alvin* observations and deep-tow magnetic inversion studies that place upper bounds on the width of the zone crustal formation (Ballard and van Andel, 1977; Macdonald, 1977). Pálmason's (1980; this volume) kinematic model does not encounter this contradiction, but does not address the problem of creating a deep rift valley since one does not exist in Iceland.

The two most applicable models are the *viscous head loss*

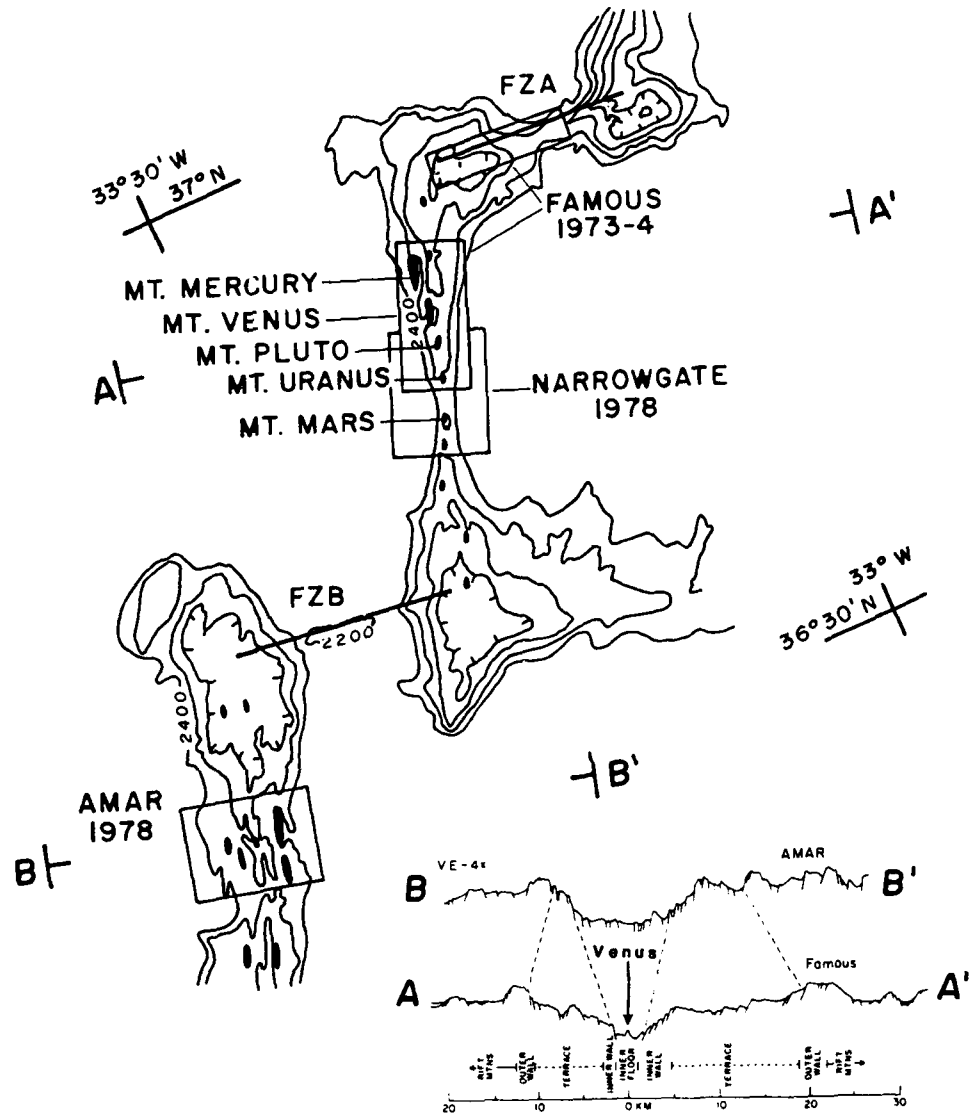


Figure 4. Charts of the FAMOUS and AMAR rifts, contour interval 200 m (see also Vogt, this volume Ch. 24). The rift segment from FZA to FZB is referred to in the literature as the *FAMOUS* rift or *rift valley 2*, while the segment south of FZB is known as the *AMAR* rift or *rift valley 3*. Areas of intensive study using submersibles are shown in red boxes. *Alvin* studies were also carried out in the rift mountains and on FZB, while other instruments such as GLORIA, Deep-Tow, and ANGUS were used over a much broader area. Inner floor volcanoes are shown as red patches and the inferred active transform fault traces are shown as red lines. Many of the volcanoes in the AMAR rift are relatively old and fault-bounded. Profile A-A' of the FAMOUS rift is typical of a V-shaped valley cross-section with a narrow inner floor and wide terraces, while deep-tow profile B-B' of the AMAR rift is typical of a U-shaped valley, a cross-section with a wide inner floor and narrow terraces. An evolutionary sequence may exist with the U- and V-shaped rift valleys as end-members in which the walls bound the width of the neovolcanic zone and influence the fidelity of the recording of magnetic anomalies. Note that the FAMOUS and AMAR rifts are 20° oblique to FZA and FZB, however they are perpendicular to the Minster and Jordan (1978) pole of opening for the North Atlantic. Hence oblique spreading here is only apparent. The short offset transform faults have a component of extension across them and do not trace small circles about the pole of opening. The resulting fracture zones, however do trace small circle paths. Note also that the AMAR and FAMOUS rifts appear to overlap at FZB. However, the neovolcanic zones have only a minimal overlap, and the large apparent overlap may be due to north-south lateral shifts of FZB as shown in Figure 9D.

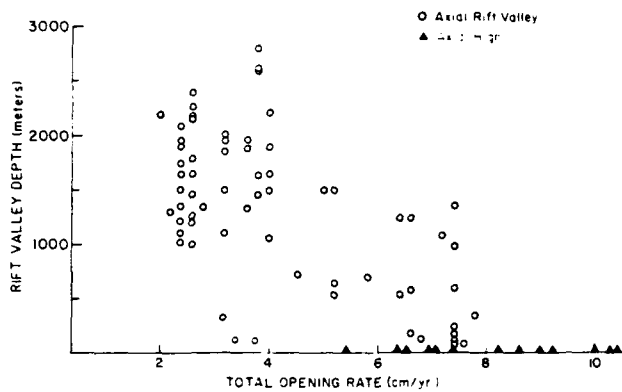


Figure 5. Depth of the median valley as a function of spreading rate. A 1.0–2.8 km deep valley is ubiquitous for spreading half-rates less than 1.7 cm/yr and an axial high is always present at half-rates above 4.5 cm/yr (solid red symbols). Between 1.7 and 4.5 cm/yr a rift valley may occur, but generally near transform fault intersections or triple junction intersections. Thus the disappearance of the rift valley as a function of spreading rate (away from transform or triple junction intersections) is gradual, occurring between half-rates of 1.7 and 4.5 cm/yr.

model of Sleep and others (Sleep, 1969; Lachenbruch, 1973, 1976; Sleep and Rosendahl, 1979), and the *steady-state necking* model (Tapponier and Francheteau, 1978). According to Sleep's model, along the sides of an idealized conduit tapping upwelling limbs of asthenospheric material, viscous forces are sufficient to cause a significant loss of hydraulic head, resulting in a topographic depression over the spreading center. To conserve energy, this head loss is regained by uplift of the rift valley walls relative to the valley floor. The head loss is directly proportional to the upwelling velocity and inversely proportional to the cube of the conduit width. A deep rift valley is present at slow spreading rates because material upwells through a relatively narrow conduit formed by the frozen lithosphere. At faster spreading rates, there is far less head loss because a wider conduit overwhelms the dependence on flow rate. The rift valley is replaced by flat topography or a crestal peak that may be caused by the presence of a low density crustal magma chamber. Thus, the cross section of fast spreading ridges closely approaches that expected from buoyancy in a relaxed state while slow spreading ridges exhibit significant dynamic effects.

In the "steady-state necking" model the rift valley is caused by necking or thinning in a ductile layer beneath the rift valley. The analogy is that of a beam plastically necking-out under tensional stress. The layer does not actually break like a necking beam because new material is added constantly from below (maintaining steady-state), while the entire region is continually uplifted by buoyancy forces. At slow spreading rates the strength of the crust and the axial zone is presumed great enough for necking to be significant, creating a rift valley. At faster rates, the young crust is too hot and weak at shallow levels for this process

to be significant. There is still considerable controversy over which models best describe rift valley dynamics.

While the large scale bilateral symmetry of the MAR suggests a symmetric spreading history, high resolution magnetic studies reveal that spreading is generally asymmetric. For example, in the FAMOUS area, the spreading rate has been grossly symmetrical for 10 m.y. (Bird and Phillips, 1975). However, deep-tow profiles reveal that the grossly symmetrical spreading is composed of episodes of highly asymmetric spreading that reverse in sense. At 37°N the spreading rates for 0–2 Ma are 0.7 cm/yr to the west and 1.3 cm/yr to the east, while the rates for 2–4 Ma are 1.3 cm/yr to the west and 1.0 cm/yr to the east (Macdonald, 1977). Asymmetric spreading that reverses in sense through time results in large scale symmetry when averaged over  $10^7$  years. Asymmetric spreading for crust 0–5 m.y. old in the Atlantic has been reported at 45°N (Loncarevic and Parker, 1971), 26°N (McGregor and Rona, 1975) and 6°S (van Andel and Heath, 1970). Adjacent segments of the MAR often have asymmetric spreading in opposite senses requiring the intervening transform fault to lengthen or shorten. Long term persistent asymmetry in spreading rate and topography has not been reported for the MAR except north of Iceland (Vogt and others, 1982).

## 2. TECTONICS AND VOLCANISM WITHIN THE RIFT VALLEY

### *The Neovolcanic Zone*

The neovolcanic zone is the area straddling the spreading axis in which most of the recent and ongoing surficial volcanism occurs. On the MAR it is characterized by a highly discontinuous chain of volcanoes that are elongate parallel to the spreading axis (Needham and Francheteau, 1974; Macdonald and others, 1975). Mount Venus, in the FAMOUS area, is a typical example with dimensions of  $1 \times 4$  km and a height of 250 m (ARCYANA, 1975). While the axial volcanoes are primarily composed of fresh sediment-free pillow basalts, thin sheet flow basalts (approximately 10–50 cm thick) are also observed, especially on flatter flanking areas and near volcanic collapse pits (Atwater, 1979). The boundaries of the neovolcanic zone are difficult to define precisely because of the lack of reliable radioactive age dating tools for young basaltic rocks. Instead we must use fine-scale sediment cover and the fresh appearance of basaltic lava morphologies. The roughness of the pillow lava surfaces shield local sediment pockets less than 50 cm deep from bottom current erosion, so that sediment cover can be a fairly reliable measure of age. Submarine lavas also exhibit a wide range of fragile ornamentation and glassy surfaces that show visible degradation in only  $10^2$ – $10^3$  years. Other useful criteria for age are the progressive inward palagonitization of pillow rims and a progressive coating of manganese that changes the surface appearance of pillows from glassy to stony (Bryan and Moore, 1977). Based on submersible and deep-tow camera studies using these criteria, it

has been estimated that the neovolcanic zone is only 1 to 3 km wide in the FAMOUS area of the MAR (Ballard and van Andel, 1977; Luyendyk and Macdonald, 1977; ARCYANA, 1975). Credence is lent to these qualitative observations by determinations of other workers at other spreading centers showing that the neovolcanic zone is rarely wider than 3 km regardless of spreading rate (RISE, 1980; Corliss and others, 1979; Rona and Grey, 1980). The neovolcanic zone at various spreading centers is bracketed by V's in Figure 2.

Observations of fresh lavas and sparse sediment cover give only an instantaneous view of the neovolcanic zone. One way to determine temporal variations in the width and location of the neovolcanic zone is through high-resolution deep-tow studies of magnetic anomaly transitions. The magnetic anomaly polarity transition width is a measure of the crustal accretion zone width, including the neovolcanic zone and underlying magnetized plutonics (Harrison, 1968). On the MAR, the transition zone appears to vary between 1 and 8 km in width (Macdonald, 1977). Thus, while the neovolcanic zone is generally only 1 to 3 km wide over short periods of time, there may be a tendency for the crustal accretion zone to wander laterally or periodically widen up to 5 or even 10 km within the rift valley inner floor.

Another way in which magnetic anomalies may be used to define the neovolcanic zone is by mapping maxima in the axial magnetization. The zones of most recent volcanism tend to be marked by very high magnetizations because the basaltic rocks have not yet been exposed to extensive low-temperature oxidation that tends to reduce magnetization (Klitgord and others, 1975). In the FAMOUS and AMAR study areas, inversion of near-bottom magnetic anomalies and direct paleomagnetic sampling show that the most recent lavas have magnetizations of approximately 20 to 40 amps per meter, relative to magnetizations of only 2 to 10 amps per meter for rocks older than 0.5 Ma. While caution must be exercised in using this approach because of other petrologic and geochemical variations that may affect the magnetization (Prévoit and others, 1979), this method has proven very useful for mapping zones of recent volcanism on many spreading centers (Klitgord and others, 1975; Macdonald, 1977; Van Wagonner and Johnson, 1983). The width of the active volcanic zone inferred from crustal magnetization in the FAMOUS area is very narrow, less than 2 to 3 km.

Off-axis volcanism does occur on the Mid-Atlantic Ridge (Heirtzler and Ballard, 1977). In the FAMOUS area, deep-tow magnetic data indicate that up to 10 percent of the volcanism occurs outside the main neovolcanic zone in crust 0.5 to 2.0 m.y. old, that is, 5 to 20 km off axis (Macdonald, 1977; Atwater, 1979).

How often do major volcanic eruptions occur along the MAR neovolcanic zone? A combination of magnetic and physical property studies coupled with seismic refraction, deep-sea drilling analyses, and ophiolite field studies suggest that the thickness of the volcanic section is approximately  $1 \pm 0.5$  km (Hall and Robinson, 1979; Fox and others, 1973; Christensen and Salisbury, 1975; Pallister and Hopson, 1981). This information can be

combined with the precise knowledge of the dimensions and spacing of volcanoes (based on multi-beam charts in the FAMOUS area) to estimate the spatial density of volcanoes in the crustal section. When combined with the spreading rate, the frequency of major eruptive cycles large enough to construct a volcano the size of Mt. Venus can be estimated to be once every 5000 to 10,000 years (Bryan and Moore, 1977; Atwater, 1979). Do these axial eruptions occur rapidly with long periods of intervening quiescence, or is actively fairly continuous at a slow rate? Analogy with terrestrial eruptions suggests the former. Perhaps the best evidence is from deep-sea drilling project (DSDP) holes. For holes greater than 500 m deep, thick crustal units occur in which magnetic, petrologic, and geochemical properties are nearly uniform and are significantly different from crustal sections above or below. In the presence of secular variation of the magnetic field, this suggests eruption episodes of short duration, 1 to 100 yrs, separated by long periods of quiescence (Hall 1976). Eruptive episodes may be far more frequent in Iceland since it is the epicenter of a major hotspot (Saemundsson, this volume).

Another indication of shifting or widening of the neovolcanic zone comes from evidence that reversely magnetized rocks exist within the inner floor of the MAR (Ade-Hall and others, 1973; Johnson and Atwater, 1977). This is quite startling because the crust here should all be of positive polarity. Small outcrops of reversely magnetized rocks sampled from *Alvin* are most likely caused by eruption during a brief reversal within the Brunhes epoch (Van Wagonner and Johnson, 1983). However, the large negative anomalies measured by surface as well as deep-tow magnetometers may be caused by blocks of older crust (>0.7 m.y.) left behind by small jumps of the neovolcanic zone and buried by subsequent lava flows (Macdonald, 1977). There is a 14 percent probability of older negative crust becoming temporarily stranded near the axis due to small lateral shifts (1–5 km) of the neovolcanic zone within the inner floor (Macdonald, 1977).

A difficult problem is how to accumulate a volcanic section approximately 1 km thick when the tallest axial volcanoes are only 250 m high. Occasionally the 1.5 km deep rift valley may be filled with a seamount (Johnson and Vogt, 1973; Vogt, this volume, Ch. 24), but this is observed at only two places along the entire length of the MAR at this time. In general the volcanic section must be approximately 3 to 6 volcanoes thick. The volcanoes must be either down-faulted (Atwater, 1979) or tilted steeply toward the axis (Moore and others, 1974) to allow for vertical accumulation of successive flows. Modelling of magnetic fields (McGregor and Rona, 1975) suggest that down-faulting must occur with, at most, only slight rotation of the volcanoes. Whether the axial volcanoes are actually split in half or transported laterally as intact units is yet another question and is still a point of debate (Atwater, 1979; Ballard and van Andel, 1977).

Observations outside the inner floor of the rift valley suggest that at least some of the axial volcanoes have survived the precarious trip into the rift mountains and onto the terraces. Small volcanoes that are elongate parallel to the spreading axis are

superposed on many of the fault blocks outside the inner floor. Curiously, most of the volcanic highs are not randomly situated, but form lips at the edges of fault blocks (Fig. 6). Of 107 volcanoes mapped outside the inner floor of the FAMOUS area rift valley, 72 (70%) were lips. If volcanoes averaging 500 m wide were randomly distributed in the rift mountains, only 30% would be lips. It is probable that these volcanic lips are created within the inner floor of the rift valley like Mount Venus. If the axial volcano has been dormant for some time, block faulting is likely to be concentrated along its edges where the crust is thinnest, resulting in a volcanic lip perched at the edge of the block fault. However, if the volcano has been recently active and the isotherms are still peaked beneath the edifice, the crust may be thinnest and weakest along its axis and it may be split in two by faulting and rifting. Both examples are common within the FAMOUS and AMAR study areas of the Mid-Atlantic Ridge.

#### Crustal Fissuring

Before the seafloor is 100,000 years old the crust becomes intensely fissured. These fissures closely resemble the *gjar* in Iceland and are typically 1 to 3 m wide, extending 10 m to 2 km along strike (Luyendyk and Macdonald, 1977; Ballard and van Andel, 1977). The most intense fissuring occurs between the distal edges of the neovolcanic zone and the inner walls delimiting the inner floor of the rift valley (the area inside the F's in Fig. 2). Their azimuth closely parallels the strike of the ridge, suggesting that they are caused by tensional failure of the crust during spreading. The tensional stresses producing pervasive fissuring are caused by horizontal acceleration of crust from zero at the idealized center of the neovolcanic zone to the full spreading rate at the edge of the plate boundary zone.

It is likely that these fissure fields provide the principal access for cold seawater to penetrate the young, hot oceanic crust (Lister, 1972; Lowell, 1975). Detailed field observations in the FAMOUS and AMAR areas, as well as recent observations in the TAG area suggest that fissuring is particularly intense on the Mid-Atlantic Ridge with average spacings of approximately 10 to 50 m between major fissures (Ballard and van Andel, 1977; Rona and others, 1982). This intense fissuring may lead to extremely rapid and efficient cooling of the oceanic crust and, as a result, high-temperature hydrothermal activity at the seafloor-ocean interface may be extremely rare. Earthquake focal depths of up to 8–10 km beneath the axis suggest that the fissures may extend to significant depths (Lilwall and others, 1978; Toomey and others, 1982). Instead, most high temperature hydrothermal activity and deposition on the Mid-Atlantic Ridge may be confined to depth with considerable subsurface mixing of fresh seawater with hydrothermal fluids.

#### Faulting

At a distance of 1 to 5 km from the spreading axis, some fissures develop large vertical offsets by normal faulting, with most of the faults dipping toward the spreading center. For the profiles shown in Figure 2, significant faulting begins near points

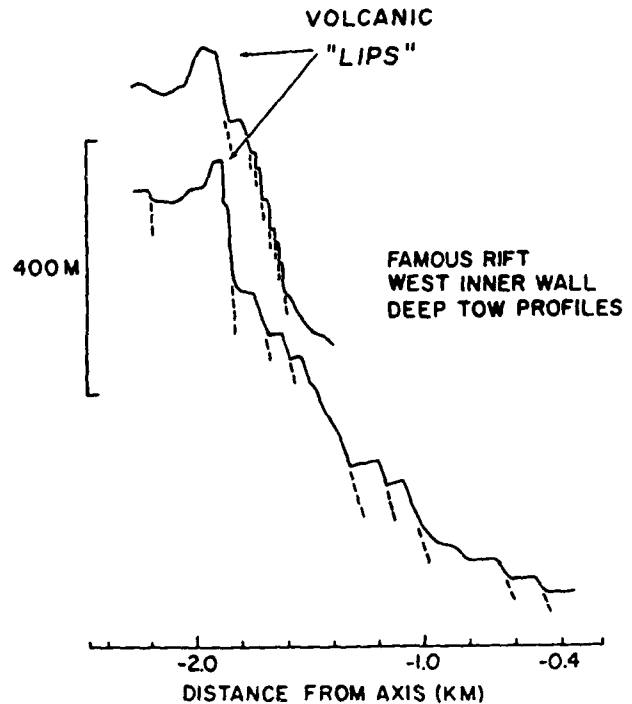


Figure 6. Two high resolution deep-tow profiles of the west inner wall of the FAMOUS rift near Mt. Venus. The character of the inner wall varies considerably even though these profiles are only 1.2 km apart. Note that the inner wall does not provide a deep "road cut" into the oceanic crust since the escarpment consists of at least nine faulted slivers. Also note the volcanic "lip" perched at the edge of the escarpment on both profiles. These volcanoes have been transported out of the inner floor by faulting. Vertical exaggeration = 2.5x.

F. The initiation of normal faulting creates the inner walls of the rift valley that bound the inner floor. Beyond the inner walls are the relatively horizontal, undulating terraces, followed by the outer walls marking the boundary between the rift valley and the rift mountains (Fig. 4, bottom).

While major escarpments on the MAR, such as the inner and outer valley walls, may reach heights of 500 to 1000 m, deep windows are not provided by these scarps because they actually consist of many closely spaced smaller normal faults. The west inner wall of the FAMOUS rift is a typical example (see Fig. 6) in which a single, narrow escarpment 500 to 700 m high actually consists of at least eight normally faulted, 20 to 100 m wide slivers with individual throws of 15 m to a maximum of 200 m. *Alvin* dives reveal that the fault scarps are further obscured by a layer of welded fault breccia.

Long range GLORIA side-scan sonar records indicate that the average spacing of major faulted escarpments on the MAR near 45°N, 40°N, and 36°N average 2 km, both inside and outside the rift valley (Laughton and Searle, 1979). The spacing is a matter of scale and resolution as *Alvin* and deep-tow records show much closer spacings (Macdonald and Luyendyk, 1977;

Ballard and van Andel, 1977). The question of average fault length and continuity encounters the same problem. Major escarpments such as the inner walls of the rift valley are continuous between transform faults and reach 40 to 60 km in length. However, as shown in Figure 6, high resolution profiles only 1.2 km apart show significant changes in fault spacing and throw. Rapid appearance and disappearance of individual faults along strike has been documented during the AMAR *Alvin* dives as well, with faults as large as 200 m in throw persisting only 1 to 2 km along strike as distinct structures.

Both the faults and the fissures result in a significant horizontal extension of the crust. In the FAMOUS area, the combined extension is 11 percent to the west and 18 percent to the east, the difference being in the same sense as the spreading rate asymmetry of 0.7 cm/yr to the west and 1.3 cm/yr to the east (Macdonald and Luyendyk, 1977). This suggests that asymmetric spreading results in asymmetric crustal extension as well as asymmetric crustal accretion.

The depth of faulting along the MAR is a critical unknown. Spectral modeling of surface waves suggest that normal faulting is shallow, only 3 to 5 km deep on the MAR (Weidner and Aki, 1973). Ocean bottom seismometer (OBS) studies on the MAR at 45°N suggest focal depths as great as 10 km (Lilwall and others, 1978), but the results are highly questionable since most of the events occur slightly outside of an array of only three OBSs. However, a recent study on the MAR near 23°N with a larger number of instruments and much better hypocentral control documents focal depths of  $8 \pm 1$  km (Toomey and others, 1982). In addition, refraction work reveals a normal 5–6 km thick oceanic crustal section beneath the inner floor of the rift (Purdy and others, 1982). Thus, normal faulting to depths of 5 to 10 km along the axis is well documented. Francis (1981) has suggested that earthquakes up to 10 kilometers deep imply that normal faulting penetrates through to the mantle near the axis of the MAR. If so, extensive serpentinization of ultramafic mantle material may occur and vertical intrusion of serpentinite may invade much of the base of the crust (Bonatti and Honnorez, 1976; OTTER Scientific team, in press).

#### *Episodicity and Variations Along Strike*

The commonly-used two-dimensional approximation of MAR structure and tectonics just discussed is a useful starting point for analysis, but recent high-resolution studies reveal important variations along-strike (Plate 8A) as well as episodicity in time. Detailed studies using deeply-towed cameras and sonars, submersibles, and multi-beam bathymetry, suggest that volcanism within the inner floor is highly episodic and may follow cycles (Francheteau and others, 1979). Mapping of various lava types and analogues with terrestrial volcanic cycles suggest that pillow lavas and sheet flows are the submarine equivalents of tube-fed and surface-fed pahoehoe, respectively (Ballard and others, 1979; Crane and Ballard, 1980). The analogy suggests that sheet flows erupt from a new volcanic vent at very high effusion rates during

the initial stage of the volcanic cycle. As the volcanic edifices build, the lava starts to flow through a volcanic catacomb of tunnels and tubes rather than erupting directly from fissures. Channeling of lava through the volcanic plumbing system and diminishing effusion rates produce pillow lavas rather than sheet flows. This sequence is supported by detailed petrologic studies in the FAMOUS and AMAR areas (Stakes and others, 1984).

Very detailed paleomagnetic studies using samples collected from *Alvin* and by precise transponder navigated dredging have helped to unravel some of the fine-scale volcano-tectonic development within the inner floor of the FAMOUS and AMAR rifts (Van Wagoner and Johnson, 1983). Magnetization of the collected samples decays by a factor of 5 in only  $10^6$  years (Vogt this volume, Ch. 15). This result agrees well with magnetization determinations made by modeling of deep-tow magnetic fields (Macdonald, 1977). Low magnetizations correlate with high Curie temperatures, suggesting that low temperature oxidation of the magnetic minerals takes place quickly after the basalts are erupted. Assuming other petrologic effects to be negligible, Van Wagoner and Johnson use the rapid decay of magnetic intensity to establish an approximate age determination technique. They find that surficial rocks representing the most recent volcanic phase are 10,000 years old in the FAMOUS area, 30,000 years old in the AMAR area, and 40,000 in the Narrowgate area. The highest magnetizations are found in the center of the Narrowgate area (84 amps/m) suggesting that this area is experiencing a renewed phase of volcanism after a long period of quiescence.

From the FAMOUS-Narrowgate area to the AMAR valley, the period of time since the last phase of volcanism increases and the terrain becomes increasingly controlled by tectonic rather than volcanic processes. During the small volume volcanic episodes in AMAR, the rate of extension and normal faulting exceeds the rate of volcanic extrusion so that no significant axial volcanoes have developed in the neovolcanic zone. While the most recent volcanism in the FAMOUS-Narrowgate area is confined to the narrow inner floor, the broad AMAR inner floor has resulted from a long phase of tectonic extension and normal faulting, combined with a long period of volcanic quiescence.

Tectonism may be quite continuous relative to the periods of quiescence (approximately 10,000 years long) between major episodes of volcanism. The entire length of the MAR under consideration here is seismically active with essentially no earthquake gaps even for short spreading center segments and for time periods as short as ten years (Einarsson, 1979). The continuity of tectonic activity extends even to a daily time span with a steady pulse of microearthquake activity of about 5 to 20 events of magnitude 0 to 1 per day (Reid and Macdonald, 1973; Spindel and others, 1974; Francis and others, 1977, 1978). Most of the microearthquake seismicity is associated with normal faulting in the inner walls of the rift.

The FAMOUS and AMAR projects (Fig. 4) produced the first detailed geologic map of a spreading center on a scale comparable to detailed studies on land. Based on these studies, volcanic and tectonic episodes of activity within the inner floor

are being described in detail. The earlier FAMOUS work is summarized in the April and May 1977 issues of *Geological Society of America Bulletin*. The very fruitful AMAR program is summarized by Atwater (1979), Crane and Ballard (1981) Stakes and others (1984) and Van Wagonner and Johnson (1983). Much of the detailed geological work is still in progress at this writing.

### 3. MODELS FOR THE AXIAL MAGMA CHAMBER

It has been proposed that crustal volcanic and plutonic rocks are formed by differentiation of mantle-derived parent magmas in a shallow axial magma chamber (AMC), rather than by injection and eruption directly from the mantle (Melson and O'Hearn, this volume). The AMC model has been strongly supported by analysis of ophiolites (e.g., Cann, 1974; Dewey and Kidd, 1976; Pallister and Hopson, 1981), petrologic studies of oceanic rocks (e.g., Natland, 1980; Bryan and Moore, 1977; Rhodes and Dungan, 1979), thermal models (Sleep, 1975, 1978; Sleep and Rosendahl, 1979), and seismic experiments (Orcutt and others, 1976). The principal evidence comes from seismic refraction, where an AMC is inferred to exist beneath the axis of the fast spreading East Pacific Rise from travel time delays, and shadow zones for P waves at shot/receiver ranges of 15–35 km (Orcutt and others, 1976; Reid and others, 1977; see Macdonald, 1982, for summary). Such data require a low velocity zone interpreted as a shallow crustal AMC beneath the spreading axis. Refraction studies have indicated AMCs at depths of 2 to 6 km beneath the EPR near 22°N (McClain and Lewis, 1980), 21°N (Reid and others, 1977), 15°N (Trehu, 1982), 13°N (Orcutt and others, in press), 12°N (Lewis and Garmany, 1982), 10°S (Bibee, 1979), and the Galapagos spreading center near 86°W (Bibee, 1979). The original refraction results at the East Pacific Rise at 9°N are substantiated by multichannel seismic reflection work (Herron and others, 1980; Hale and others, 1982). An AMC is not detectable on the EPR near 11°20'N (Bratt and Solomon, 1984) or near 12°N (Lewis, 1983). However, both of these sites are near overlapping spreading centers.

In contrast, numerous seismic refraction studies over the slow spreading MAR have not provided clear evidence for an AMC (Poehls, 1974; Whitmarsh, 1975; Fowler, 1976; Nisbet and Fowler, 1978; Fowler and Keen, 1979; Toomey and others, 1982; Bunch and Kennett, 1980). These experiments include four attempts in the FAMOUS area at 37°N, two at 45°N, one at 23°N and one on the Reykjanes Ridge. On slow spreading centers, however, it is important to keep in mind that severe limitations are imposed by closely-spaced offsets of the spreading center by transform faults. In addition, rift valley topography is large in amplitude and makes travel time corrections difficult. However, the carefully executed refraction and microearthquake experiment at 23°N clearly precludes a shallow crustal magma chamber of any significant size. Normal oceanic crustal structure with a mature thickness of 5 to 6 km occurs beneath the axis, and microearthquakes occur to depths of  $8 \pm 1$  km beneath the axis (Toomey and others, 1982; Purdy and others, 1982). While it is

possible for a seismically undetectable AMC to exist beneath the MAR, it would have to be narrower than one seismic wavelength (approximately 1–2 km).

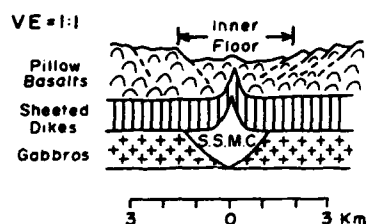
There is little doubt that AMCs have existed beneath all spreading centers at one time or another, but are they steady state features of the mid-ocean ridge system? Are they steady state at fast but not slow spreading centers? The debate continues on this topic. Unless this is a particularly unusual and unique period in the history of mid-ocean ridges, the evidence for AMCs beneath eight out of 10 ridge segments spreading faster than 6 cm/yr suggests that magma chambers are at least quasi-steady state features beneath intermediate and fast spreading centers. By quasi-steady state, I mean that they are permanent, but may vary with time in size and shape.

Numerous thermal models have been proposed for spreading centers, but unfortunately the results are somewhat ambiguous. Sleep's model (1975, 1978) addresses the fine scale thermal structure beneath the spreading center and predicts a steady state magma chamber at intermediate to fast spreading rates. More recent models that account for the importance of hydrothermal heat loss still allow for maintenance of a steady state magma chamber at intermediate to fast spreading rates but not at slow spreading rates (Sleep and Rosendahl, 1979; Sleep, 1983). Kuznir (1980) however, allows for hydrothermal cooling and still obtains a steady state magma chamber approximately 1 to 3 km wide for a slow half spreading rate of 1 cm/yr. At the other extreme, Lister (1983) maintains that hydrothermal circulation precludes the maintenance of a steady state magma chamber at even the fastest known spreading rates. The conflict in thermal models stems from poorly constrained estimates for the magnitude and areal distribution of hydrothermal heat loss at spreading centers, and ignorance of the depth and rate of crustal fissuring. Another important unknown concerns the rate at which cracks propagate downward in the axial zone versus the importance of closing of the cracks by hydrothermal precipitation.

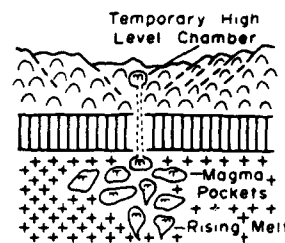
While seismic evidence for AMCs beneath the MAR is negative or at best unresolved, petrologic evidence (Melson and O'Hearn, this volume) suggests that the AMC is quasi-steady state even at slow spreading rates (Bryan and others, 1979; Bryan and Moore, 1977; Stakes and others, 1984). The very narrow range of petrologic composition of basalt samples from the MAR suggests that AMCs are steady state even at spreading rates of 2 cm/yr. If magma chambers were non-steady state (i.e. transient), very primitive or highly fractionated basalts should erupt during the formative and waning stages of the magma chamber, respectively.

In response to this controversy, a number of AMC models have been proposed (Fig. 7). The *infinite onion* model features a steady state AMC in which the edges successively freeze (Cann, 1974). This brought tears to the eyes of seismologists who had found no evidence of an AMC anywhere along the MAR. An *infinite leak* model has been proposed which features an ephemeral AMC and creates the gabbro layer by repeated freezing and coalescing of transient magma chambers (Nisbet and Fowler,

## MAR MAGMA CHAMBER MODELS

A. FUNNEL-SHAPED SEMAIL  
OPHIOLITE MODEL

## C. "INFINITE LEEK" MODEL



## B. "INFINITE ONION" MODEL

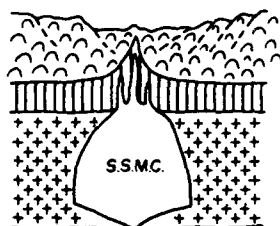
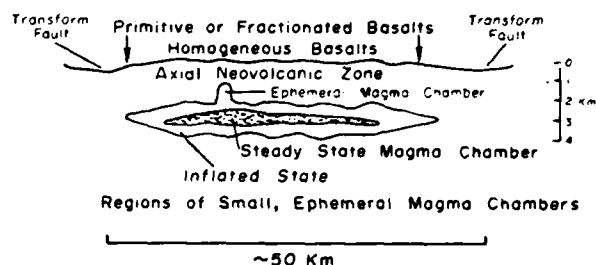
D. ALONG STRIKE VIEW OF MAGMA  
CHAMBER FOR MODELS A,B

Figure 7. Three of the possible models for axial magma chambers beneath the MAR. (A) Model based on observations in the Semail ophiolite in Oman after Pallister and Hopson (1981), (B) the *infinite onion* model after Cann (1974) and Bryan and Moore (1977), (C) the *infinite leek* model after Nisbet and Fowler (1978). The Semail and Infinite onion models predict a steady state magma chamber (S.S.M.C.). As drawn, both chamber models should be seismically detectable, but would not be if they were less than 1–2 km wide. Model (C) predicts a non-steady state magma chamber. See text for discussion. For simplicity, possible subsurface extensions of normal faults into the dike and gabbro layers are not shown. (D) shows a possible along-strike section for the steady state magma chamber models. The chamber may exist in the steady state along only 30 percent of the length of the MAR, confined to the elevated regions of the rift valley away from transform fault intersections.

1978). However, each *leek* is a closed system intrusion that would produce highly fractionated lavas upon freezing. Unless these highly fractionated magmas fail to erupt for some reason, this model directly conflicts with the detailed petrologic sampling of the FAMOUS and AMAR programs (Bryan and Moore, 1977; Stakes and others, in press).

Stakes and others (1984) have proposed an AMC model similar to that for Oman (Pallister and Hopson, 1981) for the MAR based on extensive sampling of the FAMOUS and AMAR rifts. The AMC is *funnel-shaped* with the narrow end down (Fig. 7). In this *funnel* model, steady state replenishing and continued magma mixing account for the uniform composition of the basalts collected from *Alvin*. The chamber is postulated to be only 1 to 2 km wide, sidestepping the negative seismic evi-

dence by making it too narrow to be detected. In addition, the AMC exists as a steady state feature only near the elevated mid-points of the inner floor of the rift valley, away from the cooling edge effects of transform faults. Note that Mt. Venus, which is 15 km away from FZA, is characterized by very primitive basalts that may have erupted directly from the mantle rather than fractionating in a magma chamber. Thus, given that the entire length of the FAMOUS rift is only 43 km, only the central 10 to 15 km of the rift valley or only 1/3 of its total length would retain a steady state AMC in this model. In the past I have advocated a non-steady state AMC at slow spreading rates (Macdonald, 1982), but since the petrologists have retreated to such a tiny  $1 \times 2 \times 10$  km AMC, perhaps the geophysicists should let them keep it! In any case, even if a small AMC such as this persists in a

steady state on the MAR, the lack of significant along-strike continuity of the AMC could explain many of the spreading rate-related structural, tectonic, and volcanic differences between the slow spreading MAR and the fast spreading East Pacific Rise (Macdonald, 1983a, b).

#### 4. DISRUPTION OF SPREADING CENTER PROCESSES BY CLOSELY SPACED TRANSFORM FAULTS

Transform faults are very closely and uniformly spaced on the MAR (Fig. 8). Given that the thermal and structural effects of transform faults extend 15 to 30 km away from their intersections with spreading centers (Fox and Gallo, 1984; and this volume) and that the inter-transform spacing on the MAR is 55 km (Fig. 8), there are essentially no segments of the MAR that are normal or free of transform fault edge effects. In this light it is folly to discuss the tectonics of the MAR without assessing the influences of the transform faults. I shall restrict myself to ways in which the MAR is modified near transform fault intersections. There are four processes that occur near ridge transform (RT) intersections discussed here: (1) deepening and widening of the rift valley due to increased hydraulic head loss; (2) thinning of the oceanic crust due to thermal edge effects; (3) transmission of shear stresses associated with the transform fault into the spreading center domain with resultant rotation of fault trajectories; and (4) a phenomenon I shall call apparent oblique spreading, involving small offset transform faults that do not follow small circles about the pole of opening.

##### *Valley Deepening and Crustal Thinning at RT Intersections*

The imposition of a third rigid boundary at RT intersections may increase the hydraulic head loss by 30 to 40 percent (Sleep and Biehler, 1970). This closely matches the observed increase in depth at RT intersections. For example, the intersection deep at FZA is 600 m or 40 percent deeper than "Narrowgate," which is the inner floor midway between FZA and FZB (Fig. 4). The structural effects on the rift valley are considerable. Both the inner floor and the major normal faults creating the inner and outer walls of the valley plunge towards the intersections with topographic gradients of 15 to 30 m per km (see Fig. 16 in Macdonald and Luyendyk, 1977). The inner floor also widens by as much as a factor of two. Dynamic effects associated with migration of magma along strike beneath the spreading axis may also contribute to the deepening of the valley floor (Parmentier and Forsyth, 1984). Indeed, many of the transform faults are too short (and the juxtaposed lithosphere too thin) to significantly affect the adjoining spreading segment.

In addition to the viscous effects pointed out above, transform faults have profound thermal effects on ridge structure and crustal accretion. The degree of partial melting that may occur in the rising asthenosphere is reduced and the degree of fractional crystallization is enhanced near a RT intersection because the cold bounding edge of the transform is a significant heat sink

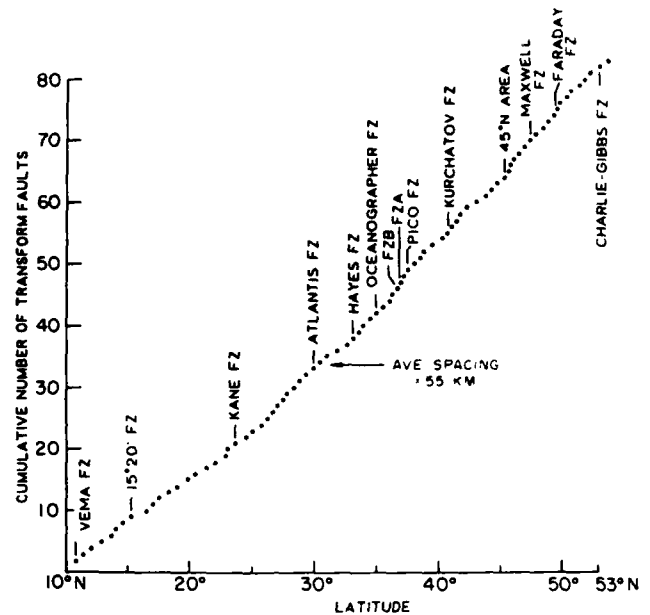


Figure 8. Cumulative number of transform faults on the MAR from 10°N–53°N. The average spacing is 55 km, so close that essentially every segment of the MAR is altered along most of its length by transform fault edge effects. See also Vogt, this volume, Ch. 12.

(Fox and others, 1980; Langmuir and Bender, 1984; Fox and Gallo, this volume). How significant a heat sink depends on the age contrast of the lithosphere near the intersection. As a result, the flux of basaltic melt is reduced and the crust is thinner. Seismic refraction results suggest that the oceanic crust may be thinned by as much as a factor of 2 near the Kane Fracture Zone (Detrick and Purdy, 1980). At large offset transforms on the MAR such as the Vema, lithosphere 30 to 50 km thick may be juxtaposed against the accreting plate boundary "all but nullifying the processes that lead to the emplacement of normal oceanic lithosphere (Fox and Gallo, 1984)." These effects are far greater on the slow spreading MAR than on the EPR because the age contrast for a given offset transform fault is 3 to 9 times greater.

##### *The Transmission of Shear Stresses Into the Spreading Center Domain*

Faults oblique to both spreading center and transform fault trends are common near RT intersections, and are hypothesized to be oblique trending normal faults (Crane, 1976; Lonsdale, 1977; Macdonald and others, 1979). Recent *Alvin* studies on the Oceanographer and Tamayo transform faults confirm that these faults are spreading center-related normal faults that are 30 to 45° oblique to the spreading axis near the RT intersection (OTTER Scientific Team, in press; Tamayo Tectonic Team, 1984). Deep-tow studies near the Vema Fracture Zone show that the normal faults follow intermediate ( $\sigma_2$ ) stress trajectories that rotate smoothly and continuously from spreading center-parallel

## INFLUENCES OF TRANSFORM FAULTS ON AXIAL MAR TECTONICS

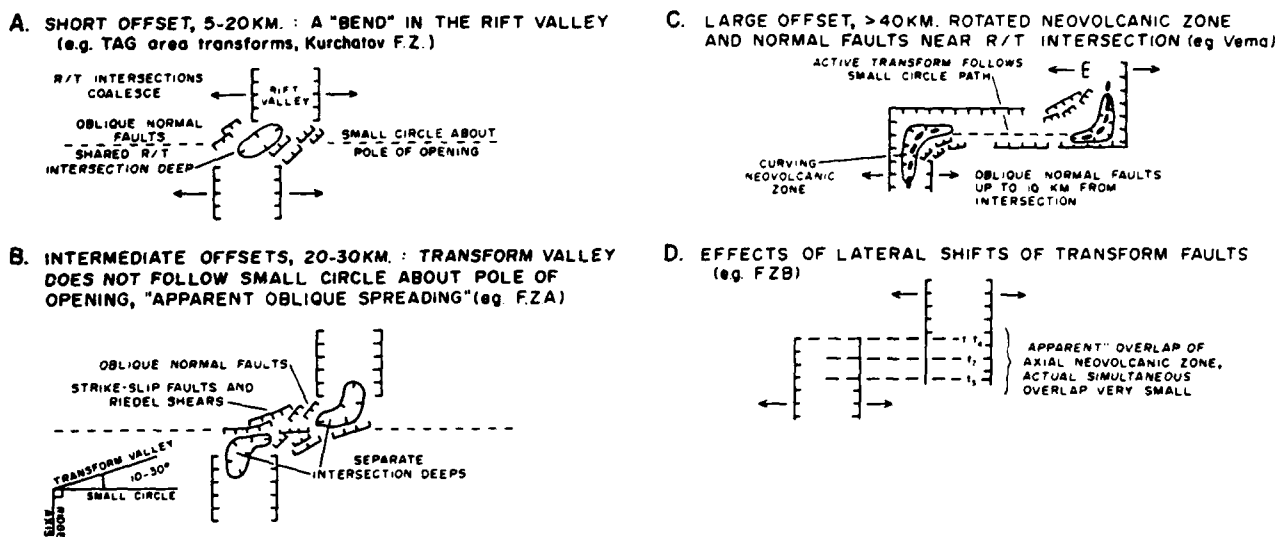


Figure 9. Various ways in which MAR structure is modified near transform fault intersections depending on the length of the offset. Small transform faults (A, B) result in a "bend" in the rift valley trend that may not follow a small circle about the pole of opening. "Apparent" oblique spreading results. Large offset transform faults (C) create a significant rotation of the neovolcanic zone and rift valley normal faults within 5-10 km of ridge/transform intersections. Another common phenomenon is the "apparent" overlapping of spreading centers caused by north-south lateral shifts of the transform fault (D). These shifts cause an echelon overlap of intersection deeps but not a large overlap of the neovolcanic zones.

to 45° oblique to the spreading axis (Macdonald and others, submitted). Rotation of stress trajectories is caused by transmission of transform-related shear stresses into the spreading center domain. Near the Vema transform fault these shear stresses extend into the MAR rift valley at least 7 km along strike (Macdonald and others, submitted).

#### "Apparent" Oblique Spreading

A fundamental premise of plate tectonics is that transform faults trace out small circles about the pole of opening (McKenzie and Parker, 1967). This may not be true for small offset transform faults on the MAR. Notice the enormous number of very small offset (<20 km) transform faults on the MAR in Figure 1 and how they are not sharp perpendicular offsets of the MAR, but appear as gentle bends in the rift valley (Vogt, this volume, Ch. 12). The Kurchatov FZ and the TAG area transform faults are well studied examples of these phenomena.

Detailed GLORIA side-scan sonar studies of the Kurchatov FZ (Searle and Laughton, 1977) do not reveal any prominent structures perpendicular to the MAR. Instead the normal faults bounding the rift valley veer approximately 45° clockwise for 18 km of offset, then back to a spreading center trend (Fig. 9). In the TAG area, where the transform offsets are even less (approx-

imately 10 to 12 km) there is only a single intersection depression shared between the two RT intersections creating a broad 45° bend in the trend of the rift valley (Rona and Gray, 1980). Similar structures have been mapped by Johnson and Vogt (1973) on the MAR from 47°N to 51°N. On transform faults whose offset is less than 15 to 20 km, the fault zone is one continuous RT intersection dominated by oblique normal faults.

Detailed studies of FZA and FZB, however, do reveal clear east-west strike slip faults that are punctuated by microearthquake activity along their entire length between RT intersections (Detrick and others, 1973; Reid and Macdonald, 1973). However, FZA and FZB are not perpendicular to the adjoining spreading centers, but intersect at angles of 70°-75°. The propensity of oblique intersections between spreading centers and their adjoining transform faults in the Atlantic led us to propose that oblique spreading is the rule, not the exception, at slow spreading centers (Atwater and Macdonald, 1977). However, it may be the transform faults rather than the spreading centers that are oblique (Collette and others, 1979; Searle and Laughton, 1977). Comparing the strikes of FZA and FZB to Minster and Jordan's predicted trends (1978), we find that spreading centers away from RT intersections are orthogonal to small circles about the pole of opening, and the transform faults are oblique relative to small circle trends.

Thus, there are essentially three types of transform faults (Fig. 9): (1) large offset ( $>30$  km) such as the Oceanographer, Kane, and Vema Fracture Zones that are parallel to small circles about the pole of opening and orthogonal to their spreading centers; (2) small offset transforms in which the entire transform valley is simply two coalesced RT intersections, and structures within the valley strike  $45^\circ$  relative to small circle trends; and (3) transitional transform faults such as FZA and FZB that have clear strike slip faults but are  $10$  to  $20^\circ$  oblique to small circle trends due to intersection effects.

Short offset transform faults (types 2 and 3) give rise to *apparent oblique spreading* because the angle between the gross morphology of the transform valley and the MAR rift valley is not  $90^\circ$ , but  $80^\circ$  to  $45^\circ$  (Vogt, this volume, Ch. 12). It is not true oblique spreading because away from the intersections the MAR is orthogonal to small circles about the pole of opening. This is not the same as postulated leaky transform faulting caused by a change in the pole of opening (Menard and Atwater, 1968).

Transform fault types 2 and 3 may be the present day equivalents to Schouten's hypothetical "zero offset transform faults" (Schouten and White, 1980). If so, then the long-term time-averaged fracture zone trends of these small offset transform faults may indeed trace small circles about the pole of opening, while the short, equidimensional transform valleys do not.

Small lateral offsets of the East Pacific Rise are manifested by "overlapping spreading centers" (OSCs) that are structurally very different from small transform faults in the Atlantic. Whether or not they have a common origin is a point of some controversy (Klitgord and Schouten, 1983; Macdonald and Fox, 1983b; Macdonald and others, 1984).

### *Heterogeneity of Crust Accreted at Slow-spreading Centers*

From the discussion above it is clear that transform faults disrupt the two-dimensionality of spreading centers and contribute significantly to heterogeneity in the physical and geochemical properties of the crust. We have reviewed evidence that the oceanic crust thins significantly near the ridge/transform intersections, that transform fault related shear stresses affect spreading center processes within approximately  $10$  km of the ridge/transform intersections, and that the dynamic forces responsible for the

maintenance of the axial rift valley may be enhanced or otherwise perturbed at the ridge transform intersection and up to several tens of kilometers along the strike of the axial rift valley. In addition, the AMC may be a steady state feature along a short length of the ridge segment removed from the RT intersection, but it is probably transient near these intersections. Considering that the MAR is disrupted every  $55$  km by a transform fault (Figs. 1 and 9), it is unlikely that any of the crust created along the MAR is free of the disrupting edge effects of transform faults. The result is a highly heterogeneous oceanic crust.

Rock magnetization is one physical property that can be inferred indirectly on a global scale via the magnetic field generated by crustal rocks, and the degree of heterogeneity of the crust should directly affect the clarity of magnetic anomalies (Vogt, this volume, Ch. 15). It has been known for some time that regional magnetic anomalies measured at the sea surface are far clearer and easier to decipher in the Pacific than in the Atlantic. For example, compare the careful magnetic anomaly study on the MAR at  $45^\circ\text{N}$  (Loncarevic and Parker, 1971) with magnetic anomalies on the East Pacific Rise at  $21^\circ\text{N}$  (Larson 1971) or  $20^\circ\text{S}$  (Rea and Blakely, 1975) or the Galapagos spreading center (Hey, 1977; Klitgord and others, 1975). To explain the difference in magnetic anomaly clarity we have suggested that crustal accretion processes and resulting magnetic structures vary significantly with spreading rate (Macdonald and others, 1983). Geologic processes that may have a spreading rate dependence and affect crustal heterogeneity include the frequency of volcanic eruptions, the stability of the neovolcanic zone, and the extent of tectonic disruption of the crust (Macdonald, 1982). An important factor to add to that list is the close spacing of transform faults in the Atlantic. If one considers transform faults whose offsets represent  $1$  m.y. age contrasts or greater (that is, the age of the lithosphere juxtaposed to the spreading center by the transform fault) then the average spacing is  $70$  km in the slow-spreading north Atlantic and approximately  $500$  km in the fast-spreading Pacific. The swath of crust disrupted by a transform fault is approximately  $30$  km, so roughly  $50$  percent of the Atlantic basin is significantly affected by transform fault edge effects while only  $5$  percent of the Pacific crust is so affected. Thus the close spacing of transform faults may be a major cause of the high degree of crustal heterogeneity observed in the Atlantic, and this factor must be considered in models of crustal accretion processes in the Atlantic.

### REFERENCES

- Ade-Hall, J. M., Aumento, F., Ryall, P.J.C., Gerstein, R. E., Brooke, J., and McKeown, D. L.  
1973 : The Mid-Atlantic ridge near  $45^\circ\text{N}$ , 21, Magnetic results from basalt drill cores from the median valley: Canadian Journal of Earth Sciences, v. 10, p. 676-696.
- ARCYANA  
1975 : Transform fault and rift valley from bathyscaph and diving saucer: Science, v. 190, p. 108-116.
- Anderson, R. N., and Noltmier, H. C.  
1973 : A model for the horst and graben structure of mid-ocean ridge crests based upon spreading velocity and basalt delivery to the oceanic crust: Geophysical Journal of the Royal Astronomical Society, v. 34:137-147.
- Atwater, T. M.  
1979 : Constraints from the FAMOUS area concerning the structure of the oceanic section; in Deep drilling results in the Atlantic Ocean: Ocean crust, eds. M. Talwani, C. G. Harrison, D. E. Hayes, 2, 33-42.
- Atwater, T. M., and Macdonald, K. C.  
1977 : Slowly spreading ridge crests: are they perpendicular to their transform faults?: Nature, v. 270, 715-719.
- Atwater, T., Ballard, R., Crane, K., Grover, N., Hopson, C., Johnson, H. P.,

- Luyendyke, B., Macdonald, K., Peirce, J., Shih, J., Shure, L., Stakes, D., Walker, N., van Andel, Tj. H.  
 1978 : AMAR 78: A coordinated submersible, photographic mapping and dredging program in the Mid-Atlantic Rift valleys near 36.5°N: Expedition Cruise Report, unpublished manuscript.
- Aumento, F.  
 1968 : The Mid-Atlantic Ridge near 45°N, 2, basalts from the area of Confederation Peak: *Canadian Journal of Earth Sciences*, v. 5, p. 1-21.
- Aumento, F., Loncarevic, B. D., and Ross, D. I.  
 1971 : Hudson geotraverse: geology of the Mid-Atlantic ridge at 45°N: *Philosophical Transactions of Royal Society, London, ser. A*, v. 268, p. 623-650.
- Ballard, R. D., Holcomb, R. T., and van Andel, Tj. H.  
 1979 : The Galapagos Rift at 86°W: 3. Sheet flows, collapse pits, and lava lakes of the rift valley: *Journal of Geophysical Research*, v. 84, p. 5407-5422.
- Ballard, R. D., and van Andel, Tj. H.  
 1977 : Morphology and tectonics of the inner rift valley at lat. 36°50'N on the Mid-Atlantic Ridge: *Geological Society of America Bulletin*, v. 88, p. 507-530.
- Barrett, D. L., and Aumento, F.  
 1970 : The Mid-Atlantic ridge near 45°N, 11, Seismic velocity, density and layering of the crust: *Canadian Journal of Earth Sciences*, v. 7, no. 4, p. 1117-1124.
- Bibee, L. D.  
 1979 : Crustal structure in areas of active crustal accretion: [Ph.D. Thesis], University of California, San Diego, p. 155.
- Bird, P., and Phillips, J. D.  
 1975 : Oblique spreading near the Oceanographer fracture zone: *Journal of Geophysical Research*, v. 80, p. 4021-4027.
- Bonatti, E., and J. Honnorez  
 1976 : Sections of the earth crust in the equatorial Atlantic: *Journal of Geophysical Research*, v. 81, p. 4104-4117.
- Bratt, S. R., and Solomon, S. C.  
 1984 : Compressional and shear wave structure of the East Pacific Rise at 11°20'N: Constraints from three-component Ocean Bottom Seismometer data: *Journal of Geophysical Research*, v. 89, p. 6095-6110.
- Bryan, W. B., and Moore, J. G.  
 1977 : Compositional variations of young basalts in the Mid-Atlantic ridge rift valley near lat. 36°49'N: *Geological Society of America Bulletin*, v. 88, p. 556-570.
- Bryan, W. B., Thompson, G., and Michael, P. J.  
 1979 : Compositional variation in a steady-state zoned magma chamber: Mid-Atlantic Ridge at 36°50'N: *Tectonophysics*, v. 55, p. 63-85.
- Bullard, E. C., and Day, A.  
 1961 : The flow of heat through the floor of the Atlantic Ocean: *Geophysical Journal*, vol. 4, p. 282-292.
- Bunch, A.W.H., and Kennett, B.L.N.  
 1980 : The crustal structure of the Reykjanes ridge at 59° 30'N: *Geophysical Journal of Royal Astronomical Society*, v. 61, p. 141-166.
- Cann, J. R.  
 1970 : New model for the structure of the oceanic crust: *Nature*, vol. 226, p. 928-930.  
 1974 : A model for oceanic crustal structure developed: *Geophysical Journal the Royal Astronomical Society*, v. 39, p. 169-187.
- Christiansen, N. I., and Salisbury, M. H.  
 1975 : Structure and constitution of the lower oceanic crust. *Reviews of Geophysics and Space Physics*, v. 13, p. 57-86.
- Colette, B. J., Sliotweg, A. P., and Twigt, W.  
 1979 : Mid-Atlantic ridge crest topography between 12° and 15°N: *Earth and Planetary Sciences Letters*, v. 42, p. 103-108.
- Corliss, J. B., Dymond, J., Gordon, L. I., Edmond, J. M., Von Herzen, R. P., Ballard, R. D., Green, K., Williams, D., Bainbridge, A., Crane, K., and van Andel, Tj. H.  
 1979 : Submarine thermal springs on the Galapagos Rift: *Science*, v. 203, p. 1073-1083.
- Crane, K.  
 1976 : The Intersection of the Siqueiros transform fault and the East Pacific Rise: *Marine Geology*, v. 21, p. 25-46.
- Crane, K., and Ballard, R. D.  
 1980 : The Galapagos rift at 86°W: 4. Structure and morphology of hydrothermal fields and their relationship to the volcanic and tectonic processes of the rift valley: *Journal of Geophysical Research*, v. 85, p. 1443-1454.  
 1981 : Volcanics and structure of the famous Narrowgate rift: evidence for cyclic evolution. AMAR1: *Journal of Geophysical Research*, v. 86, p. 5112-5124.
- Deffeyes, K. S.  
 1970 : The axial valley: a steady rate feature in the terrain. in *Megatectonics of continents and oceans*, eds. H. Johnson and B. C. Smith; Rutgers University Press, Brunswick, N.J., p. 194-222.
- Detrick, R. S., Mudie, J. D., Luyendyke, B. P., and Macdonald, K. C.  
 1973 : Near-bottom observations of an active transform fault (Mid-Atlantic ridge at 37°N): *Nature*, v. 246, no. 152, p. 59-61.
- Detrick, R. S., and Purdy, G. M.  
 1980 : The crustal structure of the Kane Fracture Zone from seismic refraction studies: *Journal of Geophysical Research*, v. 85, p. 3759-3777.
- Dewey, J. F., and Kidd, W.S.F.  
 1977 : Geometry of plate accretion: *Geological Society of America Bulletin*, v. 88, p. 960-968.
- Einarsson, P.  
 1979 : Seismicity and earthquake focal mechanisms along the Mid-Atlantic plate boundary between Iceland and the Azores: *Tectonophysics*, v. 55, p. 127-153.
- Fowler, C.M.R.  
 1976 : Crustal structure of the Mid-Atlantic ridge crest at 37°N: *Geophysical Journal of the Royal Astronomical Society*, v. 47, p. 459-491.
- Fowler, C.M.R., and Keen, C. E.  
 1979 : Oceanic crustal structure, Mid-Atlantic ridge at 45°N: *Geophysical Journal*, v. 56, p. 219-226.
- Fox, P. J., Detrick, R. S., and Purdy, G. M.  
 1980 : Evidence for crustal thinning near fracture zones: Implications for ophiolites, in *Ophiolites*, Panayiotou, A.; Proceedings of International Ophiolite Symposium, Cyprus: Geological Survey Department of Cyprus, Nicosia.
- Fox, P. J., and Gallo, D. G.  
 1984 : A tectonic model for ridge-transform-ridge plate boundaries: Implications for the structure of oceanic lithosphere: *Tectonophysics*, v. 104, p. 205-242.
- Fox, P. J., and Schreiber, E.J.J.  
 1973 : The geology of the oceanic crust: Compressional wave velocities of oceanic rocks: *Journal of Geophysical Research*, v. 78, p. 5155-5172.
- Francheteau, J., Needham, H. D., Choukroune, R., Juteau, T., Seguret, M., Ballard, R. D., Fox, P. J., Normark, W., Carranza, A., Cordoba, D., Guerrero, J., Rangan, C., Bargault, H., Cambon, P., and Hekinian, R.  
 1979 : Massive deep-sea sulfide ore deposits discovered on the East Pacific Rise: *Nature*, v. 277, p. 523-528.
- Francis, T.J.G.  
 1981 : Serpentinization faults and their role in the tectonics of slow spreading ridges: *Journal of Geophysical Research*, v. 86, p. 11, 616-11, 622.
- Francis, T.J.G., Porter, I. T., and Lilwall, R. C.  
 1978 : Microearthquakes near the eastern end of St. Paul's Fracture Zone: *Geophysical Journal of Royal Astronomical Society*, v. 53, p. 201-217.
- Francis, T.J.G., Porter, I. T., and McGrath, J. R.  
 1977 : Ocean bottom seismograph observations on the Mid-Atlantic ridge near 37°N: *Geological Society of America Bulletin*, v. 88, p. 664-677.
- Gutenberg, B., and Richter, C. F.  
 1954 : Seismicity of the earth and associated phenomena: Princeton Univer-

- sity Press, Princeton, New Jersey, p. 309.
- Hale, L. D., Morton, C. J., and Sleep, N. H.  
1982 : Reinterpretation of seismic reflection data over the East Pacific Rise: *Journal of Geophysical Research*, v. 87, p. 7707-7719.
- Hall, J. M.  
1976 : Major problems regarding the magnetization of oceanic crustal layer 2: *Journal of Geophysical Research*, v. 81, p. 4223-4230.
- Hall, J. M., and Robinson, P. T.  
1979 : Deep crustal drilling in the North Atlantic Ocean: *Science*, v. 204, p. 573-586.
- Harrison, C.G.A.  
1968 : Formation of magnetic anomaly patterns by dyke injection: *Journal of Geophysical Research*, v. 73, p. 2137-2142.  
1974 : Tectonics of mid-ocean ridges: *Tectonophysics*, v. 22, p. 301-310.
- Harrison, C.G.A., and Stieltjes, L.  
1977 : Faulting within the median valley: *Tectonophysics*, v. 38, p. 137-144.
- Harrison, C.G.A., and Watkins, N. D.  
1977 : Shallow inclinations of remanent magnetism in deep-sea drilling project igneous cores: Geomagnetic field behavior or postemplacement effects?: *Journal of Geophysical Research*, v. 82, p. 4869-4877.
- Heezen, B. C.  
1960 : The rift in the ocean floor: *Scientific American*, v. 203, no. 4, p. 99-110.
- Heezen, B. C., Sharp, M., and Ewing, M.  
1959 : The floors of the oceans, I, the North Atlantic Ocean: *Geological Society of America Special Paper* 65, 122 p.
- Heirtzler, J. R., and Ballard, R. D.  
1977 : Submersible observations at the Hole 332B area; in *Initial reports of the deep sea drilling project, Volume 37*, eds. F. Aumento, W. G. Melson, and others; p. 363-366.
- Heirtzler, J. R., and Le Pichon, X.  
1974 : FAMOUS: A plate tectonics study of the genesis of the lithosphere: *Geology*, v. 2, no. 6, p. 273-278.
- Herron, T. J., Stoffa, P. L., and Ball, P.  
1980 : Magma chamber and mantle reflection—East Pacific Rise: *Geophysical Research Letters*, v. 7, p. 989-992.
- Hess, H. H.  
1962 : History of the ocean basins, *Petrologic Studies: A volume to honor A. F. Buddington*: Geological Society of America, p. 599-620.
- Hey, R. N.  
1977 : A new class of pseudo-faults and their bearing on plate tectonics: A propagating rift model: *Earth and Planetary Science Letters*, v. 37, p. 321-325.
- Hill, M. N.  
1960 : A median valley of the Mid-Atlantic ridge: *Deep-Sea Research*, v. 6, no. 3, p. 193-205.
- Irving, E.  
1970 : The Mid-Atlantic ridge at 45°N, 14, oxidation and magnetic properties of basalt, review and discussion: *Canadian Journal of Earth Sciences*, v. 7, p. 1528-1538.
- Johnson, H. P., and Atwater, T. M.  
1977 : Magnetic study of basalts from the Mid-Atlantic ridge: *Geological Society of America Bulletin*, v. 88, p. 637-647.
- Johnson, G. L., and Vogt, P. R.  
1973 : Mid-Atlantic ridge from 47° to 51° north: *Geological Society of America Bulletin*, v. 84, p. 3443-3462.
- Keen, C. E., and Tramontini, C.  
1970 : A seismic refraction survey on the Mid-Atlantic ridge: *Geophysical Journal of the Royal Astronomical Society*, v. 20, p. 473-491.
- Klitgord, K. D., Huestis, S. P., Parker, R. L., and Mudie, J. D.  
1975 : An analysis of near-bottom magnetic anomalies: Sea floor spreading, the magnetized layer, and the geomagnetic time scale: *Geophysical Journal of the Royal Astronomical Society*, v. 43, p. 387-424.
- Kusznir, N. J.  
1980 : Thermal evolution of the oceanic crust: its dependence on spreading rate and effect on crustal structure: *Geophysical Journal of Royal Astronomical Society*, v. 61, p. 167-181.
- Lachenbruch, A. H.  
1973 : A simple mechanical model for oceanic spreading centers: *Journal of Geophysical Research*, v. 78, p. 3395-3417.  
1976 : Dynamics of a passive spreading center: *Journal of Geophysical Research*, v. 81, p. 1883-1902.
- Langmuir, C. H. and Bender, J. F.  
1984 : The geochemistry of oceanic basalts in the vicinity of transform faults: observations and implications: *Earth and Planetary Science Letters*, v. 69, p. 107-127.
- Larson, R. L.  
1971 : Near-bottom geophysical studies of the East Pacific Rise crest: *Geological Society of America Bulletin*, v. 82, p. 823-842.
- Laughton, A. S., and Searle, R. C.  
1979 : Tectonic processes on slow-spreading ridges; in *Implications of deep drilling results in the Atlantic Ocean: Ocean crust*, eds. M. Talwani and others; Maurice Ewing Series, American Geophysical Union, v. 2, p. 15-32.
- Lewis, B.R.T.  
1983 : The process of formation of ocean crust: *Science*, v. 220, p. 151-156.
- Lewis, B.T.R., and Garmany, J. D.  
1982 : Constraints on the structure of the East Pacific Rise from seismic refraction data: *Journal of Geophysical Research*, v. 87, p. 8417-8425.
- Lilwall, R. C., Francis, T.J.G., and Porter, I. T.  
1978 : Ocean bottom seismograph observations on the Mid-Atlantic ridge near 45°N—further results: *Geophysical Journal of Royal Astronomical Society*, v. 55, p. 255-262.
- Lister, C.R.B.  
1972 : On the thermal balance of a mid-ocean ridge: *Geophysical Journal of Royal Astronomical Society*, v. 26, p. 515-535.  
1983 : On the intermittency and crystallization mechanisms of sub-sea-floor magma chambers: *Geophysical Journal of Royal Astronomical Society*, v. 73, p. 351-365.
- Loncarevic, B. D., Mason, C. S., and Matthews, D. H.  
1966 : The Mid-Atlantic ridge near 45°N, I, The median valley: *Canadian Journal of Earth Sciences*, v. 3, p. 327-349.
- Loncarevic, B. D., and Parker, R. L.  
1971 : The Mid-Atlantic ridge near 45°N, 17, Magnetic anomalies and sea-floor spreading: *Canadian Journal of Earth Sciences*, v. 8, p. 883-898.
- Lonsdale, P.  
1977 : Structural geomorphology of a fast-spreading rise crest: The East Pacific Rise near 3°25'S: *Marine Geophysical Research*, v. 3, p. 251-293.
- Lowell, R. P.  
1975 : Circulation in fractures, hot springs and convective heat transport on mid-ocean ridge crests: *Geophysical Journal of Royal Astronomical Society*, v. 40, p. 351-365.
- Luyendyk, B. P., and Macdonald, K. C.  
1977 : Physiography and structure of the inner floor of the Famous rift valley: observations with a deeply towed instrument package: *Geological Society of America Bulletin*, v. 88, p. 648-663.
- MacDonald, K. C.  
1976 : Geomagnetic reversals and the deep drill hole at DSDP site 32: *Journal of Geophysical Research*, v. 81, p. 4163-4165.  
1977 : Near-bottom, magnetic anomalies, asymmetric spreading, oblique spreading, and tectonics of the Mid-Atlantic ridge near 37°N: *Geological Society of America Bulletin*, v. 88, p. 541-555.  
1982 : Mid-ocean ridges: Fine-scale tectonic, volcanic and hydrothermal processes within the plate boundary zone: *Annual Review of Earth and Planetary Sciences*, v. 10, p. 155-190.  
1983a : Crustal processes at spreading centers: *Reviews of Geophysics and Space Physics*, v. 21, p. 1441-1453.

- 1983b: A geophysical comparison between fast and slow spreading centers: constraints on magma chamber formation and hydrothermal activity; in *Hydrothermal processes at seafloor spreading centers*, eds. P. Rona and others; p. 27-51, NATO Conference series IV: 12, Plenum, N.Y. 796 pp.
- MacDonald, K. C., and Atwater, T. M.  
1978a: AMAR78, Preliminary results, I. Evolution of the median rift (abstract): EOS, v. 59, p. 1198.  
1978b: Evolution of rifted ocean ridges: *Earth and Planetary Sciences Letters*, v. 39, p. 319-327.
- MacDonald, Ken C., Castillo, D., Miller, S., Fox, P. J., Kastens, K. A., and Bonatti, E.  
submitted: Deep tow studies of the Vema fracture zone: I. The tectonics of a major slow-slipping transform fault and its intersection with the Mid-Atlantic Ridge: *Journal of Geophysical Research*.
- MacDonald, K. C., and Fox, P. J.  
1983a: Overlapping spreading centres: new accretion geometry on the East Pacific Rise: *Nature*, v. 302, p. 55-58.  
1983b: Overlapping spreading centers on the East Pacific Rise—discussion and reply: *Nature*, v. 303, p. 549-550.
- MacDonald, K. C., Kastens, K., Spiess, F. N., and Miller, S. P.  
1979: Deep tow studies in the Tamayo Transform Fault: *Marine Geophysical Research*, v. 4, p. 37-70.
- MacDonald, K. C., and Luyendyk, B. P.  
1977: Deep-tow studies of the structure of the Mid-Atlantic ridge crest near 37°N (Famous): *Geological Society of America Bulletin*, v. 88, p. 621-636.
- MacDonald, K. C., Luyendyk, B. P., Mudie, J. D., and Spiess, F. N.  
1975: Near-bottom geophysical study of the Mid-Atlantic Ridge median valley near lat. 37°N: Preliminary observations: *Geology*, v. 3, p. 211-215.
- MacDonald, K. C., Miller, S. P., Luyendyk, B. P., Atwater, T. M., and Shure, L.  
1983: Investigation of a Vine-Matthews magnetic lineation from a submersible: The source and character of marine magnetic anomalies: *Journal of Geophysical Research*, v. 88, p. 3403-3418.
- MacDonald, K. C., Sempere, J. C., and Fox, P. J.  
1984: The East Pacific Rise from the Siqueiros to the Orozco fracture zones: along-strike continuity of the neovolcanic zone and the structure and evolution of overlapping spreading center: *Journal of Geophysical Research*, v. 89, no. B7, p. 6049-6306.
- McClain, J. S., and Lewis, B.T.R.  
1980: A seismic experiment of the axis of the East Pacific Rise: *Marine Geology*, v. 35, p. 147-169.
- McGregor, B. A., and Rona, P. A.  
1975: Crest of the Mid-Atlantic ridge at 26°N: *Journal of Geophysical Research*, v. 80, p. 3307-3314.
- McKenzie, D. P., and Parker, R. L.  
1967: The North Pacific: An example of tectonics on a sphere: *Nature*, v. 216, p. 1276-1280.
- Maury, M. F.  
1963: *The physical geography of the sea*: Cambridge, Mass., Harvard University Press, (from eighth edition, published 1861).
- Menard, H. W., and Atwater, T.  
1968: Changes in the direction of seafloor spreading: *Nature*, v. 219, p. 463-467.
- Minster, J. B., and Jordan, T. H.  
1978: Present-day plate motions: *Journal of Geophysical Research*, v. 83, p. 5331-5354.
- Moore, J. G., Fleming, H. S., and Phillips, J. D.  
1974: Preliminary model for extrusion and rifting of the axis of the Mid-Atlantic ridge, 36°48'N: *Geology*, v. 2, p. 437-440.
- Natland, J. H.  
1980: Effect of axial magma chambers beneath spreading centers on the compositions of Basaltic Rocks: Initial Report Deep Sea Drilling Project LIV, p. 833-850.
- Needham, H. D., and Francheteau, J.  
1974: Some characteristics of the rift valley in the Atlantic Ocean near 36°48'N: *Earth and Planetary Sciences Letters*, v. 22, p. 29-43.
- Nelson, K. D.  
1981: A simple thermal-mechanical model for mid-ocean ridge topographic variation: *Geophysical Journal of Royal Astronomical Society*, v. 65, p. 19-30.
- Nisbet, E. G., and Fowler, C.M.R.  
1978: The Mid-Atlantic ridge at 37 and 45°N: some geophysical and petrologic constraints: *Geophysical Journal Royal Astronomical Society*, v. 54, p. 631-660.
- Normark, W. R.  
1976: Delineation of the main extrusion zone of the East Pacific Rise at Lat. 21°N: *Geology*, v. 4, p. 681-685.
- Orcutt, J. A., Kennett, B.L.N., and Dorman, L. M.  
1976: Structure of the East Pacific Rise from an ocean bottom seismometer array: *Geophysical Journal of the Royal Astronomical Society*, v. 45, p. 305-320.
- Orcutt, J. A., McClain, J. S., and Burnett, M.  
in press: Seismic constraints on the generation, evolution and structure of the ocean crust: *Geological Society of London Special Publication*.
- Osmaston, M. F.  
1971: Genesis of ocean ridge median valleys and continental rift valleys: *Tectonophysics*, v. 11, p. 387-405.
- OTTER Scientific Team  
in press: The geology of the Oceanographer Transform: The eastern ridge-transform intersection: *Marine Geophysical Research*.
- Pallister, J. S., and Hopson, C. A.  
1981: Semail ophiolite plutonic suite: Field relations, phase variation, cryptic variation and layering, and a model of a spreading ridge magma chamber: *Journal of Geophysical Research*, v. 86, p. 2593-2644.
- Pålmason, G.  
1980: A continuum model of crustal generation in Iceland kinematic aspects: *Journal of Geophysics*, v. 47, p. 7-18.
- Phillips, J. P., Thompson, G., Von Herzen, R. P., and Bowen, V. T.  
1969: Mid-Atlantic ridge near 43°N latitude: *Journal of Geophysical Research*, v. 74, p. 3069-3081.
- Poehls, K.  
1974: Seismic refraction on the Mid-Atlantic ridge at 37°N: *Journal of Geophysical Research*, v. 79, p. 3370-3373.
- Prevot, M., Lecaillon, A., Hekinian, R.  
1979: Magnetism of the Mid-Atlantic ridge crest near 37°N from FAMOUS and DSDP results: A review; in *Deep sea drilling results in the Atlantic ocean: Ocean crust*, eds. M. Talwani, C. G. Harrison, D. E. Hayes: Maurice Ewing Series 2, American Geophysical Union, Washington, D.C., 431 p.
- Parmentier, E. M., and Forsyth, D. W.  
1985: Three-dimensional flow beneath a slow-spreading ridge axis: a dynamic contribution to the deepening of the median valley toward fracture zones: *Journal of Geophysical Research*, v. 90, p. 678-684.
- Purdy, G. M., Detrick, R. S., and Cormier, M.  
1982: Seismic constraints on the crustal structure at a ridge-fracture zone intersection: EOS, v. 63, p. 1100.
- Ramberg, I. B., Gray, D. F., and Reynolds, R.G.H.  
1977: Tectonic evolution of the FAMOUS area of the Mid-Atlantic Ridge, lat. 35°50' to 37°20'N: *Geological Society of America Bulletin*, v. 88, p. 609-620.
- Rea, D. K.  
1978: Evolution of the East Pacific Rise between 3°S and 13°S since the middle miocene: *Geophysical Research Letters*, v. 5, p. 561-564.
- Rea, D. K., Blakely, R. J.  
1975: Short-wavelength magnetic anomalies in a region of rapid seafloor spreading: *Nature*, v. 255, p. 126-128.
- Reid, I. D., and Jackson, H. R.

- 1981 : Oceanic spreading rate and crustal thickness: *Marine Geophysical Research*, v. 5, p. 165-172.
- Reid, I. D., and MacDonalD, K. C.  
 1973 : Microearthquake study of the Mid-Atlantic Ridge near 37°N using sonobuoys: *Nature*, v. 246, p. 88-90.
- Reid, I. D., Orcutt, J. A., and Prothero, W. A.  
 1977 : Seismic evidence for a narrow zone of partial melting underlying the East Pacific Rise at 21°N: *Geological Society of American Bulletin*, v. 88, p. 678-682.
- Rhodes, J. M., and Dungan, M. A.  
 1979 : The evolution of ocean-floor basaltic magmas, in *Deep drilling results in the Atlantic Ocean: Ocean Crust*; eds. M. Talwani and others; v. 2, p. 262-272.
- RISE Team  
 1980 : East Pacific Rise: Hot springs and geophysical experiments: *Science*, v. 207, p. 1421-1433.
- Rona, P. A., Thompson, G., Mottl, M. J., Karson, J., Jenkins, W. J., Graham, D., Von Damm, K., and Edmond, J. M.  
 1982 : Direct observations of hydrothermal mineralization at the TAG hydrothermal field, Mid-Atlantic ridge 26°N: *EOS*, v. 63, p. 1014.
- Rona, P. A., and Gray, D. F.  
 1980 : Structural behavior of fracture zones symmetric and asymmetric about a spreading axis: Mid-Atlantic ridge (latitude 23°N to 27°N): *Geological Society of America Bulletin*, v. 91, p. 485-494.
- Schouten, H., and Klitgord, K. D.  
 1982 : The memory of the accreting plate boundary and the continuity of fracture zones: *Earth and Planetary Sciences Letters*, v. 59, p. 255-266.  
 1983 : Overlapping spreading centers on the East Pacific Rise—comment: *Nature*, v. 303, p. 549-550.
- Schouten, H., and White, R. S.  
 1980 : Zero-offset fracture zones: *Geology*, v. 8, p. 175-179.
- Searle, R. C.  
 1979 : Side-scan sonar studies of North Atlantic fracture zones: *Journal of the Geological Society*, v. 136, part 3, p. 283-292.
- Searle, R. C., and Loughton, A. S.  
 1977 : Sonar studies of the Mid-Atlantic ridge and Kurchatov Fracture Zone: *Journal Geophysical Research*, v. 82, p. 5313-5328.
- Shand, S. J.  
 1949 : Rocks of the Mid-Atlantic ridge: *Journal Geology*, v. 57, p. 89-91.
- Shih, J.S.F.  
 1980 : The nature and origin of fine-scale seafloor relief; [Ph.D. thesis] Massachusetts Institute of Technology, Cambridge, Mass., 222 pp.
- Sleep, N. H.  
 1969 : Sensitivity of heat flow and gravity to the mechanism of seafloor spreading: *Journal of Geophysical Research*, v. 74, p. 542-549.  
 1975 : Formation of ocean crust: Some thermal constraints: *Journal of Geophysical Research*, v. 80, p. 4037-4042.  
 1978 : Thermal structure of mid-oceanic ridge axes, some implications to basaltic volcanism: *Geophysical Research Letters*, v. 5, p. 426-428.
- Sleep, N. H., and Biehler, S.  
 1970 : Topography and tectonics at the intersections of fracture zones with central rifts: *Journal of Geophysical Research*, v. 75, p. 2748-2752.
- Sleep, N. H., and Rosendahl, B. R.  
 1979 : Topography and tectonics of mid-ocean ridge axes: *Journal of Geophysical Research*, v. 84, p. 6831-6839.  
 1983 : Hydrothermal convection at ridge axes: in *Hydrothermal processes at seafloor spreading centers*, ed. P. A. Rona: NATO conference series, series 4, v. 12, Plenum Press, New York, p. 71-82.
- Spindel, R. C., Davis, S. B., Macdonald, K. C., Porter, R. P., and Phillips, J. D.  
 1974 : Microearthquake survey of median valley of the Mid-Atlantic ridge at 36°30'N: *Nature*, v. 248, p. 577-579.
- Stakes, D., Shervais, J. W., and Hopson, C. A.  
 1984 : The volcano-tectonic cycle of the FAMOUS and AMAR valleys, Mid-Atlantic Ridge (36°47'N): Evidence from basalt glass and basalt phenocryst compositional variations for a steady-state magma chamber beneath the valley midsections: *Journal of Geophysical Research*, v. 89, p. 6995-7028.
- Tamayo Tectonic Team  
 1984 : Tectonics at the Intersection of the East Pacific Rise with the Tamayo Transform Fault: *Marine Geophysical Research*, v. 6, p. 159-185.
- Tapponnier, P., and Francheteau, J.  
 1978 : Necking of the lithosphere and the mechanics of slowly accreting plate boundaries: *Journal of Geophysical Research*, v. 83, p. 3955-3970.
- Toomey, D. R., Murray, M. H., Purdy, G. M., and Murray, M. H.  
 1982 : Microearthquakes on the Mid-Atlantic ridge near 23°N: new observations with a large network: *EOS*, v. 63, p. 1103.
- Trenu, A. M.  
 1982 : Seismicity and structure of the Orozco transform from ocean bottom seismic observation, WHOI-reference-82-13; [Ph.D. dissertation] Woods Hole Oceanographic Institution/Massachusetts Institute of Technology.
- van Andel, Tj. H., and Ballard, R. D.  
 1979 : The Galapagos Rift at 86°W, 2. Volcanism, structure and evolution of the rift valley: *Journal of Geophysical Research*, v. 84, p. 5390-5406.
- van Andel, Tj. H., and Bowin, C. O.  
 1968 : Mid-Atlantic ridge between 22° and 23°N latitude and the tectonics of mid-ocean rises: *Journal of Geophysical Research*, v. 73, p. 1279-1298.
- van Andel, Tj. H., and Heath, C. R.  
 1970 : Tectonics of the Mid-Atlantic ridge 6-8° south latitude: *Marine Geophysical Research*, v. 1, p. 5-36.
- Van Wagoner, N. A., and Johnson, H. P.  
 1983 : Magnetic properties of three segments of the Mid-Atlantic ridge at 37°N: FAMOUS, Narrowgate and AMAR: *Journal of Geophysical Research*, v. 88, p. 5065-5083.
- Verosub, K. L., and Moores, E. M.  
 1981 : Tectonic rotations in extensional regimes and their paleomagnetic consequences for oceanic basalts: *Journal of Geophysical Research*, v. 86, p. 6335-6350.
- Vine, F. J.  
 1966 : Ocean floor spreading: new evidence: *Science*, v. 154, no. 3755, p. 1405-1415.
- Vine, F. J., and Matthews, D. H.  
 1963 : Magnetic anomalies over oceanic ridges: *Nature*, v. 199, p. 947-949.
- Weidner, D. J. and Aki, K.  
 1973 : Focal depth and mechanism of mid-ocean ridge earthquakes: *Journal of Geophysical Research*, v. 78, p. 1818.
- Vogt, P. R., Kovacs, L. C., Bernero, C., and Srivastava, S. P.  
 1982 : Asymmetric geophysical signatures in the Greenland-Norwegian and south Labrador seas and the Eurasian basin, *Tectonophysics*, v. 89, p. 95-160.
- Whitmarsh, R. B.  
 1975 : Axial intrusion zone beneath the median valley of the Mid-Atlantic ridge at 37°N detected by explosion seismology: *Geophysical Journal of Royal Astronomical Society*, v. 42, p. 189-215.

MANUSCRIPT ACCEPTED BY THE SOCIETY JULY 1, 1984

#### Acknowledgments

I would like to thank C. Hopson whose review was so thorough he should probably be a co-author, P. Vogt who cajoled me into writing this paper, and P. J. Fox, E. Bonatti, A. Palmer, D. Stakes, R. Haymon, J. Bicknell, and P. Vogt who improved the paper with their careful reviews. My efforts in the research presented in this paper have been supported by the National Science Foundation and the Office of Naval Research.